Ministry of Higher Education and Scientific Research

Hassiba Benbouali University of Chlef

Faculty of Exact Sciences and Informatics
Department of Physics
Laboratory of Theoretical Physics and Material Physics

Doctoral Thesis in Theoretical Physics

Ultra-cold gases in Low Dimensionality

Presented by: Mr Medani Mohammed

Defended on May 23, 2026 before the thesis defense committee:

RACHED HABIB	Professor	Chlef University	President
BOUKABCHA HOCINE	Professor	University of Khemis-Meliana	Examiner
BILEL HAMIL	MCA	University of Constantine 1	Examiner
DRIS BOUBAA	MCA	University of Khenchla	Examiner
BENAROUS MOHAMED	ProfessOR	Chlef University	Advisor
HOCINE AHMED	Professeur	Chlef University	Co-advisor

Academic Year 2025–2026

Dedication

To my mother and father,
To my brother and my sisters

Acknowledgements

First , I wish to express my profound gratitude to Allah Almighty for give me this opportunity to undertake this research study and complete it satisfactorily

I also extend my deepest gratitude to all those who contributed, in one way or another, to the completion of this doctoral thesis.

I am profoundly grateful to my supervisor, Professor Benarous Mohamed, for his continuous guidance, unwavering support, and invaluable scientific insight throughout the course of this research. His rigorous approach to physics, his patience, and his constant encouragement have been a source of inspiration and motivation at every stage of this work. His contribution has been instrumental in shaping the direction of this research.

I would also like to extend my sincere thanks to my co-supervisor, my old friend Professor Hocine Ahmed, for his thoughtful advice, constructive remarks, and the fruitful scientific discussions that have significantly enriched this thesis.

I am deeply honoured that Professor Rached Habib accepted to chair the jury committee of this doctoral defence. His presence and engagement are greatly appreciated.

I wish to express my heartfelt gratitude to the members of the examination committee, Professor Boukabcha , Dr Hamil and Dr Boubaa, for accepting to review and evaluate this work. Their careful reading, critical comments, and valuable suggestions have undoubtedly contributed to improving the quality of this manuscript.

I would also like to express my sincere gratitude to all the faculty members of the Department of Physics for their dedication, continuous support, and the friendship they have shown throughout my academic journey.

Finally, and above all, I owe an immense debt of gratitude to all my family, whose unconditional love, patience, and moral support have been my greatest strength.

Abstract

This thesis investigates the thermodynamic properties of ideal Bose gases within the framework of the Dunkl formalism, a generalization of quantum mechanics based on the deformed Heisenberg algebra introduced through the Wigner-Dunkl differential-difference operator. Starting from the mathematical foundations of deformed algebras and revisiting the seminal contributions of Wigner, Yang, and Dunkl, we systematically extend the standard Bose-Einstein condensation theory to the Dunkl-deformed setting, covering both homogeneous and confined systems in arbitrary spatial dimension D. For ideal Bose gases confined by general power-law trapping potentials, we show that all thermodynamic quantities depend solely on a single universal parameter s that encoding the combined effects of dimensionality and trap geometry η. This reveals the existence of universality classes applicable to any power-law potential regardless of its specific form. Bose-Einstein condensation occurs exclusively for $s > 1$, consistently with the Mermin-Wagner-Hohenberg theorem, and the BEC transition remains second order for all $s \neq 2$, while $s = 2$ it exhibits a continuous transition of Berezinskii-Kosterlitz-Thouless type. The Dunkl deformation parameter ν tunes the thermodynamic behavior continuously, and thermodynamic consistency requires $0 < \nu \leq 2$, a constraint shown to hold for arbitrary regular potentials in any dimension. These results establish a unified description of Dunkl-deformed Bose gases and clarify the fundamental interplay between confinement geometry and algebraic deformation.

résumé

Cette thèse étudie les propriétés thermodynamiques des gaz de Bose idéaux dans le cadre du formalisme de Dunkl qui est une généralisation de la mécanique quantique basée sur l'algèbre de Heisenberg déformée introduite via les opérateurs différentiel-différentiels de Wigner-Dunkl. En partant des fondements mathématiques des opérateurs déformés et en revisitant les contributions fondamentales de Wigner, Yang et Dunkl, nous étendons systématiquement la théorie standard de la condensation de Bose-Einstein à l'ensemble déformé de Dunkl, couvrant à la fois les systèmes homogènes et confinés dans un espace de dimension D.

Pour des gaz de Bose idéaux confinés par un potentiel en loi de puissance, nous montrons que toutes les grandeurs thermodynamiques dépendent uniquement d'un paramètre universel noté s;

qui incluent les effets combinés de la dimension et de la géométrie du piège η. Cela révèle l'existence de classes d'universalité applicables à tout potentiel de puissance, indépendamment de sa forme spécifique.

La condensation de Bose-Einstein se produit exclusivement pour $s > 1$, conformément au théorème de Mermin-Wagner-Hohenberg, et la fraction condensée reste nulle pour $s \leq 2$, tandis que $s = 2$ elle montre une arbitraire transition continue de type Berezinskii-Kosterlitz-Thouless. Le paramètre de déformation de Dunkl ν influence de manière continue le comportement thermodynamique, et le critère de consistance thermodynamique requiert $0 < \nu \leq 2$, une contrainte nécessaire et valable pour tout potentiel régulier arbitraire pour toute dimension.

Ces résultats fournissent une description unifiée des gaz de Bose déformés de Dunkl et clarifient l'interaction fondamentale entre la géométrie du confinement et la déformation algébrique .

Contents

List of Figures

General introduction

In the 1924s, Albert Einstein put forward one of the most importante prediction in the history of modern physics that transforms our understanding of matter at its most fundamental level.The origin of this prediction goes to the Indian physicist who formulated a statistical framework for describing the photon. Recognizing the originality of Bose's approach, Einstein extended Bose's quantum-statistical formalism to apply not only to photons but to any collection of indistinguishable integer-spin particles (bosons) [1, 2]. Einstein predicted that, when a bosonic gas system is cooled below a critical temperature, it undergoes a quantum phase transition and a macroscopic fraction of the particles simultaneously "condenses" into the single lowest-energy quantum state, giving rise to a new state of matter called Bose-Einstein condensate (BEC). The first experimental confirmation of this 70 year old prediction, was obtained; in 1995, by Eric Cornell and Carl Wieman who successfully produced the first BEC using Rubidium-87 atoms. Within months, Wolfgang Ketterle at MIT independently achieved BEC with Sodium atoms [3, 4].

The Quantum statistical mechanics provides the theoretical framework for understanding collective phenomena arising from the microscopic laws of quantum mechanics and Bose–Einstein condensation occupies a central position as one of the most physical realization of quantum coherence at macroscopic scales. The thermodynamic behavior of Bose gases is known to depend sensitively on the density of states, which in turn is governed by both spatial dimensionality and external trapping.

Its study has revealed the profound role played by dimensionality and confinement geometry in determining the properties of many-body systems. Advances in experimental techniques now allow unprecedented control over trapping potentials, dimensionality, and effective interactions, opening new avenues for exploring non-standard quantum regimes.

While homogeneous systems provide valuable insight, most experimentally relevant realizations involve trapped gases, often confined by potentials that deviate significantly from the harmonic approximation.

Power-law trapping potentials offer a natural and flexible framework for studying such systems. They interpolate continuously between homogeneous gases and strongly confined regimes, allowing systematic exploration of how geometry influences thermodynamic and critical properties.

In parallel with experimental, theoretical progress have brought up important concerns regarding the uniqueness of the canonical formulation of quantum mechanics. It has long been recognized that the standard Heisenberg commutation relations do not represent the only mathematically consistent realization of quantum dynamics. To explore generalized commutation relations that preserve the Hilbert space structure while modifying the operator algebra; algebraic deformations of quantum mechanics provide a systematic way. This formalism has found applications across various fields of physics [5–24] and mathematic [25–33],

Among the various deformation schemes proposed in the literature such as κ-deformation [10, 34, 35] and q-deformation [36, 37],or Tsallis non-extensive statistics [38, 39] , the Dunkl formalism [40] occupies a distinctive position due to its explicit connection with reflection symmetry and parity sectors. Such deformation have been motivated by diverse considerations, including effective descriptions of interactions, parity-dependent dynamics, low-dimensional systems, and possible signatures of physics beyond the standard quantum framework.

The Dunkl formalism introduces differential-difference operators associated with reflection groups, leading to a deformation of the canonical momentum operator [41]. As a consequence, the fundamental commutation relations acquire an explicit dependence on parity, giving rise to modified quantum statistics. This parity-dependent algebra naturally interpolates between different quantum regimes and offers a controlled framework for studying deformed quantum systems.

Despite its mathematical elegance, the physical consequences of Dunkl deformation for quantum statistical mechanics, and in particular for Bose–Einstein condensation in trapped systems, remain only partially explored.

The primary objective of this thesis is to develop a comprehensive and self-consistent thermodynamic theory of ideal Bose gases confined by general power-law potentials within the Dunkl-deformed framework.

To this end, we will first

Generalize the density of states to arbitrary spatial dimension and power-law confinement of ideal gases within the Dunkl deformation framework. Then, we investigate its effects on various thermodynamic quantities. Most importantly we identify universal parameters governing thermodynamic behavior and classify systems into universality classes. This allow us to establish rigorous conditions for the

existence of Bose-Einstein condensation. We analyze the critical properties, including the behavior of the heat capacity and the nature of the phase transition; and at the end to investigate the classical limit and derive physical consistency constraints on the deformation parameter.

By addressing these questions, this thesis aims at clarifying the interplay between geometry, algebraic structure, and macroscopic quantum phenomena.

This thesis is organized as follows. Chapter 1 introduces the mathematical foundations of the deformed algebra. Chapter 2 concerns the deformed algebra by Dunkl formalism and its underlying deformed quantum mechanics . Chapter 3 is devoted to quantum statistical mechanics as framework to investigate Bose–Einstein condensation . Chapter 4 analyzes the ideal Bose gases in Dunkl-framework for different harmonic confinement potentials. Chapter 5 investigates the ideal Dunkl-Bose gases in arbitrary dimension with power-law confinement and the physical consistency with classical limits. Finally, the thesis concludes with a general discussion and perspectives for future research.

Chapter 1

Introduction to deformed algebra

The concept of deformed algebras is based on the idea that classical algebraic structures, such as Lie-Poisson algebra or associative algebras, can be continuously modified without altering their essential structural properties. Such deformations provide a powerful framework for interpolating between different mathematical theories and for incorporating corrections to classical models motivated by physical considerations.

The mathematical foundations of deformation theory were established in the 1960s through the work of Gerstenhaber [42], who introduced the concept of deforming associative algebras to investigate their structural properties perturbatively. This approach was later extended by Bayen et al [43], who formulated deformation quantization and showed that quantum mechanics naturally emerges as a deformation of classical mechanics.

In general, a deformation replaces the original algebraic relations by modified ones depending on a set of parameters, such that the classical algebra is recovered in an appropriate limit.

We begin by introducing Lie algebras as the algebraic structures underlying continuous symmetries in mathematics and theoretical physics. We then explore the historical emergence of deformation theory, Gerstenhaber's cohomological framework, deformation quantization, quantum groups, and their applications in modern mathematical physics.

1.1 Lie algebra

A Lie algebra is a vector space $\mathfrak{g}$ over a field $\mathbb{F}$ (typically $\mathbb{R}$ or $\mathbb{C}$) equipped with a bilinear operation, called the Lie bracket, $[\,\cdot\,,\cdot\,] : \mathfrak{g} \times \mathfrak{g} \to \mathfrak{g}$, such that for all

$X, Y, Z \in \mathfrak{g}$ and all scalars $a, b \in \mathbb{F}$,

$$[aX + bY, Z] = a[X, Z] + b[Y, Z], \quad [Z, aX + bY] = a[Z, X] + b[Z, Y]. \tag{1.1}$$

The Lie bracket satisfies two fundamental properties. First, it is antisymmetric:

$$[X, Y] = -[Y, X], \quad \text{for all } X, Y \in \mathfrak{g}, \tag{1.2}$$

implying in particular that $[X, X] = 0$. Second, it obeys the Jacobi identity:

$$[X, [Y, Z]] + [Y, [Z, X]] + [Z, [X, Y]] = 0 \quad \text{for all } X, Y, Z \in \mathfrak{g}. \tag{1.3}$$

These properties encode a compatibility condition that distinguishes Lie algebras from arbitrary bilinear operations and capture the essential algebraic structure underlying infinitesimal symmetries.

Lie's insight was that the local structure of a continuous group—now known as a Lie group—is completely determined by its infinitesimal generators, which themselves form a Lie algebra.

Concrete examples of Lie algebras abound in mathematics and physics.For instance, the vector space of all $n \times n$ matrices over $\mathbb{F}$, denoted $\mathfrak{gl}(n, \mathbb{F})$, becomes a Lie algebra under the commutator bracket

$$[A, B] = AB - BA, \quad A, B \in \mathfrak{gl}(n, \mathbb{F}). \tag{1.4}$$

Important subalgebras include $\mathfrak{sl}(n, \mathbb{F})$ of traceless matrices; $\mathfrak{Tr}(sl(n, F)) = 0$, $\mathfrak{so}(n)$ of skew-symmetric matrices $\mathfrak{Tr}(so(n)) = -so(n)$, and $\mathfrak{su}(n)$ of skew-Hermitian traceless matrices; $\mathfrak{su}^+(n) = -\mathfrak{su}(n)$ and $\mathfrak{Tr}(su(n, F)) = 0$.

Infinite-dimensional examples also play a central role, particularly in differential geometry. The space of smooth vector fields on a manifold M, denoted $\mathfrak{X}(M)$, forms a Lie algebra with the Lie bracket defined by

$$[X, Y] = \big(X^i \partial_i Y^j - Y^i \partial_i X^j\big)\partial_j, \tag{1.5}$$

where $X = X^i \partial_i$ and $Y = Y^j \partial_j$. This structure links Lie algebras directly to the symmetries of geometric objects and smooth manifolds.

In physics, the canonical commutation relations of quantum mechanics provide another fundamental example. The Heisenberg algebra is generated by the position

operator $\hat{q}$, the momentum operator $\hat{p}$, and the identity $\hat{1}$, satisfying

$$\begin{aligned} [\hat{q}, \hat{p}] &= i\hbar\hat{1}, \\ [\hat{q}, \hat{1}] &= 0, \\ [\hat{p}, \hat{1}] &= 0. \end{aligned} \tag{1.6}$$

This three-dimensional nilpotent Lie algebra underlies the structure of quantum mechanics and provides the simplest nontrivial example of a Lie algebra in physics.

Let us recall that a Lie algebra $\mathfrak{g}$ is nilpotent if its lower central series

$$\mathfrak{g}^0 = \mathfrak{g}, \qquad \mathfrak{g}^{k+1} = [\mathfrak{g}, \mathfrak{g}^k], \tag{1.7}$$

terminates at zero, i.e., $\mathfrak{g}^n = \{0\}$ for some integer n.

1.1.1 Lie algebra and continuous symmetries

According to Noether's theorem [44], every continuous symmetry of the action in a physical system gives rise to a conserved quantity. The algebraic structure governing these conserved quantities is naturally encoded in a Lie algebra, with the Poisson bracket providing the relevant algebraic operation.

On a phase space with canonical coordinates (q_i, p_i), the Poisson bracket of two observables f and g is given by

$$\{f, g\} = \frac{\partial f}{\partial q_i}\frac{\partial g}{\partial p_i} - \frac{\partial f}{\partial p_i}\frac{\partial g}{\partial q_i}. \tag{1.8}$$

Under this bracket, the space of smooth functions on phase space forms an infinite-dimensional Lie algebra. In particular, observables generating spatial symmetries—such as the components of angular momentum L_x, L_y, L_z—satisfy relations that reproduce the Lie algebra of rotations,

$$\{L_x, L_y\} = L_z, \quad \{L_y, L_z\} = L_x, \quad \{L_z, L_x\} = L_y, \tag{1.9}$$

which corresponds to the algebra $\mathfrak{so}(3)$.

This algebraic structure persists in quantum mechanics through the procedure of canonical quantization, whereby classical observables are promoted to operators and the Poisson bracket is replaced by the commutator according to the correspondence

$$\{f, g\} \longrightarrow \frac{1}{i\hbar}[\hat{f}, \hat{g}]. \tag{1.10}$$

This transition, often referred to as the correspondence principle [45–47], highlights the fact that quantum mechanics may be viewed as a deformation of classical mechanics, with Planck's constant $\hbar$ acting as the deformation parameter that governs deviations from classical behavior.

1.2 Historical Foundations of Deformation Theory: From Classical to Quantum Structures

The conceptual foundations of deformation theory arose from one of the central questions of twentieth-century physics: the precise relationship between classical and quantum mechanics [43]. Although the mathematical formalism of quantum theory was established in the 1920s through the work of Heisenberg [46], Schrödinger [48], Dirac [45], and others, the manner in which quantum mechanics should recover classical mechanics in an appropriate limit remained conceptually unclear.

A particularly illuminating insight was provided by Dirac in 1926. He observed that the algebraic structure of classical observables endowed with the Poisson bracket and that of quantum observables equipped with the commutator share the same fundamental properties, namely those of a Lie algebra. This structural analogy led him to propose the correspondence

$$\{f, g\}_{\text{Poisson}} \longleftrightarrow \frac{1}{i\hbar}[\hat{f}, \hat{g}]_{\text{commutator}}. \tag{1.11}$$

From this perspective, quantum mechanics may be viewed not as a radical departure from classical mechanics, but rather as a deformation controlled by Planck's constant $\hbar$. In the formal limit $\hbar \to 0$, the quantum theory is expected to reduce smoothly to classical mechanics, much as a family of geometric or algebraic structures continuously deforms into another.

This viewpoint also highlights the limitations of the traditional approach known as canonical quantization. In its simplest form, this procedure associates classical observables with operators on a Hilbert space, replaces Poisson brackets by commutators according to the correspondence principle, and promotes the canonical variables q and p to operators satisfying the first Eq:(1.6)

Despite its conceptual appeal, this approach encounters serious mathematical difficulties. One immediate issue is the ambiguity in operator ordering: a classical observable such as qp admits multiple inequivalent quantum realizations, including $\hat{q}\hat{p}$, $\hat{p}\hat{q}$, or the symmetrized combination $\frac{1}{2}(\hat{q}\hat{p} + \hat{p}\hat{q})$, with no canonical criterion for selecting one over the others.

A further obstruction arises from the nonlinearity of the quantization map. In general, the commutator does not act as a derivation in both arguments. For example, if $f = q^2$, one finds

$$[\hat{q}^2, \hat{p}] = 2i\hbar\hat{q}, \tag{1.12}$$

which accidentally coincide with the naive quantization of the classical expression $\{q^2, p\} = 2q$. But if we consider the classical observable $f = q^2 p$ quantized via the Weyl (symmetric) ordering:

$$f \longrightarrow \hat{f} = \frac{1}{2}\left(\hat{q}^2\hat{p} + \hat{p}\hat{q}^2\right). \tag{1.13}$$

Using the canonical commutation relation $[\hat{q}, \hat{p}] = i\hbar$, we compute:

$$\frac{1}{i\hbar}\left[\hat{f},\, \hat{q}\right] = \frac{1}{i\hbar} \cdot \left(-\frac{i\hbar}{2}\hat{q}^2\right) = -\frac{1}{2}\hat{q}^2, \tag{1.14}$$

whereas the naive quantization of the classical Poisson bracket gives:

$$\{q^2 p,\, q\} = -q^2 \quad \longrightarrow \quad -\hat{q}^2. \tag{1.15}$$

Similarly, for the second bracket:

$$\frac{1}{i\hbar}\left[\hat{f},\, \hat{p}\right] = \hat{q}\hat{p} + \hat{p}\hat{q} = 2\hat{q}\hat{p} - i\hbar, \tag{1.16}$$

while the classical correspondence predicts:

$$\{q^2 p,\, p\} = 2qp \quad \longrightarrow \quad 2\hat{q}\hat{p}. \tag{1.17}$$

In both cases, the quantum result differs from the classically expected one, explicitly revealing the ordering ambiguity inherent to canonical quantization.

The result depends explicitly on the chosen operator ordering, revealing an intrinsic limitation of canonical quantization and motivating the search for a more systematic deformation-based framework.

1.3 Deformation of Lie algebra

Let A be an algebra over a field $\mathbb{K}$, typically $\mathbb{R}$ or $\mathbb{C}$, endowed with an associative multiplication $\mu_0 : A \otimes A \to A$. A formal deformation of A is constructed by extending the multiplication to the space $A[[\hbar]]$ of formal power series in a parameter

$\hbar$, according to

$$\mu_\hbar(a,b) = \mu_0(a,b) + \sum_{n=1}^{\infty} \hbar^n \mu_n(a,b), \tag{1.18}$$

where each $\mu_n : A \otimes A \to A$ is a bilinear map. To preserve its algebraic structure, this deformed product $\mu_\hbar$ must remain associative. the order of evaluating a product of three or more elements affect the result. This requirement of associativity imposes the constraint

$$\mu_\hbar(\mu_\hbar(a,b),c) = \mu_\hbar(a,\mu_\hbar(b,c)), \qquad \forall\, a,b,c \in A[[\hbar]].$$

Expanding this order by order in $\hbar$, each coefficient μ_n must satisfy a compatibility condition involving all previous μ_k with $k < n$. At first order, this yields precisely the Hochschild cocycle condition:

$$\mu_0(a,\mu_1(b,c)) + \mu_1(a,\mu_0(b,c)) = \mu_0(\mu_1(a,b),c) + \mu_1(\mu_0(a,b),c).$$

The requirement that the deformed product $\mu_\hbar$ remain associative imposes a hierarchy of consistency conditions on the maps μ_n, ensuring that $(A[[\hbar]], \mu_\hbar)$ defines a well-posed algebraic structure. By construction, the original algebra is recovered in the classical limit $\hbar \to 0$.

The parameter $\hbar$ thus plays the role of a deformation variable measuring the departure from the initial algebraic structure. Although introduced here as a formal mathematical parameter, in many physical applications $\hbar$ is naturally identified with Planck's constant, thereby establishing a deep conceptual connection between algebraic deformation theory and the transition from classical to quantum descriptions.

Lie algebras, which encode infinitesimal symmetries of geometric and physical systems, provide a particularly important illustration of this general deformation framework. Let $(\mathfrak{g}, [\cdot,\cdot]_0)$ be a Lie algebra with bracket $[\cdot,\cdot]_0$. A deformation of $\mathfrak{g}$ consists of a family of brackets $[\cdot,\cdot]_\hbar$ that satisfy the Jacobi identity for all values of the deformation parameter. In the formal setting, this family may be written as

$$[X,Y]_\hbar = [X,Y]_0 + \sum_{n=1}^{\infty} \hbar^n C_n(X,Y), \tag{1.19}$$

where the maps $C_n : \mathfrak{g} \times \mathfrak{g} \to \mathfrak{g}$ are bilinear, and the deformed bracket is required to remain antisymmetric and to satisfy the Jacobi identity order by order in $\hbar$.

1.4 Quantization by deformation

Quantization by deformation, provides a rigorous mathematical framework that connects classical mechanics and quantum mechanics through the systematic deformation of algebraic structures. Rather than promoting classical observables to operators acting on a Hilbert space, this approach constructs a noncommutative associative product directly on the space of classical observables.

More precisely, given a smooth manifold M endowed with a Poisson bracket $\{\cdot,\cdot\}$, one introduces a deformed product—known as the star product—on the algebra $C^\infty(M)$ of smooth functions. This product is expressed as a formal power series in the deformation parameter $\hbar$,

$$f \star_\hbar g = fg + \sum_{n=1}^{\infty} \hbar^n B_n(f,g), \tag{1.20}$$

where each $B_n : C^\infty(M) \times C^\infty(M) \to C^\infty(M)$ is a bidifferential operator. The star product is required to be associative and to reproduce the Poisson bracket at first order in $\hbar$, in the sense that

$$\frac{1}{i\hbar}\big(f \star_\hbar g - g \star_\hbar f\big) = \{f,g\} + O(\hbar). \tag{1.21}$$

This condition ensures that the classical limit is recovered as $\hbar \to 0$.

A paradigmatic example is provided by the Moyal product on $\mathbb{R}^{2n}$ equipped with the canonical Poisson structure $\{q_i, p_j\} = \delta_{ij}$. In this case, the star product admits the explicit expression

$$(f \star_\hbar g)(q,p) = \exp\left[\frac{i\hbar}{2}\left(\overleftarrow{\partial}_{q_i}\overrightarrow{\partial}_{p_i} - \overleftarrow{\partial}_{p_i}\overrightarrow{\partial}_{q_i}\right)\right] f(q,p)\, g(q,p), \tag{1.22}$$

and serves as the prototypical example of a star product encoding the structure of standard quantum mechanics. A fundamental requirement of any deformation quantization scheme is the recovery of classical mechanics in the limit $\hbar \to 0$. This requirement is encoded in the correspondence principle, which states that the commutator of quantized observables, when divided by $i\hbar$, reduces to the Poisson bracket in the classical limit.

For a star product $\star_\hbar$, the classical limit is defined by

$$\{f,g\} = \lim_{\hbar\to 0} \frac{1}{i\hbar}\big(f \star_\hbar g - g \star_\hbar f\big). \tag{1.23}$$

This condition guarantees that the deformed algebraic structure admits the classical

Poisson manifold as its $\hbar \to 0$ reduction.

The existence of a well-defined classical limit plays a crucial role in establishing the physical consistency of deformed theories, ensuring that quantum corrections encoded by the deformation vanish smoothly as the classical regime is approached.

Chapter 2

Deformed Quantum Mechanics: Wigner-Dunkl deformation

In recent decades, the study of quantum systems has been enriched by the development of mathematical frameworks that extend beyond the conventional formalism of quantum mechanics. Among these approaches, the Dunkl formalism has attracted significant attention. Originally introduced in the context of harmonic analysis and special functions [41], Dunkl operators provide a natural generalization of differential operators by incorporating reflection symmetries. This structure introduces a deformation parameter that modifies the usual momentum operator, giving rise to non-trivial algebraic and analytical properties.

Instead of the usual derivative, one employs the Dunkl derivative, that combine ordinary derivative operator with reflection operators. This modification alters the momentum operator, leading to a generalized algebra of observables of the ordinary Heisemberg algbra. As a result, the transition from classical to quantum dynamics is no longer unique: the Dunkl framework provides a consistent but deformed version of quantization, where reflection symmetries and deformation parameters influence the physical behavior of the system.This modification leads to new physical effects such as altered energy spectra, generalized commutation relations, and the possibility of describing interactions that are not captured by the standard Heisenberg algebra.

In this chapter, we begin by recalling the usual correspondence that allows us to pass from classical to quantum mechanics. In the classical framework, the motion of a particle is described by Newton's laws or, more generally, through the Hamiltonian formalism, where observables are smooth functions of position and momentum. Moving to the quantum domain, the procedure of quantization replaces these observables with operators acting on a Hilbert space, and the Poisson brackets of classical mechanics are elevated to quantum commutation relations. Within this setting, the momentum operator acquires its well-known differential representation $\hat{p} = -i\hbar\frac{d}{dx}$; which generates translations and encodes the canonical commutation relation $[\hat{x}, \hat{p}] = i\hbar$ The second point concerns Wigner's investigation [49], where he addressed the question "Do the Equations of Motion Determine the Quantum Mechanical Commutation Relations?" and this by taking as example the classical harmonic oscillator. Subsequently, L. M. Yang [50] revisited this problem, extending the analysis by replacing the classical harmonic oscillator considered by Wigner with its quantum counterpart. In the following, we investigate the Dunkl deformed-algebra and its fundamental properties, including the Dunkl operator, given as a combination of the partial derivative and a linear combination of difference–differential operators. We then analyze its algebraic structure, emphasizing its non-commutative character and commutation relations with other operators. Furthermore, we illustrate the application of the Dunkl formalism in one-dimensional quantum mechanics, focusing on Dunkl derivatives, and refer to the work of Chung and Hassanabadi [10] for further illustrations.

2.1 The Classical–Quantum mechanic Correspondence

- **Classical Hamiltonian Formalism and Its Quantum Formulation**

  In classical mechanics, the Hamiltonian formalism provides a powerful framework for describing the dynamics of physical systems. A system consisting of N degrees of freedom is characterized by canonical coordinates (q_i, p_i), where q_i denotes generalized positions and p_i the conjugate momenta. The Hamiltonian $H(q_i, p_i, t)$ represents the total energy of the system, typically as the sum of potential and kinetic energies. The temporal evolution of any observable $F(q_i, p_i, t)$ is governed by Hamilton's equations and can also be expressed using the Poisson bracket:

$$\dot{q}_i = \{q_i, H\}, \tag{2.1}$$

$$\dot{p}_i = \{p_i, H\}, \tag{2.2}$$

  where

$$\{F, G\} = \sum_i \left(\frac{\partial F}{\partial q_i} \frac{\partial G}{\partial p_i} - \frac{\partial F}{\partial p_i} \frac{\partial G}{\partial q_i} \right). \tag{2.3}$$

  is the Lie-Poisson bracket already discussed.

  Adiscussed previously, the transition to quantum mechanics promotes classical observables to operators acting on a Hilbert space, and replaces Poisson brackets by commutators.

  The operators form a non-commutative algebra with analogous properties:linearity, antisymmetry, Jacobi identity and Leibniz rule.

  Thus, the algebraic structure of classical mechanics is preserved in quantum mechanics, albeit in a non-commutative form, providing a systematic bridge from classical trajectories to quantum evolution. The study of these operator algebras forms the backbone for understanding more advanced quantum structures, such as Dunkl operators and deformed algebras.

- **Heinsemberg formulation**

  Within the Heisenberg picture [46], the dynamical variables of the system, such as the position operator $\hat{q}(t)$ and the momentum operator $\hat{p}(t)$, explicitly depend on time, whereas the state vectors themselves remain constant. This representation shifts the dynamical content of quantum mechanics from the states to the operators. The time evolution of an arbitrary operator $\hat{A}(t)$, possibly with explicit time dependence, is determined by the Heisenberg equation of motion, which provides the quantum analogue of Hamilton's equations in classical mechanics:

$$\frac{d\hat{A}(t)}{dt} = \frac{1}{i\hbar}\left[\hat{A}(t), \hat{H}\right] + \frac{\partial \hat{A}(t)}{\partial t}. \tag{2.4}$$

  As an illustration, let us consider the time evolution of the fundamental operators $\hat{q}(t)$ and $\hat{p}(t)$. Applying the Heisenberg equation (2.4) to the position operator yields

$$\frac{d\hat{q}(t)}{dt} = \frac{1}{i\hbar}\left[\hat{q}(t), \hat{H}\right]. \tag{2.5}$$

  For the Hamiltonian of a particle in a potential,

$$\hat{H} = \frac{\hat{p}^2}{2m} + V(\hat{q}), \tag{2.6}$$

  this commutator gives

$$\frac{d\hat{q}(t)}{dt} = \frac{\hat{p}(t)}{m}. \tag{2.7}$$

  Similarly, for the momentum operator $\hat{p}(t)$ we obtain

$$\frac{d\hat{p}(t)}{dt} = \frac{1}{i\hbar}\left[\hat{p}(t), \hat{H}\right]. \tag{2.8}$$

  A straightforward calculation leads to

$$\frac{d\hat{p}(t)}{dt} = -\frac{\partial V(\hat{q})}{\partial \hat{q}}. \tag{2.9}$$

  Equations (2.7) and (2.9) represent the quantum-mechanical analogues of Hamilton's equations, showing the direct correspondence between the Heisenberg picture and classical dynamics.

  we see finally that the transition from classical to quantum mechanics is fundamentally based on the correspondence between Poisson brackets and commutators. Within the Heisenberg picture, this correspondence guarantees that

the structure of the classical equations of motion is preserved, while embedding the inherently non-commutative nature of quantum observables through the canonical commutation relations. Moreover, since the commutator $\frac{i}{\hbar}[\hat{A}, \hat{H}]$ plays the role of the time derivative of $\hat{A}$,see Eq (2.4), one may ask: is the sole requirement that quantum operators obey the same equations of motion as their classical counterparts sufficient to uniquely fix the commutation relations? In other words, rather than postulating the canonical commutation relations as an independent axiom, can they be derived from the dynamical structure alone?

This question will be examined in detail in the following section.

2.2 Beyond the standard Heisenberg Algebra

2.2.1 a-E.P.Wigner contribution

[49]

The first steps toward the concept of the deformed Heisenberg algebra were initiated by Wigner [49], who, in his study of the classical harmonic oscillator, show that the commutation relations between operators are not uniquely determined, but rather depend on the specific form of the Hamiltonian operator. Let us explain. As we know, in Heisenberg representation, the operators obey the classical differential equations:

$$\dot{q} = \frac{p}{m}, \qquad \dot{p} = -\frac{\partial V}{\partial x}. \tag{2.10}$$

but by assuming that the Hamiltonian of the system is given by

$$H = \frac{1}{2}\left(\frac{p^2}{m} + V(x)\right), \tag{2.11}$$

and Since, in the Heisenberg picture, the time evolution of operators is governed by their commutators with the Hamiltonian, we have:

$$\frac{i}{\hbar}[H, q] = \frac{p}{m}, \qquad \frac{i}{\hbar}[H, p] = -\frac{\partial V}{\partial q}. \tag{2.12}$$

However, these equations are usually derived from the Heisenberg–Born–Jordan relation,

$$[p, q] = -i\hbar, \tag{2.13}$$

from which we obtain

$$\frac{i}{\hbar}\left[\frac{p^2}{2m}, q\right] = \frac{p}{m}, \qquad \frac{i}{\hbar}[V, p] = -\frac{\partial V}{\partial x}. \tag{2.14}$$

Since Eqs. (2.10) and (2.12) possess a more immediate physical interpretation than Eq. (2.13), it is natural to ask whether, conversely, Eq. (2.13) can be derived from Eq. (2.12). Nevertheless, the fundamental status of relations of the type (2.12) is open to question, since the classical equations of motion are not, in general, satisfied by operator-valued observables in quantum theory.

Moreover, owing to the intrinsically non-commutative nature of the canonical operators p and q, the Hamiltonian operator is not uniquely defined. Different choices of operator ordering may lead to formally distinct Hamiltonians which are not, in general, unitarily equivalent. In particular, in the example discussed below, the Hamiltonian

$$H = 2(x + iv)(x - iv) \tag{2.15}$$

could equally well have been chosen instead of

$$H = \frac{1}{2}\left(x^2 + v^2\right), \tag{2.16}$$

a choice that would modify the resulting operator equations of motion and, consequently, alter the final physical conclusions.

The example to be considered is that of the harmonic oscillator, which is chosen for its simplicity. Since the aim of the preceding considerations is to avoid an explicit use of Hamiltonian theory, we express the energy of an oscillator of unit mass and classical frequency $\frac{1}{2\pi}$ in terms of the coordinate and the velocity, rather than in terms of coordinates and conjugate momenta. The energy is therefore written as

$$H = \frac{1}{2}\left(x^2 + v^2\right). \tag{2.17}$$

With this choice, the fundamental equations (2.12) reduce to

$$\dot{x} = i[H, x] = v, \qquad \dot{v} = i[H, v] = -x. \tag{2.18}$$

to solve the system (2.17) and (2.18), let assume that the Hamiltonian H is diagonal. Its diagonal elements, which are positive , will be denoted by $E_0, E_1, E_2, \ldots$. Let x_{mn} and v_{mn} denote the matrix elements of the operators x and v, respectively.

Equations (2.18) then yield, for the matrix elements,

$$v_{mn} = i(E_m - E_n)\, x_{mn}, \qquad -x_{mn} = i(E_m - E_n)\, v_{mn}, \tag{2.19}$$

Combining these two relations, one obtains

$$x_{mn} = (E_m - E_n)^2\, x_{mn}. \tag{2.20}$$

It follows that x_{mn} can be nonvanishing only if

$$(E_m - E_n)^2 = 1. \tag{2.21}$$

Moreover, the first Eq.of (2.18) implies that the matrix elements v_{mn} vanish whenever x_{mn} does. Consequently, the energy eigenvalues connected by a nonvanishing matrix element of either x or v must differ by one unit and therefore form an arithmetic progression,

$$E_n = E_0 + n. \tag{2.22}$$

Among the matrix elements x_{mn}, only those of the form $x_{n,n+1}$ and $x_{n+1,n}$ can be non-vanishing. The elements $x_{n,n+1}$ can be chosen to be real and positive by a suitable unitary transformation with a diagonal matrix. Due to the Hermitian nature of x, the elements $x_{n+1,n} = x_{n,n+1}$ are then real as well. The corresponding matrix elements of v are purely imaginary. Specifically, one has

$$v_{n,n+1} = -ix_{n,n+1} = -ix_{n+1,n}, \qquad v_{n+1,n} = ix_{n+1,n} = -v_{n,n+1}. \tag{2.23}$$

as follows from Eqs. (2.19) and (2.22).

So far, the elements $x_{01}, x_{12}, x_{23}, \ldots$ are arbitrary, and only Eq. (2.18) is satisfied. In order to fulfill Eq. (2.17), it is necessary to compute $\frac{1}{2}\left(x^2 + v^2\right)$. One observes that, as a consequence of the above structure, this combination is automatically diagonal. The diagonal element corresponding to energy E_n is

$$\frac{1}{2}\left(x^2 + v^2\right)_{nn} = E_n - E_0 + n = x_{n,n+1}^2 + x_{n-1,n}^2, \tag{2.24}$$

with the convention $x_{0,1}^2 = E_0$. This allows one to determine the elements $x_{n,n+1}$ recursively:

$$x_{n,n+1} = \begin{cases} \left(E_0 + \frac{1}{2}n\right)^{\frac{1}{2}}, & \text{for even } n, \\ \left(\frac{1}{2}n + \frac{1}{2}\right)^{\frac{1}{2}}, & \text{for odd } n. \end{cases} \tag{2.25}$$

The commutator $[v, x]$ is also automatically diagonal as a result of Eq (2.23), with diagonal elements

$$[v, x]_{nn} = -2i(x^2_{n,n+1} - x^2_{n-1,n}), \tag{2.26}$$

yielding, in the usual solution, $E_0 = \frac{1}{2}$ and therefore

$$[v, x] = -i, \tag{2.27}$$

in agreement with the canonical commutation relation. A more general solution can be written as

$$([v, x] - i)^2 = -(2E_0 - 1), \tag{2.28}$$

where E_0 is a constant characterizing the solution.

The analysis above highlights that the commutation relations between operators are not uniquely fixed, but rather depend on the choice of Hamiltonian and operator ordering, as initially observed by Wigner.

By expressing the harmonic oscillator in terms of position x and velocity v and assuming a diagonal Hamiltonian, the Heisenberg equations of motion constrain the matrix elements of x and v. Only the nearest-neighbor elements $x_{n,n+1}$ and $x_{n+1,n}$ are non-vanishing, forming a ladder structure.

Thus, this construction shows that the standard Heisenberg algebra is only a particular realization of a broader class of operator algebras, and the ladder structure of x and v provides a natural framework for introducing the deformed Heisenberg algebra.

2.2.2 b-L.M.Yang contribution

[50] The aim of the present study is to demonstrate, through a simple illustrative example, that the commutation relations—often postulated as fundamental axioms in quantum mechanics—are in fact not arbitrary. Their form can be systematically derived, provided one adopts a more rigorous definition of the Hilbert space and applies a precise expansion theorem.

The central question is whether the commutation relations can be derived from the classical equations of motion, supplemented by the postulate that the Hamiltonian generates time translations. That is, for any dynamical variable f of a given system, one assumes

$$\dot{f} = \frac{i}{\hbar}[H, f], \tag{2.29}$$

To investigate this question, we consider the specific case of a harmonic oscillator, for which the Hamiltonian is taken as

$$H = \frac{1}{2}\left(x^2 + \dot{x}^2\right), \tag{2.30}$$

where $\dot{x}$ denotes the time derivative of x, and natural units with $\hbar = \omega = 1$ are used. From the given Hamiltonian and the equation of motion

$$\ddot{x} + x = 0 \tag{2.31}$$

it follows that

$$\ddot{x} = [\dot{x}, H], \qquad \ddot{x}^2 = \frac{1}{2}\big([\dot{x}, x] + [x, \ddot{x}]\big).$$

Introducing

$$D = [x, \dot{x}] - 1, \tag{2.32}$$

one has

$$\{D, \ddot{x}\} = 0, \tag{2.33}$$

where the curly bracket is the anti-commutator. From (2.29) and (2.30) one has similarly

$$\{D, x\} = 0 \tag{2.34}$$

From (2.33) and (2.34), it can easily be shown that

$$[D^2, x] = [D^2, \dot{x}] = 0, \qquad [D, H] = 0, \tag{2.35}$$

which shows that D is a constant of motion, and that D^2 is a real numerical constant.

In the x-representation, (2.34) becomes

$$(x' + x'')\, X(x', x'')\, D(x', x'') = 0. \tag{2.36}$$

Hence it follows that

$$X(x', x'') = c(x')\, \delta(x' + x''), \tag{2.37}$$

where $c(x')$ is an arbitrary function of x'.

The hermitian property of D requires that

$$c(x') = c^*(-x'). \tag{2.38}$$

Hence in the x-representation one can write

$$D = c(x)\, R, \tag{2.39}$$

where R is the reflection operator defined by

$$R|x\rangle = |-x\rangle. \tag{2.40}$$

From this representation of D, one obtains the explicit operational form of $\dot{x}$:

$$\dot{x} = -\,i\,\frac{d}{dx} + f(x) + \frac{c(x)}{2x}\,R, \tag{2.41}$$

where $f(x)$ is a real function. It can be demonstrated that the term $f(x)$ can be eliminated by an appropriate choice of the phase factor in the x-representation. Denoting operators in the transformed representation by a star, one obtains:

$$\begin{gathered}\left(\frac{d}{dx}\right)^{*} = e^{-iy}\,\frac{d}{dx}\,e^{iy} = \frac{d}{dx} + i\,\frac{dy}{dx}, \\ R^{*} = e^{-iy}\,R\,e^{iy} = e^{-2iy_{-}}\,R.\end{gathered} \tag{2.42}$$

where y is a real function of x, and y_{-} is the odd part of y. If one chooses

$$y_{-} = \int f(x)\,dx, \tag{2.43}$$

equation (2.41) becomes

$$\dot{x} = -\,i\left(\frac{d}{dx}\right)^{*} + \frac{c^{*}(x)}{2x}\,R^{*}, \qquad c^{*}(x) = c(x)\,e^{2iy_{-}}. \tag{2.44}$$

Dropping the stars and the dash, and with the help of (2.33), one can show that $c(x)$ is a numerical constant, thus obtaining

$$\dot{x} = -\,i\,\frac{d}{dx} + \frac{c}{2x}\,R. \tag{2.45}$$

The explicit form of $\dot{x}$ derived above, featuring the reflection operator, naturally motivates the introduction of a generalized derivative operator. In this context, the Dunkl derivative provides a systematic extension of the conventional derivative by incorporating reflection symmetries. The following subsection presents its formal definition and illustrates how it generalizes standard differentiation, offering a broader framework for the operator structures encountered in the present analysis.

2.2.3 C.Dunkel contribution on the impulsion

[41]

As highlighted in the previous subsection, Dunkl significantly advanced the study of differential-difference operators by incorporating reflection symmetries, leading to a generalized derivative that extends the traditional partial derivative. We first recall some fundamental properties of reflections and the corresponding groups they form

We begin by recalling some fundamental facts about reflections and the groups they generate.

For a nonzero vector $v \in \mathbb{R}^N$, define the reflection $\theta_v \in O(N)$ (the orthogonal group) by

$$y\theta_v := y - 2\frac{\langle y, v\rangle}{|v|^2}v, \quad y \in \mathbb{R}^N, \tag{2.46}$$

where

$$\langle y, v\rangle := \sum_{i=1}^{N} y_i v_i \tag{2.47}$$

denotes the standard inner product and

$$|v|^2 := \langle v, v\rangle \tag{2.48}$$

is the squared norm. In particular,

$$v\theta_v = -v, \quad \text{and} \quad y\theta_v = y \text{ if and only if } \langle y, v\rangle = 0. \tag{2.49}$$

Any collection of such reflections generates a subgroup of $O(N)$, which is finite under suitable conditions. Such a group is referred to as a finite reflection group .

Now, suppose that G is a Coxeter group as shown in Appendix C with the set of reflections

$$\{\theta_j : 1 \le j \le m\}. \tag{2.50}$$

Let

$$\{v_j : 1 \le j \le m\} \subset \mathbb{R}^N \tag{2.51}$$

be vectors such that

$$\theta_j = \theta_{v_j} \quad \text{for each } j, \tag{2.52}$$

and assume

$$|v_i| = |v_j| \quad \text{whenever } \theta_i \sim \theta_j \text{ in } G \tag{2.53}$$

(i.e., θ_i is conjugate to θ_j), which implies

$$v_i = \pm v_j \tag{2.54}$$

for some element of G.

Next, choose positive parameters β_j such that

$$\beta_i = \beta_j \quad \text{whenever } \theta_i \sim \theta_j. \tag{2.55}$$

We then define the G-invariant function

$$l(y) := \prod_{j=1}^{m} |\langle y, v_j \rangle|^{\beta_j}, \tag{2.56}$$

where "l" is used as shorthand to denote the collection of the parameters v_j and β_j. Finally, let

$$B := \{y \in \mathbb{R}^N : |y| = 1\} \tag{2.57}$$

denote the unit sphere, by ∇ the gradient operator and by

$$\Delta := \sum_{i=1}^{N} \left(\frac{\partial}{\partial y_i} \right)^2 \tag{2.58}$$

the Laplacian on $\mathbb{R}^N$.

following these considerations, Dunkl defines the generalized Laplacian and gradient as follows

$$\Delta_l f(x) := \Delta f(x) + \sum_{j=1}^{m} \beta_j \left[\frac{2 \langle \nabla f(x), v_j \rangle}{\langle x, v_j \rangle} - |v_j|^2 \frac{f(x) - f(x\theta_j)}{\langle x, v_j \rangle^2} \right]. \tag{2.59}$$

$$\nabla_l f(x) := \nabla f(x) + \sum_{j=1}^{m} \beta_j \frac{f(x) - f(x\theta_j)}{\langle x, v_j \rangle} v_j. \tag{2.60}$$

Starting from the l-gradient (2.60)associated with a previously defined reflection group $O(N)$, one defines the Dunkl operator as the projection of ∇_l onto a direction $\xi \in \mathbb{R}^N$,

$$T_\xi f(x) = \langle \nabla_l f(x), \xi \rangle. \tag{2.61}$$

This leads to the general form of the Dunkl derivative

$$T_\xi f(x) = \partial_\xi f(x) + \sum_{v\in R_+} k(v)\,\frac{\langle v,\xi\rangle}{\langle v,x\rangle}\big(f(x) - f(\theta_v x)\big). \tag{2.62}$$

In one dimension, the Euclidean space reduces to $\mathbb{R}$ and the root system is given by

$$R = \{\pm 1\}, \tag{2.63}$$

corresponding to the Coxeter system of type A_1; the smallest nontrivial Coxeter group . The associated reflection group is the finite Coxeter group $G \simeq \mathbb{Z}_2$, generated by the single reflection

$$\nu(x) = -x. \tag{2.64}$$

Its action on functions is represented by the reflection operator $\hat{R}$, defined as

$$\hat{R} f(x) = f(-x), \qquad \hat{R}^2 = 1. \tag{2.65}$$

Choosing the set of positive roots as $R_+ = \{1\}$, the multiplicity function reduces to a single real parameter $k(1) = \theta$. The general definition of the l-gradient,

$$\nabla_l f(x) = \nabla f(x) + \sum_{v\in R_+} k(v)\,\frac{f(x) - f(\sigma_v x)}{\langle x,v\rangle}\,v, \tag{2.66}$$

simplifies considerably in this setting. Since the scalar product coincides with ordinary multiplication in one dimension, and $v = 1$, one obtains

$$\nabla_l f(x) = \frac{df}{dx} + \theta\,\frac{f(x) - f(-x)}{x}. \tag{2.67}$$

The Dunkl derivative is defined as the projection of the h-gradient along the unique spatial direction. Therefore, in one dimension, the Dunkl operator coincides directly with the h-gradient and takes the explicit form

$$Df(x) = \frac{df}{dx} + \frac{\theta}{x}\big(f(x) - f(-x)\big). \tag{2.68}$$

Introducing the reflection operator $\hat{R}$, this expression can be written compactly as

$$D = \frac{d}{dx} + \frac{\theta}{x}(1 - \hat{R}). \tag{2.69}$$

This operator interpolates between the ordinary derivative, recovered in the limit $\theta = 0$, and a purely reflection–induced finite–difference operator. The presence

of the factor $1/x$ reflects the scale invariance of the operator. Indeed, under the dilation $x \to \lambda x$, the derivative transforms as $\frac{d}{dx} \to \frac{1}{\lambda}\frac{d}{dx}$, while the term $\frac{1}{x}(1-\hat{R})$ transforms as $\frac{1}{\lambda x}(1-\hat{R})$. Both contributions therefore scale in the same way, leaving the structure of the operator unchanged.

The singular factor $1/x$ also signals the presence of a reflection hyperplane at the origin. In one dimension the reflection associated with the root system $R = \{\pm 1\}$ is $\sigma(x) = -x$, whose fixed point is $x = 0$. Hence the origin plays the role of the reflection hyperplane (which reduces to a single point in one dimension). The operator D is therefore the one–dimensional Dunkl derivative associated with the root system R.

For any dimension the most frequently used position representation is given by [41]

$$\hat{D}_j^{\theta} = \frac{\partial}{\partial x_j} + \frac{\theta_j}{x_j}\left(1 - \hat{R}_j\right). \tag{2.70}$$

where ν_j represents the Wigner(deformation) parameter and $\hat{R}_j$ the reflection operators that satisfy

$$\hat{R}_i\hat{R}_j = \hat{R}_j\hat{R}_i \qquad \hat{R}_j x_i = -\delta_{ij}\frac{\partial}{\partial x_j}\hat{R}_i \tag{2.71}$$

Here, we see that the reflection operator naturally leads to two distinct cases, depending on the parity of the function.

If f is an even function, it satisfies

$$f(-x) = f(x). \tag{2.72}$$

The action of the reflection operator $\hat{R}$ on f therefore leaves it invariant:

$$(\hat{R}f)(x) = f(-x) = f(x). \tag{2.73}$$

Thus, even functions are eigenfunction of the reflection operator with eigenvalue $+1$.

If f is an odd function, it satisfies

$$f(-x) = -f(x). \tag{2.74}$$

In this case, the action of the reflection operator yields

$$(\hat{R}f)(x) = f(-x) = -f(x). \tag{2.75}$$

Hence, odd functions are eigenfunction of the reflection operator with eigenvalue -1.

The reflection operator $\hat{R}$ induces a decomposition of the function space into even and odd subspaces, corresponding to its two eigenvalues ± 1. This decomposition is fundamental in the construction of one-dimensional Dunkl operators associated with the Coxeter system of type A_1.

2.3 Properties of the one-dimensional Dunkl operator

Let $\hat{D}_j$ denote the Dunkl operator associated with the j-th variable x_j:

$$\hat{D}_j f(x_j) = \frac{d}{dx_j} f(x_j) + \frac{\theta_j}{x_j} (1 - \hat{R}_j) f(x_j), \tag{2.76}$$

where $\hat{R}_j$ is the reflection operator: $(\hat{R}_j f)(x_j) = f(-x_j)$, and θ_j is the deformation parameter. we can easilly show that it satisffies the following proprities :

1. Linearity

For any functions $f(x_j)$, $g(x_j)$ and constants $a, b \in \mathbb{R}$, the Dunkl operator is linear:

$$\hat{D}_j\big(af(x_j) + bg(x_j)\big) = a\,\hat{D}_j f(x_j) + b\,\hat{D}_j g(x_j). \tag{2.77}$$

2. Modified Leibniz rule (product rule)

For the product of two functions $f(x_j)$ and $g(x_j)$, we have the modified Leibniz rule:

$$\hat{D}_j\big(f(x_j)g(x_j)\big) = (\hat{D}_j f(x_j))\, g(x_j) + f(x_j)\, (\hat{D}_j g(x_j)) - \frac{\theta_j}{x_j} (1-\hat{R}_j) f(x_j)\, (1-\hat{R}_j) g(x_j). \tag{2.78}$$

3. Chain rule

In general, the Dunkl derivative does not satisfy the usual chain rule:

$$\hat{D}_x f(u(x)) = \frac{df}{du}\,\frac{du}{dx} + \frac{\nu}{x}\Big(f(u(x)) - f(u(-x))\Big). \tag{2.79}$$

However, if $u(x)$ is an even function, $u(-x) = u(x)$, the standard chain rule is restored:

$$\hat{D}_x f(u(x)) = \frac{df}{du}\,\hat{D}_x u(x). \tag{2.80}$$

4. Square of the Dunkl operator

The square of $\hat{D}_j$ is given by

$$\hat{D}_j^2 f(x_j) = \frac{d^2}{dx_j^2} f(x_j) + \frac{2\theta_j}{x_j} \frac{d}{dx_j} f(x_j) - \frac{\theta_j}{x_j^2} \big(f(x_j) - f(-x_j)\big). \tag{2.81}$$

These properties reduce to the usual derivative properties when $\theta_j = 0$. The reflection operator $\hat{R}_j$ introduces a nonlocal correction, which modifies the Leibniz rule and the square form.

Having discussed mathematical properties, it is natural to turn to their physical implications. In the following section, we explore how this deformed differential structure can be consistently embedded into the formalism of quantum mechanics.

2.4 Quantum Mechanics in the Wigner–Dunkl Framework

In this subsection, we present a formulation of quantum mechanics within the Wigner–Dunkl framework, which combines the phase-space approach introduced by Wigner with the use of Dunkl operators. This construction provides a natural generalization of standard quantum mechanics by incorporating reflection symmetries and deformation parameters through Dunkl derivatives. Such a framework allows one to describe quantum systems with nonlocal and parity-dependent interactions in a systematic way. The present approach follows and extends the ideas developed in [10].

In Wigner–Dunkl quantum mechanics, the momentum operator is defined in terms of the Dunkl derivative rather than the ordinary derivative. In the coordinate representation, the fundamental operators are given by

$$\hat{p} = \frac{1}{i} \hat{D}_x, \qquad \hat{x} = x, \tag{2.82}$$

where we have set $\hbar = 1$. The Dunkl derivative is defined as

$$\hat{D}_x = \hat{\partial}_x + \frac{\theta}{x}(1 - \hat{R}), \tag{2.83}$$

with $\hat{R}$ the reflection operator. The reflection operator can be expressed in a convenient form using the dilation generator $x\partial_x$. Indeed, $x\partial_x$ generates scale transformations according to

$$e^{ax\partial_x} f(x) = f(e^a x), \tag{2.84}$$

where a is a complex parameter. Since reflection corresponds to $x \mapsto -x$, and $-1 = e^{i\pi}$, choosing $a = i\pi$ yields

$$e^{i\pi x\partial_x} f(x) = f(-x), \tag{2.85}$$

which coincides exactly with the action of the reflection operator. Hence, one can write

$$\hat{R} = e^{i\pi x\partial_x} = (-1)^{x\partial_x}. \tag{2.86}$$

This representation is consistent with the action of $\hat{R}$ on monomials: for $f(x) = x^n$,

$$x\partial_x x^n = nx^n, \qquad \hat{R}x^n = (-1)^n x^n = (-x)^n.$$

The parameter θ, known as the Wigner parameter, is restricted to $\theta > -\frac{1}{2}$, as will see later.

With this in hand , we can check that for an arbitrary function $f(x)$, we find

$$\begin{aligned}[\hat{x}, \hat{p}]f(x) &= x\left(\frac{1}{i}\hat{D}_x f(x)\right) - \frac{1}{i}\hat{D}_x\big(xf(x)\big) \\ &= i\big(1 + 2\theta\hat{R}\big)f(x),\end{aligned} \tag{2.87}$$

which yields the commutation relation

$$[\hat{x}, \hat{p}] = i\big(1 + 2\theta\hat{R}\big). \tag{2.88}$$

Thus, we see that in the Wigner -Dunkl formalism the Heisemberg algebra is non-locally modified Now, we explicitly apply the Dunkl operator to elementary polynomial functions, and in particular to monomials, in order to elucidate the fundamental mechanisms induced by this generalized differential operator. The action of the Dunkl operator on a monomial provides a transparent illustration of how reflection symmetries and deformation terms enter the calculus at a basic level.

Acting on the monomial x^n, the Dunkl derivative gives

$$\hat{D}_x x^n = [n]_\theta x^{n-1}, \tag{2.89}$$

where the θ-deformed number is defined by

$$[n]_\theta = n + \theta\big(1 - (-1)^n\big). \tag{2.90}$$

The first few θ-deformed numbers are

$$[0]_\theta = 0, \qquad [1]_\theta = 1 + 2\theta, \qquad [2]_\theta = 2, \qquad [3]_\theta \quad = 3 + 2\theta, \qquad [4]_\theta = 4, \quad (2.91)$$

and, in general,

$$[2k]_\theta = 2k, \qquad [2k+1]_\theta = 2k + 1 + 2\theta, \quad k = 0, 1, 2, \ldots \quad (2.92)$$

All θ-deformed numbers are non-negative provided $\theta > -\frac{1}{2}$.

From these results, it follows that the Dunkl derivative reduces to the ordinary derivative ∂_x when acting on even functions, while for odd functions it behaves as

$$\hat{D_x} = \hat{\partial}_x + \frac{2\theta}{x}. \quad (2.93)$$

Within the Wigner–Dunkl formalism, the time evolution of a quantum state is governed by the time-dependent Schrödinger equation

$$i\frac{\partial}{\partial t}\psi(x,t) = \hat{H}(\hat{x},\hat{p})\psi(x,t) = \left(\frac{\hat{p}^2}{2m} + \hat{V}(\hat{x})\right)\psi(x,t) \quad (2.94)$$

where $\hat{p} = \hat{D}_x/i$ Replacing $\hat{p}^2$ by equation (2.81), we find the time-dependent Dunkl-Schrödinger equation

$$i\frac{\partial}{\partial t}\Psi(x,t) = \left[-\frac{1}{2m}\frac{\partial^2}{\partial x^2} + \frac{2\theta}{x}\frac{\partial}{\partial x} - \frac{\theta}{x^2}\left(1 - \hat{R}\right) - V(x)\right]\Psi(x,t)\,. \quad (2.95)$$

Upon defining the weighted inner product

$$\langle f|g\rangle = \int_{-\infty}^{\infty} g^*(x) f(x)\,|x|^{2\theta}\,dx, \quad (2.96)$$

on e immediately obtain

$$\int_{-\infty}^{\infty} |x|^{2\theta}\,\hat{D}_x f(x)\,dx = 0, \quad (2.97)$$

For an odd function $f(x) = -f(-x)$, one has $(1 - \hat{R})f = 2f$, and the Dunkl derivative takes the form

$$\hat{D}_x f(x) = \partial_x f(x) + \frac{2\theta}{x} f(x). \quad (2.98)$$

Assuming the boundary condition

$$\lim_{x\to\pm\infty} x^{2\theta} f(x) = 0, \qquad \theta > 0, \tag{2.99}$$

an integration by parts shows that

$$\int_{-\infty}^{\infty} |x|^{2\theta}\, \hat{D}_x f(x)\, dx = 0. \tag{2.100}$$

For both even and odd admissible functions. The integral of the Dunkl-derivative vanishes with respect to the weighted measure. Moreover, assuming the boundary condition

$$\lim_{x\to\pm\infty} |x|^{2\theta} \big(\psi^* \hat{D}_x \psi - \psi \hat{D}_x \psi^*\big) = 0$$

The norm $\int_{-\infty}^{\infty} |\psi(x,t)|^2 |x|^{2\theta} dx$ is conserved in time, allowing for a consistent normalization of the wave function.

Having established the basic properties of the Dunkl derivative, the associated weighted Hilbert space, and the hermiticity of the momentum operator, we are now in a position to investigate concrete quantum–mechanical systems within the Wigner–Dunkl framework.

In the following subsection, we apply the formalism to two paradigmatic one–dimensional models: the particle confined in a box and the harmonic oscillator. These systems provide a natural testing ground for the Dunkl deformation, as they allow one to analyze explicitly the effects of reflection symmetry and the parameter θ on the energy spectrum and the structure of the eigenfunctions. Moreover, they illustrate how the modified kinetic operator $\hat{D}_x^2$ and the weighted inner product enter consistently into the formulation and solution of the corresponding Schrödinger equations.

2.4.1 Illustrations

- **a) Particle in a box**.

  Let us consider a spinless particle with mass m confined in a one-dimensional potential given by

$$V(x) = \begin{cases} 0, & -L < x < L, \\ \infty, & \text{otherwise.} \end{cases} \tag{2.101}$$

  In the position representation, the time-independent Schrödinger equation for a particle in a box is given by:

$$-\frac{1}{2m}\left(\frac{\partial^2}{\partial x^2}+\frac{2\theta}{x}\frac{\partial}{\partial x}-\frac{\theta}{x^2}(1-\hat{R})\right)\psi(x)=E\psi(x). \tag{2.102}$$

according to the parity of the solution the equation (2.102) can be divided into two equations. Let us denote the even parity solution by ψ_+:

$$-\frac{1}{2m}\left(\frac{\partial^2}{\partial x^2}+\frac{2\theta}{x}\frac{\partial}{\partial x}\right)\psi_+=E_+\psi_+. \tag{2.103}$$

Assuming the following formal series for :

$$\psi_+^{(\lambda)}(x)=\sum_{n=0}^{\infty}a_n^+x^{2n}|x|^{\lambda}. \tag{2.104}$$

We obtain:

$$\sum_{n=0}^{\infty}a_n(2n+\lambda)(2n+\lambda-1+2\nu)x^{2n+\lambda-2}=-2mE_+\sum_{n=0}^{\infty}a_nx^{2n+\lambda}. \tag{2.105}$$

Solving for a_n leads to the recurrence relation

$$a_n=\frac{2mE_+}{(2n+\lambda)(2n-1+\lambda+2\theta)}a_{n-1}. \tag{2.106}$$

The recurrence relation obtained for the coefficients determines the whole series in terms of the initial coefficient a_0. Iterating this relation shows that the coefficients possess the general structure of products of rising factorials. Consequently, the Frobenius series solution

$$\psi(x)=\sum_{n=0}^{\infty}a_nx^{2n+\lambda} \tag{2.107}$$

can be written in a form that matches the standard power-series representation of the confluent hypergeometric function ${}_0F_1$, defined by

$${}_0F_1(b;x)=\sum_{n=0}^{\infty}\frac{x^n}{(b)_n\,n!}, \tag{2.108}$$

where $(b)_n$ denotes the Pochhammer symbol(the detail is presented in Appendix-A. Therefore, the solution obtained from the Frobenius expansion can be expressed compactly in terms of the hypergeometric function ${}_0F_1$.

By rearranging the terms according to the powers of x, the characteristic equation at order x^{-2} is

$$\lambda(\lambda - 1 + 2\theta) = 0. \tag{2.109}$$

For $\lambda = 0$, the solution is given by the confluent hypergeometric function

$$\psi_+^{\lambda=0} = {}_0F_1\left(;\, \frac{1}{2} + \theta;\, -\frac{mE_+x^2}{2}\right). \tag{2.110}$$

For $\lambda = 1 - 2\theta$, one finds

$$\psi_+^{1-2\theta} = |x|^{1-2\theta}\, {}_0F_1\left(;\, \frac{3}{2} - \theta;\, -\frac{mE_+x^2}{2}\right). \tag{2.111}$$

In the limit $\theta \to 0$, Eq. (2.110) reduces to the standard even-parity solution

$$\psi_+ \longrightarrow \cos\left(\sqrt{2mE_+}\, x\right). \tag{2.112}$$

And the solution $\psi_+^{1-2\theta}$ of equation (2.111) that lead in the limit $\theta \to 0$,to

$$|x|^{1/2} \sin\left(\sqrt{2mE_+}\, x\right) \tag{2.113}$$

is discarded since it's doesn't reproduce the standard even free particle solution $\cos\left(\sqrt{2mE_+}\, x\right)$.

Using the relation

$$J_n(x) = \frac{1}{n!}\left(\frac{x}{2}\right)^n {}_0F_1\left(n+1;\, -\frac{x^2}{4}\right), \tag{2.114}$$

between Bessel functions J_n and ${}_0F_1$, Eq.(2.110) can be written as:

$$\psi_+^{\lambda=0} = N_+\, x^{\frac{1}{2}-\theta} J_{\theta-\frac{1}{2}}\left(\sqrt{2mE_+}\, x\right), \tag{2.115}$$

where

$$N_+ = \frac{\Gamma\left(\theta - \frac{1}{2}\right)}{2}\left(2mE_+\right)^{\frac{\theta-1/2}{2}} \tag{2.116}$$

is the normalization constant.

The boundary condition $\psi_+(\pm L) = 0$ leads to

$$J_{\theta-\frac{1}{2}}\left(\sqrt{2mE_+}\, L\right) = 0. \tag{2.117}$$

Hence, the energy spectrum is

$$E_n^+ = \frac{1}{2mL^2}\,\alpha^2_{\theta-\frac{1}{2},n}, \qquad n = 1, 2, \ldots \tag{2.118}$$

where $\alpha_{\theta-\frac{1}{2},n}$ is the n-th zero of $J_{\theta-\frac{1}{2}}$.

Next, let us consider the case of the odd functions, denoted by ψ^-, which satisfy the equation

$$-\frac{1}{2m}[\partial^2 + \frac{2\theta}{x}\partial - \frac{2\theta}{x^2}]\psi^- = E_-\psi_-. \tag{2.119}$$

We can transform the solution (2.104) for the odd case as follows:

$$\psi_-^\lambda = \sum_{n=0}^{\infty} a_n^- x^{2n+1}|x|^\lambda. \tag{2.120}$$

By substituting equation (2.120) into equation (2.119) and solving, we obtain the charac teristic equation:

$$\lambda(\lambda + 2\theta + 1) = 0. \tag{2.121}$$

The recurrence relation for the odd case is given by:

$$a_n^- = -\frac{2mE^-}{(2n+\lambda)(2n+1+\lambda+2\theta)}a_{n-1}^-. \tag{2.122}$$

We now write all the terms as a function of a_0. We find for $\lambda = 0$

$$\psi_-^{\lambda=0} = x\,{}_0F_1\left(;\frac{3}{2}+\theta;-\frac{mE^-x^2}{2}\right). \tag{2.123}$$

For $\lambda = 1 - 2\theta$ we have

$$\psi_-^{\lambda=-1-2\theta} = |x|^{-1-2\theta}x\,{}_0F_1\left(;\frac{1}{2}-\theta;-mE^-x^2\right). \tag{2.124}$$

For the case of $\theta = 0$ we have the odd parity solution

$$\psi_- \to \sin\sqrt{2mE^-}\,x. \tag{2.125}$$

We discard the solution $\psi^-_{\lambda=-1-\theta}$ since it leads to

$$\frac{|x|}{x}\cos\sqrt{2mE^-}\,x \tag{2.126}$$

in the limit $\theta \to 0$. In terms of the Bessel function, equation (2.123) can be written as

$$\psi_- = N_- x^{\frac{1}{2}-\theta} J_{\frac{1}{2}+\theta}\left(\sqrt{2mE^-}\, x\right), \tag{2.127}$$

where

$$\frac{\left(\theta-\frac{1}{2}\right)!}{\frac{1}{2}\sqrt{\left(2mE^-\right)^{\theta-\frac{1}{2}}}} \tag{2.128}$$

is the normalization constant. The boundary condition $\psi^-(\pm L) = 0$ determines the energy levels for this case

$$\begin{cases} J_{\theta+\frac{1}{2}}\left(\sqrt{2mE^+}\, L\right) = 0 \\ J_{\theta+\frac{1}{2}}\left(-\sqrt{2mE^+}\, L\right) = 0 \end{cases} \tag{2.129}$$

Solving this condition leads to the relationship

$$\sum_{n=0}^{\infty} \frac{\left(\sqrt{2mE^-}\, L\right)^n}{n!} = 0. \tag{2.130}$$

After some manipulation, we obtain the energy levels as

$$E_n^- = \frac{1}{2mL^2}\alpha^2_{\theta+\frac{1}{2},n}, \quad n = 1, 2, \ldots \tag{2.131}$$

where $\alpha_{\theta+\frac{1}{2},n}$ is an-th zeros of $J_{\theta+\frac{1}{2}}$.

- **b) Harmonic oscillator**

Let us consider the one-dimensional harmonic oscillator problem with reflection symmetry. The Schrödinger equation is written as

$$-\frac{1}{2m}D_x^2\psi + \frac{1}{2}m\omega^2 x^2\psi = E\psi. \tag{2.132}$$

By introducing the dimensionless variable $\zeta = \sqrt{m\omega}\, x$, the equation becomes

$$-D_\zeta^2\psi + \zeta^2\psi = \epsilon\psi. \tag{2.133}$$

where

$$\epsilon = \frac{2E}{\omega}$$

Assuming a solution of the form $\psi(\xi) = e^{-\zeta^2/2}y(\zeta)$, we obtain

$$D_\zeta^2 y - D_\zeta(\zeta y) - \zeta D_\zeta y + y = 0, \tag{2.134}$$

which can be rewritten as

$$D_\zeta^2 y - 2\zeta D_\zeta(-1 - 2\theta R)y = 0. \tag{2.135}$$

This is an Hermite differential equation,wich can be solved by the Frobenius method [51,52] , which consists of taking a power series Ansatz and we will find that the solutions behaves differently according to the parity of the function

- Even Solution

  For the even solution, we set

$$y = \sum_{k=0}^{\infty} a_n \zeta^{2k}. \tag{2.136}$$

  Substituting this into Eq. (2.135) gives the recurrence relation

$$a_{n+1} = \frac{2[2n]_\theta + 1 + 2\theta - \epsilon_+}{[2n+2]_\theta[2n+1]_\theta} a_n. \tag{2.137}$$

  Requiring that the series terminate yields

$$(\epsilon_+)_N = 2[2N]_\theta + 1 + 2\theta, \quad N = 0, 1, 2, \ldots. \tag{2.138}$$

  Thus, the energy levels for the even solutions are

$$E_N^+ = \frac{\omega}{2}(2[2N]_\theta + 1 + 2\theta). \tag{2.139}$$

  The polynomial solution has the recurrence

$$a_{n+1} = \frac{2([2n]_\theta - [2N]_\theta)}{[2n+2]_\theta[2n+1]_\theta} a_n. \tag{2.140}$$

  We denote the corresponding polynomial by H_N^+, and the first few polynomials are

$$
\begin{aligned}
H_0^+(x) &= 1, \\
H_1^+(x) &= 1 - \frac{2}{[1]_\theta}x^2, \\
H_2^+(x) &= 1 - \frac{2[4]_\theta}{[2]_\theta!}x^2 + \frac{2([4]_\theta([4]_\theta - [2]_\theta))}{[4]_\theta!}x^4
\end{aligned}
\tag{2.141}
$$

- Odd Solution

  For the odd solution, we set

$$
y = \sum_{n=0}^{\infty} b_n \, \xi^{2k+1}. \tag{2.142}
$$

  Substituting into Eq. (2.135) gives the recurrence

$$
b_{n+1} = \frac{2[2n+1]_\theta + 1 - 2\theta}{[2n+3]_\theta[2n+2]_\theta} b_n. \tag{2.143}
$$

  The termination condition is

$$
(\epsilon_-)_N = 2[2N+1]_\theta + 1 - 2\theta, \quad N = 0, 1, 2, \ldots \tag{2.144}
$$

  Hence, the energy levels for the odd solutions are

$$
E_N^- = \frac{\omega}{2}(2[2N+1]_\theta + 1 - 2\theta). \tag{2.145}
$$

  The corresponding polynomial solution has the recurrence

$$
b_{n+1} = \frac{2([2n+1]_\theta - [2N+1]_\theta)}{[2n+3]_\theta[2n+2]_\theta} b_n. \tag{2.146}
$$

  We denote the polynomial by H_N^-, and the first few polynomials are

$$
\begin{aligned}
H_0^-(x) &= x, \\
H_1^-(x) &= x - \frac{2([3]_\theta - [1]_\theta)}{[3]_\theta!}x^3, \\
H_2^-(x) &= x - \frac{2([5]_\theta - [1]_\theta)}{[3]_\theta!}x^3 + \frac{2([5]_\theta - [3]_\theta)([5]_\theta - [1]_\theta)}{[5]_\theta!}x^5
\end{aligned}
\tag{2.147}
$$

  The two forms of the solution can be combined and represented in a single, unified expression:

$$\psi_M(\xi) = e^{-\xi^2/2} H_M^\theta(\xi), \quad M = 0, 1, 2, \dots \tag{2.148}$$

with

$$H_M^\theta(\xi) = \begin{cases} H^+_{M/2}(\xi), & M \text{ even}, \\ H^-_{(M-1)/2}(\xi), & M \text{ odd}, \end{cases} \qquad E_M = \frac{\omega}{2}([M]_\theta + [M+1]_\theta). \tag{2.149}$$

2.4.2 Operator Method for Harmonic oscillator

An alternative and elegant approach to solving the Dunkl-deformed harmonic oscillator is the operator method, which generalizes the standard creation and annihilation operators of the harmonic oscillator to include the Dunkl derivative. By defining suitable step operators, one can construct the Hamiltonian in a factorized form and derive the energy spectrum algebraically. This method also naturally introduces the number operator and Fock space structure, allowing for a systematic construction of all eigenstates.

Upon defining the step operators (recall that $\hbar = 1$:

$$a = \sqrt{\frac{m\omega}{2}} x + \frac{1}{\sqrt{2m\omega}} D_x, \quad a^\dagger = \sqrt{\frac{m\omega}{2}} x - \frac{1}{\sqrt{2m\omega}} D_x. \tag{2.150}$$

wich satisfy the commutation relations

$$[a, a^\dagger] = 1 + 2\theta \hat{R}, \qquad [a, a] = 0, \qquad [a^\dagger, a^\dagger] = 0. \tag{2.151}$$

The Hamiltonian writes

$$H = \frac{\omega}{2} \left(2a^+ a + 1 + 2\theta R \right) \tag{2.152}$$

Introducing the number operator N such that $[N, a^\dagger] = a^\dagger$ and $[N, a] = -a$, we have

$$a^\dagger a = [N]_\theta, \quad a a^\dagger = [N+1]_\theta, \tag{2.153}$$

and the Fock space is defined as

$$N|n\rangle = n|n\rangle, \quad n = 0, 1, 2, \dots \tag{2.154}$$

Finally, the energy levels are

$$E_n = \frac{\omega}{2}([n]_\theta + [n+1]_\theta), \quad n = 0, 1, 2, \dots, \tag{2.155}$$

In summary, the harmonic oscillator problem involving Dunkl derivatives can be solved using two equivalent approaches: a direct method based on polynomial series expansions, and an operator formalism constructed from generalized creation and annihilation operators. Both approaches lead to the same energy spectrum, as given in Eqs. (2.149) and (2.155), and yield eigenfunctions expressed in terms of the generalized polynomial functions $H_M^{\theta}(\xi)$, which naturally distinguish between even and odd states. However, despite their equivalence, these two methods and their underlying expressions do not explicitly reveal the new interaction terms that emerge from the Dunkl formalism. Indeed, The Hamiltonian written in terms of the Dunkl number operator $\hat{N}_\theta = \hat{a}_\theta^\dagger \hat{a}_\theta$ becomes:

$$\hat{H} = \hbar\omega \left(\hat{N} + \frac{1}{2} + \theta \hat{R} \right), \tag{2.156}$$

where the term $\theta\hat{R}$ is entirely new and has no counterpart in the standard harmonic oscillator. Expressing $\hat{H}$ back in terms of the original undeformed operators $\hat{x}$, $\hat{p}$, and $\hat{R}$:

$$\hat{H}_\theta = \underbrace{\frac{\hat{p}^2}{2m} + \frac{1}{2} m\omega^2 \hat{x}^2}_{\hat{H}_{\text{standard}}} + \underbrace{\frac{\hbar^2\theta}{m} \frac{1}{\hat{x}^2} \left(\theta + \hat{R} \right)}_{\text{interaction terms}}, \tag{2.157}$$

revealing two new interaction terms absent from the original Hamiltonian. The first is a centrifugal-like inverse-square potential:

$$V_1 = \frac{\hbar^2\theta^2}{m\hat{x}^2}, \tag{2.158}$$

which introduces a singular repulsive barrier at the origin. The second is a parity-dependent interaction:

$$V_2 = \frac{\hbar^2\theta}{m} \frac{\hat{R}}{\hat{x}^2}, \tag{2.159}$$

which couples the spatial dynamics to the discrete parity symmetry through $\hat{P}$. It acts with opposite signs on even and odd states:

$$V_2 \, \psi_\pm = \pm \frac{\hbar^2\theta}{m\hat{x}^2} \, \psi_\pm, \tag{2.160}$$

thereby lifting the parity degeneracy present in the standard harmonic oscillator. This is the key advantage of the Dunkl formalism: interactions emerge naturally from the deformation.

Chapter 3

Bose–Einstein Condensation of an ideal Bose gas

3.1 Introduction

The theoretical framework for describing BEC rests upon the principles of quantum statistical mechanics, particularly the treatment of indistinguishable particles. Unlike classical particles, which retain their individual identities, quantum particles of the same species are fundamentally indistinguishable. This indistinguishability, combined with the symmetry properties of the quantum mechanical wave function, leads to profoundly different statistical behaviors for bosons and fermions. Bosons, characterized by integer spin and symmetric wave functions, are not subject to the Pauli exclusion principle and can therefore accumulate in the same quantum state without restriction. This unrestricted occupation is the key feature that enables Bose–Einstein condensation.

In this chapter, we develop a rigorous treatment of Bose–Einstein condensation from first principles using the grand canonical ensemble formalism. We derive the Bose–Einstein distribution function, analyze the conditions for condensation, calculate the critical temperature, and explore the physical implications of this remarkable quantum phase transition.

This is a standard textbook traitement and is introduce here to make this document self-contained

3.1.1 The Continuum Limit and Density of States

For a macroscopic system in a container of volume V, the single-particle energy levels form a quasi-continuum. For free particles in a three-dimensional box with

periodic boundary conditions, the allowed wave vectors are

$$\mathbf{k} = \frac{2\pi}{L}(n_x, n_y, n_z), \quad n_x, n_y, n_z \in \mathbb{Z}, \tag{3.1}$$

where $L = V^{1/3}$ is the linear dimension of the box. The energy of a free particle is

$$\epsilon(\mathbf{k}) = \frac{\hbar^2 k^2}{2m}, \tag{3.2}$$

where m is the particle mass.

In the thermodynamic limit, we convert sums over discrete states to integrals using the density of states. The number of states in a volume element d^3k in $\mathbf{k}$-space is

$$\frac{V}{(2\pi)^3} d^3k. \tag{3.3}$$

In spherical coordinates, $d^3k = 4\pi k^2 dk$, so the density of states as a function of wave vector magnitude is

$$\rho(k)dk = \frac{V}{(2\pi)^3} 4\pi k^2 dk = \frac{V k^2}{2\pi^2} dk. \tag{3.4}$$

yielding

$$\rho(\epsilon)d\epsilon = \frac{V}{2\pi^2} \left(\frac{2m}{\hbar^2}\right)^{3/2} \sqrt{\epsilon}\, d\epsilon. \tag{3.5}$$

Therefore, the density of states for free particles in three dimensions is

$$\rho(\epsilon) = \frac{V}{2\pi^2} \left(\frac{2m}{\hbar^2}\right)^{3/2} \sqrt{\epsilon} = CV\sqrt{\epsilon}, \tag{3.6}$$

where $C = (2m)^{3/2}/(2\pi^2\hbar^3)$.

3.1.2 Particle Number in Excited States

The total number of particles can now be written as

$$N = N_0 + N_{\text{ex}}, \tag{3.7}$$

where N_0 is the number of particles in the ground state ($\epsilon = 0$) and N_{ex} is the number in excited states. For excited states, we convert the sum to an integral:

$$N_{\text{ex}} = \int_0^\infty \frac{\rho(\epsilon)}{e^{\beta(\epsilon-\mu)} - 1} d\epsilon = \int_0^\infty \frac{CV\sqrt{\epsilon}}{e^{\beta(\epsilon-\mu)} - 1} d\epsilon. \tag{3.8}$$

Therefore:

$$N_{\text{ex}} = CV\left(\frac{1}{\beta}\right)^{3/2}\frac{\sqrt{\pi}}{2}\sum_{n=1}^{\infty}\frac{z^n}{n^{3/2}} = V\left(\frac{mk_BT}{2\pi\hbar^2}\right)^{3/2}g_{3/2}(z), \tag{3.9}$$

where we have defined the Bose function as shown in Appendix B

$$g_\nu(z) = \frac{1}{\Gamma(\nu)}\sum_{n=1}^{\infty}\frac{z^n}{n^\nu}. \tag{3.10}$$

For $\nu = 3/2$:

$$g_{3/2}(z) = \sum_{n=1}^{\infty}\frac{z^n}{n^{3/2}}. \tag{3.11}$$

It is convenient to define the thermal de Broglie wavelength:

$$\lambda_T = \sqrt{\frac{2\pi\hbar^2}{mk_BT}}, \tag{3.12}$$

which represents the typical wavelength of a particle at temperature T. In terms of λ_T:

$$N_{\text{ex}} = \frac{V}{\lambda_T^3}g_{3/2}(z). \tag{3.13}$$

3.1.3 The Critical Temperature for Condensation

The crucial observation is that $g_{3/2}(z)$ is a monotonically increasing function of z for $0 < z < 1$, and it reaches its maximum value at $z = 1$:

$$g_{3/2}(1) = \sum_{n=1}^{\infty}\frac{1}{n^{3/2}} = \zeta(3/2) \approx 2.612, \tag{3.14}$$

where ζ is the Riemann zeta function.

Since N_{ex} cannot exceed the total number of particles N, and since $g_{3/2}(z)$ has a maximum value, there is a maximum number of particles that can occupy excited states at a given temperature:

$$N_{\text{ex}}^{\max} = \frac{V}{\lambda_T^3}\zeta(3/2). \tag{3.15}$$

When $N > N_{\text{ex}}^{\max}$, the "excess" particles must occupy the ground state. This occurs below a critical temperature T_c defined by the condition $N = N_{\text{ex}}^{\max}$ with

$\mu = 0$ (corresponding to $z = 1$):

$$N = \frac{V}{\lambda_{T_c}^3}\zeta(3/2). \tag{3.16}$$

Solving for T_c:

$$\lambda_{T_c}^3 = \frac{V\zeta(3/2)}{N}, \tag{3.17}$$

$$\frac{2\pi\hbar^2}{mk_BT_c} = \left(\frac{V\zeta(3/2)}{N}\right)^{2/3}, \tag{3.18}$$

$$T_c = \frac{2\pi\hbar^2}{mk_B}\left(\frac{N}{V\zeta(3/2)}\right)^{2/3}. \tag{3.19}$$

Defining the particle density $n = N/V$:

$$T_c = \frac{2\pi\hbar^2}{mk_B}\left(\frac{n}{\zeta(3/2)}\right)^{2/3} \approx \frac{3.31\hbar^2n^{2/3}}{mk_B}. \tag{3.20}$$

This is the critical temperature for Bose–Einstein condensation in a non-interacting Bose gas in three dimensions.

3.1.4 Condensate Fraction and heat capacity

For $T < T_c$, a macroscopic number of particles occupy the ground state. The number of particles in the ground state is

$$N_0 = N - N_{\text{ex}} = N - \frac{V}{\lambda_T^3}g_{3/2}(1), \tag{3.21}$$

where we set $z = 1$ (i.e., $\mu = 0$) for $T < T_c$.

The condensate fraction is defined as

$$\frac{N_0}{N} = 1 - \frac{N_{\text{ex}}}{N} = 1 - \frac{V}{N\lambda_T^3}\zeta(3/2). \tag{3.22}$$

Using the definition of T_c:

$$\frac{N_0}{N} = 1 - \frac{\lambda_{T_c}^3}{\lambda_T^3} = 1 - \left(\frac{T}{T_c}\right)^{3/2}. \tag{3.23}$$

This result shows that the condensate fraction increases continuously from zero at $T = T_c$ to unity at $T = 0$. The behavior near T_c is characteristic of a second-order phase transition, with N_0/N serving as the order parameter. Indeed near T_c, the condensate fraction vanishes according to a power law. To see this, write $T = T_c - \varepsilon$

with $\varepsilon \to 0^+$:

$$\frac{N_0}{N} = 1 - \left(\frac{T_c - \varepsilon}{T_c}\right)^{3/2} = 1 - \left(1 - \frac{\varepsilon}{T_c}\right)^{3/2}. \tag{3.24}$$

Expanding to first order in $\varepsilon/T_c \ll 1$:

$$\frac{N_0}{N} \approx \frac{3}{2}\frac{\varepsilon}{T_c} = \frac{3}{2}\left(1 - \frac{T}{T_c}\right). \tag{3.25}$$

This result takes the form of a power law:

$$\frac{N_0}{N} \sim (T_c - T)^{\beta} \tag{3.26}$$

where the exponent $\beta = 1$ is a critical exponent. It is the fundamental quantity that characterizes the universality class of the transition. We can also see that the heat capacity presents two different values below and above T_c.indeed, knowing that the internal energy for an ideal gas is given by:

$$U = \frac{3}{2} N k_B T \frac{g_{5/2}(z)}{g_{3/2}(z)}.$$

and the definition of the heat capacity at constant volume:

$$C_V = \left(\frac{\partial U}{\partial T}\right)_V.$$

and by carrying out the derivative we get its expression for $T > T_c$

$$C_V^{>} = \frac{15}{4} N k_B \frac{g_{5/2}(z)}{g_{3/2}(z)} - \frac{9}{4} N k_B \frac{g_{3/2}(z)}{g_{1/2}(z)}. \tag{3.27}$$

But for $T < T_c$ the chemical potential becomes $\mu = 0$ so that $z = 1$. The internal energy becomes

$$U = \frac{3}{2} N k_B T \frac{\zeta(5/2)}{\zeta(3/2)} \left(\frac{T}{T_c}\right)^{3/2}. \tag{3.28}$$

Hence, the heat capacity in this case became:

$$C_V^{<} = \left.\frac{\partial U}{\partial T}\right|_V = \frac{15}{4} N k_B \frac{\zeta(5/2)}{\zeta(3/2)} \left(\frac{T}{T_c}\right)^{3/2}. \tag{3.29}$$

The specific heat C_V evaluated from the expressions obtained above and below T_c yields two distinct finite values at the critical point, revealing a discontinuity — a cusp — at $T = T_c$. This jump in C_V and with the order parameter vanishing

continuously, constitutes a definitive thermodynamic signature of a second-order phase transition:

At $T = 0$, all particles are in the ground state ($N_0 = N$), representing a pure quantum state. As temperature increases, thermal excitations populate higher energy states, reducing the condensate fraction. At $T = T_c$, the condensate vanishes ($N_0 = 0$), and for $T > T_c$, all particles are in excited states distributed according to the Bose–Einstein distribution with $\mu < 0$.

3.2 Conclusion

The grand canonical ensemble provides a natural framework for understanding Bose-Eistein condensation, with the grand partition function factorizing over single-particle states and yielding the Bose–Einstein distribution. The key insight is that the chemical potential must remain below the ground state energy, and when it saturates at this value, excess particles accumulate in the ground state, forming the condensate.

The critical temperature for condensation in three dimensions, $T_c \propto n^{2/3}$, reflects the quantum degeneracy condition where thermal de Broglie wavelength becomes comparable to interparticle spacing. Below this temperature, a macroscopic fraction of particles condenses, with the condensate fraction growing continuously from zero at T_c to unity at $T = 0$, characteristic of a second-order phase transition.

Chapter 4

Quantum Statistics of Ideal Dunkl Bosons

In this chapter, we investigate the statistical mechanics of ideal Dunkl–boson systems. Our analysis introduces a novel approach based on symmetry and reflection operators to study the thermodynamic behavior of an ideal Bose gas within the framework of Dunkl formalism. The results obtained in this generalized setting are systematically compared with those of the conventional ideal Bose gas, allowing us to identify the key differences arising from the presence of Dunkl operators and to discuss their physical implications.

A central ingredient of our approach is the role played by reflection symmetry in extending the conventional quantum state space to Dunkl space. This extension is implemented through the Dunkl derivative, defined by (see chap 2, sect 2)

$$\hat{D}_x = \frac{\partial}{\partial x} + \frac{\theta}{x}\left(1 - \hat{R}_x\right), \tag{4.1}$$

where $\hat{R}_x$ denotes the reflection operator, We will conduct a systematic way to investigate the thermodynamic properties of Dunkl–boson systems in comparison with their standard bosonic counterparts.

The theoretical foundations of the transformation from the standard Hilbert space to Dunkl space are discussed in subsction 2.4 of chap 2 where the mathematical tools underlying this transformation are presented in detail and leads to a generalized description of bosonic systems governed by Dunkl operators.

We will derive explicit analytical expressions for fundamental thermodynamic quantities, including the partition function, the internal energy and the heat capacity. These results are then compared with the corresponding expressions for the non-deformed ideal Bose gas. In addition, we also investigate ideal Dunkl–boson

systems confined in external potentials, particularly harmonic traps, and study the effects of such confinement on the transition temperature.

Let us recall that the standard flat measure dx is not adapted to the Dunkl derivative $\hat{D}_{x_i}$. The appropriate Hilbert space is the weighted space defined as:

$$\mathcal{H}_D = L^2(\mathbb{R}, \omega_\theta(x)\, dx), \qquad \omega_\theta(x) = |x|^{2\theta}, \tag{4.2}$$

equipped with the inner product

$$\langle f, g \rangle_\theta = \int_{-\infty}^{+\infty} f(x)\, g(x)\, |x|^{2\theta}\, dx. \tag{4.3}$$

Within $\mathcal{H}_D$, the Dunkl derivative satisfies the skew-adjointness relation

$$\hat{D}_{x_i}^\dagger = -\hat{D}_{x_i}, \tag{4.4}$$

which mirrors the corresponding property of the ordinary derivative in $L^2(\mathbb{R}, dx)$. The multiplication operator x_i is self-adjoint, and the reflection operator $\hat{R}_i$ is self-adjoint and unitary.

The creation and annihilation operators are defined as

$$b_i = \frac{1}{\sqrt{2}} \left(x_i + \hat{D}_{x_i} \right), \qquad b_i^\dagger = \frac{1}{\sqrt{2}} \left(x_i - \hat{D}_{x_i} \right), \tag{4.5}$$

where adjoints are taken with respect to the inner product of $\mathcal{H}_\nu$. Introducing the notation

$$\phi_i \equiv b_i, \qquad \bar{\phi}_i \equiv b_i^\dagger, \tag{4.6}$$

their explicit expressions follow from $\hat{D}_{x_i} = \partial_{x_i} + \frac{\theta}{x_i}(1 - \hat{R}_i)$:

$$\phi_i = \frac{1}{\sqrt{2}} \left(x_i + \partial_{x_i} + \frac{\theta}{x_i}(1 - \hat{R}_i) \right), \tag{4.7}$$

$$\bar{\phi}_i = \frac{1}{\sqrt{2}} \left(x_i - \partial_{x_i} - \frac{\theta}{x_i}(1 - \hat{R}_i) \right). \tag{4.8}$$

Therefore the deformed commutation relation is

$$[\phi_i, \bar{\phi}_j] = \delta_{ij} \left(1 + \theta \hat{R}_i \right). \tag{4.9}$$

which is a generalization to N particles of (2.88) Knowing that the ideal gas can be considered as an ensemble of independent harmonic oscillator modes, the number

operator is defined by

$$\hat{N}_i = \bar{\phi}_i \phi_i = b_i^\dagger b_i, \tag{4.10}$$

which is self-adjoint and non-negative on $\mathcal{H}_\theta$. Its explicit form reads

$$\hat{N}_i = \frac{1}{2}\left(x_i^2 - \hat{D}_{x_i}^2\right) - \frac{1}{2} - \theta \hat{R}_i. \tag{4.11}$$

Acting on number states $|n_i\rangle$, with $|n_i\rangle \equiv |n_1, n_2, n_3, ...\rangle$,one finds

$$\bar{\phi}_i |n_i\rangle = \sqrt{n_i + 1}|n_i + 1\rangle \tag{4.12}$$

$$\phi_i |n_i\rangle = \left[\sqrt{n_i} + \frac{\theta}{\sqrt{n_i}}\left(1 - (-1)^{n_i}\right)\right]|n_i\rangle \tag{4.13}$$

and

$$\hat{N}_i |n_i\rangle = \lambda_{n_i}|n_i\rangle, \qquad \lambda_{n_i} = n_i + \theta\big(1 - (-1)^{n_i}\big), \tag{4.14}$$

or equivalently,

$$\hat{N}_i |n_i\rangle = \begin{cases} n_i |n_i\rangle, & n_i \text{ even}, \\ (n_i + 2\theta)|n_i\rangle, & n_i \text{ odd}. \end{cases} \tag{4.15}$$

This result shows how the spectrum of the occupation number operator splits into two parts: it retains the standard behavior for states with an even number of particles, while for states with an odd number of particles acquire a modified eigenvalue due to the Dunkl deformation

The single-mode Hamiltonian is defined using symmetric ordering,

$$H_i = \frac{1}{2}\left(b_i b_i^\dagger + b_i^\dagger b_i\right) = \hat{N}_i + \frac{1}{2} + \theta \hat{R}_i. \tag{4.16}$$

Its action on the Fock states yields the energy spectrum

$$E_{n_i} = n_i + \theta + \frac{1}{2}, \tag{4.17}$$

which we note is independent of parity .

4.1 Ideal Bose gas in Dunkl framework

4.1.1 A)Partition function

Within the grand canonical ensemble, the partition function of the Dunkl–boson system is constructed by summing over all occupation numbers, each weighted by its corresponding energy. By reorganizing this sum, the partition function can be decomposed into two separate contributions associated with even and odd parity sectors. its general form in the grand canonical ensemble is given by:

$$Z_D = \sum_{N_1,N_2,N_3,\ldots} e^{-\beta \sum_i N_i(\varepsilon_i-\mu)}. \tag{4.18}$$

which can be written as

$$Z_D = \prod_i \sum_{N_i} \xi_i. \tag{4.19}$$

where

$$\xi_i = e^{-\beta N_i(\varepsilon_i-\mu)}. \tag{4.20}$$

by using the previous equation (4.15) one can subdivide this expression into two functions according to the parity

$$\xi_i \equiv \xi_i^{\text{odd}} + \xi_i^{\text{even}}. \tag{4.21}$$

Odd parity.

$$\begin{aligned}\xi_i^{\text{odd}} &= e^{-\beta(1+2\theta)(\varepsilon_i-\mu)} + e^{-\beta(3+2\theta)(\varepsilon_i-\mu)} + e^{-\beta(5+2\theta)(\varepsilon_i-\mu)} + \cdots \\ &= e^{-2\beta\theta(\varepsilon_i-\mu)} \left(e^{-\beta(\varepsilon_i-\mu)} + e^{-5\beta(\varepsilon_i-\mu)} + \cdots\right).\end{aligned} \tag{4.22}$$

since this is a geometric series

we obtain

$$\xi_i^{\text{odd}} = \frac{e^{-\beta(1+2\nu)(\varepsilon_i-\mu)}}{1-e^{-2\beta(\varepsilon_i-\mu)}}. \tag{4.23}$$

Even parity.

$$\begin{aligned}\xi_i^{\text{even}} &= 1 + e^{-2\beta(\varepsilon_i-\mu)} + e^{-4\beta(\varepsilon_i-\mu)} + \cdots \\ &= \frac{1}{1-e^{-2\beta(\varepsilon_i-\mu)}}.\end{aligned} \tag{4.24}$$

Subsequently, we write the Dunkl partition function as

$$Z_D = \prod_i \frac{1 + e^{-\beta(1+2\theta)(\varepsilon_i - \mu)}}{1 - e^{-2\beta(\varepsilon_i - \mu)}}. \tag{4.25}$$

In the limit $\theta \to 0$, this expression reduces to the well-known partition function of the ideal Bose gas

$$Z = \prod_i \frac{1}{1 - ze^{-\beta\varepsilon_i}}, \tag{4.26}$$

with the fugacity $z = e^{\beta\mu}$.

4.1.1.1 B)The average particle number

Using

$$N_D = \frac{1}{\beta}\left(\frac{\partial \ln Z_D}{\partial \mu}\right)_{T,V}. \tag{4.27}$$

we get,

$$N_D = N_0^D + N_e^D, \tag{4.28}$$

where

$$N_0^D = \frac{2}{z^{-2} - 1} + (1 + 2\theta)\frac{1}{z^{-(1+2\theta)} + 1} \tag{4.29}$$

denotes the occupation number of the ground state, and

$$N_e^D = \sum_{i \neq 0}\left[\frac{2}{e^{2\beta\varepsilon_i} z^{-2} - 1} + \frac{1 + 2\theta}{e^{\beta(1+2\theta)\varepsilon_i} z^{-(1+2\theta)} + 1}\right] = \sum_{i \neq 0} n_\theta(\varepsilon_i). \tag{4.30}$$

the occupation number of the excited states. One notices that the condition $\mu < 0$,required for a non-deformed ideal case is sufficient here to ensure positivity of N_ϵ^D

4.2 Ideal Dunkl-Bose gases 3D: homogeneous case

In the thermodynamic limit , the energy spectrum becomes quasi-continuous allowing the replacement of sums by integrals, so, the total particles number given by

$$N = \sum_{i=0}^{\infty} n_\theta(\varepsilon_i) \tag{4.31}$$

where $n_\theta(\epsilon_i)$ is the deformed Bose-Eistein distrubtion function; becomes

$$N = \int_0^\infty n_\theta(\varepsilon)\,\rho(\varepsilon)\,d\varepsilon \tag{4.32}$$

and $\rho(\epsilon)$ is the density of states. Using the deformed partition function given by Eq: (4.30) we get:

$$n_\theta(\varepsilon_i) = \frac{2}{\left(z^{-1}e^{\beta\varepsilon_i}\right)^2 - 1} + \frac{1+2\theta}{\left(z^{-1}e^{\beta\varepsilon_i}\right)^{1+2\theta} + 1}. \tag{4.33}$$

By substituting the density of state $\rho(\varepsilon_i)$ given by Eq: (3.6) chapter-3 we obtain: :

$$\frac{N_e^D}{V} = \frac{1}{\lambda^3\sqrt{2}}\left[g_{3/2}(z^2) - \sqrt{\frac{2}{1+2\theta}}g_{3/2}(-z^{1+2\theta})\right], \tag{4.34}$$

where $g_s(z)$ is the Bose function defined by (3.10)

$$g_s(z) = \frac{1}{\Gamma(s)}\int_0^\infty \frac{x^{s-1}}{z^{-1}e^x - 1}\,dx, \tag{4.35}$$

and

$$\lambda = \left(\frac{2\pi\hbar^2\beta}{m}\right)^{1/2}. \tag{4.36}$$

is the Broglie wavelength Thus, the total number of particles can be written as

$$N^D = \frac{2}{z^{-2}-1} + \frac{1+2\theta}{z^{-(1+2\theta)}+1} + \frac{V}{\lambda^3}\left[\sqrt{2}\,g_{3/2}(z^2) - \frac{2}{1+2\theta}\,g_{3/2}\big(-z^{1+2\theta}\big)\right]. \tag{4.37}$$

using the following property of the polylogarithmic function,

$$g_s(z) + g_s(-z) = 2^{1-s}g_s(z^2), \tag{4.38}$$

we rewrite equation (4.37) as

$$\frac{N^D}{V} = \frac{N_0^D}{V} + \frac{1}{\lambda^3}\,g_{3/2}(z,\theta), \tag{4.39}$$

where

$$g_{3/2}(z,\theta) = g_{3/2}(z) + g_{3/2}(-z) - \frac{1}{\sqrt{1+2\theta}}\,g_{3/2}\big(-z^{1+2\theta}\big)\,. \tag{4.40}$$

We notice on (4.34) that N_e^D becomes complex for $1+2\theta < 0$, so physical consistency

requires that,

$$\theta > -\frac{1}{2}.$$

. we also note that; in the limit of $\theta \to 0$, equation (4.39) reduces to the standard result:

$$\frac{N_D}{V} = \frac{N_0^D}{V} + \frac{1}{\lambda^3}\, g_{3/2}(z), \tag{4.41}$$

- **Dunkl-transition Temperature and Dunkl-condensed Fraction**

  The transition temperature marks the onset of Bose–Einstein condensation (BEC), characterized by a macroscopic occupation of the lowest energy state and a null chemical potential ($z = 1$). The equation(4.39) leads to:

$$N^D = \frac{V}{\lambda_c^3}\, g_{3/2}(1)\left(1 + \frac{g_{3/2}(-1)}{g_{3/2}(1)}\left(1 - \frac{1}{\sqrt{1+2\theta}}\right)\right) \equiv N, \tag{4.42}$$

  where N denotes the total number of particles in the system. From this relation, the critical temperature is deduced as

$$T_c^D = \frac{2\pi\hbar^2}{mk_B}\left(\frac{N}{V\, g_{3/2}(1)}\right)^{2/3}\left[1 + \frac{g_{3/2}(-1)}{g_{3/2}(1)}\left(1 - \frac{1}{\sqrt{1+2\theta}}\right)\right]^{-2/3}. \tag{4.43}$$

  which clearly demonstrates the dependence of the transition temperature on the Wigner parameter. By setting $\theta = 0$, we recover the critical temperature of the undeformed case.

$$T_c^0 = \frac{2\pi\hbar^2}{mk_B}\left(\frac{N}{V g_{3/2}(1)}\right)^{2/3}. \tag{4.44}$$

  The impact of the Dunkl formalism is better seen by considering the ratio of the critical temperature to that of the ordinary case.

$$\frac{T_c^D}{T_c^0} = \left[1 + \frac{g_{3/2}(-1)}{g_{3/2}(1)}\left(1 - \frac{1}{\sqrt{1+2\theta}}\right)\right]^{-2/3} \tag{4.45}$$

Finally, below the transition temperature, one may use Eqs. (4.39) and (4.40) to derive the fraction of particles in the ground state,

$$\frac{N_0^D}{N} = 1 - \left(\frac{T}{T_c^D}\right)^{3/2}. \tag{4.46}$$

This result shows that the condensate fraction remains structurally identical to that of the standard Bose–Einstein condensation, while the parameter θ modifies the condensation threshold without altering the underlying mechanism of condensation.

4.3 Ideal Dunkl-Bose gas in Arbitrary Dimension

the density of states for a free massive particle in a d-dimensional system of volume V is obtained via the semi-classical framework [53, 54] using its definition

$$\rho(\epsilon) = \frac{dN}{d\epsilon} \tag{4.47}$$

The number of states in a phase-space element is

$$dN = \frac{V}{(2\pi\hbar)^d} d^d p. \tag{4.48}$$

Upon transforming to hyperspherical coordinates in momentum space, one obtains

$$d^d p = S_{d-1} p^{d-1} dp, \qquad S_{d-1} = \frac{2\pi^{d/2}}{\Gamma(d/2)}, \tag{4.49}$$

so that

$$dN = \frac{V}{(2\pi\hbar)^d} S_{d-1} p^{d-1} dp. \tag{4.50}$$

Using the dispersion relation

$$\varepsilon = \frac{p^2}{2m}, \tag{4.51}$$

one obtains

$$\rho(\varepsilon)^{(d)} = \frac{V}{\Gamma(d/2)} \left(\frac{2\pi m}{h^2}\right)^{d/2} \varepsilon^{\frac{d}{2}-1} \equiv C\, \varepsilon^{\frac{d}{2}-1}. \tag{4.52}$$

Note that in the limit $\varepsilon \to 0$, the density of states $\rho^{(2)}$ remains constant, while $\rho^{(1)}$ diverges. For dimensions $d > 3$, one finds

$$\lim_{\varepsilon \to 0} \rho^{(d)}(\varepsilon) = 0. \tag{4.53}$$

These distinct asymptotic behaviors of $\rho^{(d)}(\varepsilon)$ near zero energy imply that a finite Bose–Einstein condensation critical temperature T_c exists only in three dimensions in the thermodynamic limit.Hence a true BEC exist only in 3D.For $D < 3$, we rather have a quasi condensation wich we will discuss later. However, for systems trapped of finite size, a non-zero critical temperature can arise regardless of the dimensionality.

Consider an ideal Dunkl–Bose gas in arbitrary dimensions. In the thermodynamic limit ($V, N \to \infty$ with $n = N/V$ fixed) by using the eaquation (4.32) and the deformed distrubtion function from equation (4.29) and (4.30) we get the number of particles:

$$N = N_0^D + 2\int_0^\infty \frac{\rho(\varepsilon)}{e^{2\beta\varepsilon} - 1}\, d\varepsilon + (1+2\theta)\int_0^\infty \frac{\rho(\varepsilon)}{e^{\beta(1+2\theta)\varepsilon} + 1}\, d\varepsilon. \tag{4.54}$$

where $\rho(\epsilon)$ is given by Eq. (4.52) we easily obtain:

$$N = N_0^D + \frac{V}{\lambda_{\text{th}}^d} g_{d/2}(z,\theta), \tag{4.55}$$

where the generalized Dunkl-Bose-Einstein function is defined as

$$g_{d/2}(z,\theta) = g_{d/2}(z) + g_{d/2}(-z) - (1+2\theta)^{1-d/2} g_{d/2}(-z^{1+2\theta}). \tag{4.56}$$

In the limit $\theta \to 0$,we recovers the standard case :

$$N = N_0 + \frac{g_{d/2}(z)}{\lambda^d}. \tag{4.57}$$

- **Dunkl-transition temperature and Dunkl condensate fraction** For a finite number of particles, the Dunkl critical temperature T_c^D is obtained by setting $\mu = 0$ and $N_0 = 0$. we then got

$$N = \frac{1}{\lambda_c^D}\Big[g_{d/2}(1) + g_{d/2}(-1) - (1+2\theta)^{1-d/2} g_{d/2}(-1)\Big]. \tag{4.58}$$

where λ_c is the critical de Broglie wavelength

the Dunkl critical temperature can be expressed as:

$$\frac{T_c^D}{T_c^0} = \left[1 + \frac{g_{d/2}(-1)}{\zeta(d/2)}\left(1 - (1+2\theta)^{d/2-1}\right)\right]^{-2/d}, \tag{4.59}$$

where $\zeta(s)$ is the Riemann-Zeta function and T_c^0;

$$T_c^0 = \frac{h^2}{2\pi m k_B}\left(\frac{N}{V\zeta(d/2)}\right)^{2/d} \tag{4.60}$$

is the standard Bose-Einstein condensation temperature.

The condensate fraction can easily be derived :

$$\frac{N_0^D}{N} = 1 - \left(\frac{T}{T_c^D}\right)^{d/2}. \tag{4.61}$$

Expressing this result in terms of the Bose condensation temperature, we find

$$\frac{N_0^D}{N} = 1 - \left[1 + \frac{g_{d/2}(-1)}{\zeta(d/2)}\left(1 - (1+2\theta)^{d/2-1}\right)\right]^{-d/2}\left(\frac{T}{T_c^0}\right)^{d/2}. \tag{4.62}$$

These findings provide a generalization of the standard Bose-Einstein condensation fraction to the Dunkl-deformed system in arbitrary dimensions. When $\theta = 0$, the standard expression is exactly recovered:

$$\frac{N_0^D}{N} = 1 - \left(\frac{T}{T_c^0}\right)^{d/2}. \tag{4.63}$$

This demonstrates the consistency of the Dunkl-deformed formulation with respect the conventional Bose-Einstein condensation in the undeformed limit.

4.4 Ideal Dunkl-Bose gases in Confined Potentials

So far we have only considered free (homogeneous) gases. In recent years, however, considerable attention has been given to the study of Bose–Einstein condensation in the presence of external confining potentials, particularly harmonic traps. These trapping potentials impose spatial confinement, which can substantially alter the properties of the condensate and give rise to a range of intriguing physical phenomena, including quantized vortices and modified thermodynamic behavior [55].

We begin by considering the three-dimensional harmonic oscillator and analazing the thermodynamic properties of the trapped bosonic gas. Investigating BEC in trapped systems within the context of Dunkl statistics provides a distinctive approach to the relation between external confinement and generalized statistical effects. In particular, this approach highlights the influence of the Wigner parameter on condensate formation, density distributions, and the thermodynamic characteristics of trapped gases.

4.4.1 Ideal Dunkl-Bose gas trapped in a three dimensional harmonic potential

- **transition temperature and condensate fraction**:

  Consider a system of N neutral atoms behaving as a Bose gas and confined in

a three-dimensional harmonic trap

$$V(x,y,z) = \frac{m\omega_1^2}{2}x^2 + \frac{m\omega_2^2}{2}y^2 + \frac{m\omega_3^2}{2}z^2, \tag{4.64}$$

where m denotes the atomic mass and ω_i are the trapping frequencies in three space directions. The spectrum of the system is given by the sum of the individual particle energies

$$\epsilon_{n_1,n_2,n_3} = \hbar(\omega_1 n_1 + \omega_2 n_2 + \omega_3 n_3) + \epsilon_0, \tag{4.65}$$

with $n_i = 0, 1, 2, \ldots$ $(i = 1, 2, 3)$. The single particle ground-state energy reads

$$\epsilon_0 = \frac{\hbar}{2}(\omega_1 + \omega_2 + \omega_3). \tag{4.66}$$

Within the Dunkl formalism, the grand canonical ensemble yields expressions for the number of atoms occupying the ground state and the excited states, respectively :

$$N = N_0^D + N_e^D, \tag{4.67}$$

where N_0^D and N_ϵ^D are given by (4.28), (4.29), (4.30) The discrete sums ((4.29), (4.30)) are quite hard to compute , even numerically . An alternative way is to use the continuous limit by using the density if state $\rho(\epsilon)$ Here $\beta = (k_B T)^{-1}$, where k_B is the Boltzmann constant, and

$$z = e^{\beta(\mu - E_0)} \tag{4.68}$$

Following Grossmann and Holthaus approximation of the density states [56,57] , we get

$$\rho(\epsilon) = \frac{1}{2}\frac{\epsilon^2}{(\hbar\omega)^3} + \gamma\,\frac{\epsilon}{(\hbar\omega)^2}, \tag{4.69}$$

where $\omega = (\omega_1\omega_2\omega_3)^{1/3}$ is the geometric mean of the trapping frequencies, and γ is a numerical factor depending on $(\omega_1, \omega_2, \omega_3)$. For a symmetric harmonic oscillator, one finds $\gamma = 3/2$ [56].

This approximation is valid in the regime of small energy level spacing. After a straightforward calculations, the total number of particles reads:

$$
\begin{aligned}
N = N_0^D &+ \frac{1}{4}\left(\frac{k_B T}{\hbar\omega}\right)^3 \left[g_3(z^2) - \frac{g_3(-z^{1+2\theta})}{(1+2\theta)^2}\right] \\
&+ \frac{\gamma}{2}\left(\frac{k_B T}{\hbar\omega}\right)^2 \left[g_2(z^2) - \frac{g_2(-z^{1+2\theta})}{1+2\theta}\right] \\
&= N_0^D + \left(\frac{k_B T}{\hbar\Omega}\right)^3 g_3(z,\theta) + \gamma\left(\frac{k_B T}{\hbar\Omega}\right)^2 g_2(z,\theta)
\end{aligned}
\tag{4.70}
$$

In the limit $\theta \to 0$, the Dunkl–Bose function reduces to the standard Bose function, and Eq. (4.70) coincides with the corresponding result obtained in Ref. [56]. The Dunkl Bose–Einstein condensation temperature T_c^D can also be expressed as:

$$
T_c^D \simeq \frac{\hbar\omega}{k_B}\left(\frac{N}{g_3(1,\theta)}\right)^{1/3}\left[1 - \frac{\gamma}{3}\frac{g_2(1,\theta)}{g_3^{2/3}(1,\theta)}\frac{1}{N^{1/3}}\right]. \tag{4.71}
$$

It is important to note that the Dunkl critical temperature depends on several factors: the total number of particles N, the individual oscillator frequencies ω_i, the coefficient γ, as well as the Wigner parameter θ. When $\theta \to 0$, one recovers the standard Bose condensation temperature T_c^0 reported in Ref. [56]:

$$
T_c^0 \simeq \frac{\hbar\omega}{k_B}\left(\frac{N}{g_3(1)}\right)^{1/3}\left[1 - \frac{\gamma}{3}\frac{g_2(1)}{g_3^{2/3}(1)}\frac{1}{N^{1/3}}\right]. \tag{4.72}
$$

By comparing Eqs. (4.71) and (4.72), we obtain the ratio

$$
\frac{T_c^D}{T_c^0} = \left(\frac{\zeta(3)}{g_3(1,\theta)}\right)^{1/3} \frac{1 - \dfrac{\gamma}{3N^{1/3}}\dfrac{g_2(1,\nu)}{g_3^{2/3}(1,\theta)}}{1 - \dfrac{\gamma}{18N^{1/3}}\dfrac{\pi^2}{\zeta^{2/3}(3)}}, \tag{4.73}
$$

For a very large number of particles ($N \to \infty$), the second term in Eq. (4.71) can be neglected, yielding

$$
T_c^D = \frac{\hbar\omega}{k_B}\left(\frac{N}{g_3(1,\theta)}\right)^{1/3}, \tag{4.74}
$$

which reduces to the ordinary case for $\theta = 0$ [56]:

$$
T_c^B = \frac{\hbar\Omega}{k_B}\left(\frac{N}{\zeta(3)}\right)^{1/3}. \tag{4.75}
$$

By comparing Eqs. (4.74) and (4.75), we obtain

$$\frac{T_c^D}{T_c^B} = \left(\frac{\zeta(3)}{g_3(1,\theta)}\right)^{1/3}. \tag{4.76}$$

Using Eq. (4.75) in Eq.(5.45), the condensate fraction ground-state population becomes

$$\frac{N_0^D}{N} = 1 - \frac{g_3(1,\theta)}{\zeta(3)}\left(\frac{T}{T_c^B}\right)^3 - \gamma\frac{g_2(1,\theta)}{\zeta^{2/3}(3)}\frac{1}{N^{1/3}}\left(\frac{T}{T_c^B}\right)^2. \tag{4.77}$$

and by using the equation (4.76) we obtain :

$$\frac{N_0^D}{N} = 1 - \left(\frac{T}{T_c^D}\right)^3 - \gamma\,\frac{g_2(1,\theta)}{g_3^{2/3}(1,\theta)}\,\frac{1}{N^{1/3}}\left(\frac{T}{T_c^D}\right)^2 \tag{4.78}$$

In the large-N limit, the second term vanishes and one recovers the simple form:

$$\frac{N_0^D}{N} \approx 1 - \left(\frac{T}{T_c^D}\right)^3, \tag{4.79}$$

which is structurally identical to the standard BEC result, with T_c^D replacing T_c^0.

4.4.2 Thermodynamics of Ideal Dunkl-Bose trapped gas

We now proceed to investigate the thermodynamic behavior of an ideal Bose gas confined in 3D harmonic trapp within the framework of Dunkl statistics. In particular, our analysis focuses on the determination of the internal energy of the system and the associated heat capacity. In this generalized setting, the internal energy of the system is defined as

$$U = \sum_i N_i\varepsilon_i. \tag{4.80}$$

Replacing the summation by an integral in the continuous case, yields the internal energy in the Dunkl framework:

$$U^D = 2\int_0^\infty \frac{\varepsilon\rho(\varepsilon)\,d\varepsilon}{e^{2\beta\varepsilon}z^{-2}-1} + (1+2\theta)\int_0^\infty \frac{\varepsilon\rho(\varepsilon)\,d\varepsilon}{e^{\beta(1+2\theta)\varepsilon}z^{-(1+2\theta)}+1}. \tag{4.81}$$

Substituting $\rho(\epsilon)$ (4.69) yields

$$\frac{U^D}{\hbar\omega} = 3\left(\frac{k_BT}{\hbar\omega}\right)^4 g_4(z,\theta) + 2\gamma\left(\frac{k_BT}{\hbar\omega}\right)^3 g_3(z,\theta). \tag{4.82}$$

The constant volume heat capacity,

$$C_V = \left(\frac{\partial U}{\partial T}\right)_{z,N}. \tag{4.83}$$

should be computed as fellows
For $T < T_c^D$, one way safety set $z = 1$,and, therefore

$$\frac{C_<^D}{Nk_B} = 12\frac{g_4(1,\theta)}{\zeta(3)}\left(\frac{T}{T_c^B}\right)^3 + 6\gamma\frac{g_3(1,\theta)}{\zeta^{2/3}(3)}\frac{1}{N^{1/3}}\left(\frac{T}{T_c^B}\right)^2. \tag{4.84}$$

For large N, we may neglect the second term in Eq(4.84), and thus

$$\frac{C_<^D}{Nk_B} = 12\frac{g_4(1,\theta)}{\zeta(3)}\left(\frac{T}{T_c^B}\right)^3 \tag{4.85}$$

For $T > T_c^D$, since z depend on T

$$\begin{aligned}\frac{C_>^D}{Nk_B} = {} & 12\frac{g_4(z,\theta)}{\zeta(3)}\left(\frac{T}{T_c^B}\right)^3 + 6\frac{\gamma}{N^{1/3}}\frac{g_3(z,\theta)}{\zeta^{2/3}(3)}\left(\frac{T}{T_c^B}\right)^2 \\ & + \Big[\frac{3g_3(z,\theta)}{\zeta(3)}\left(\frac{T}{T_c^B}\right)^4 + 2\frac{\gamma}{N^{1/3}}\frac{g_2(z,\theta)}{\zeta^{2/3}(3)}\left(\frac{T}{T_c^B}\right)^3\Big]\frac{T_c^B}{z}\frac{dz}{dT}.\end{aligned} \tag{4.86}$$

Using

$$\frac{dg_s(z^n)}{dz} = \frac{n}{z}g_{s-1}(z^n), \tag{4.87}$$

and imposing $dN/dT = 0$, we obtain

$$\frac{T_c^B}{z}\frac{dz}{dT} = -3\frac{T_c^B}{T}\frac{g_3(z,\theta)}{g_2(z,\theta)}\frac{1+\frac{2\gamma}{3}\frac{\zeta^{1/3}(3)}{N^{1/3}}\frac{g_2(z,\theta)}{g_3(z,\theta)}\frac{T_c^B}{T}}{1+\gamma\frac{\zeta^{1/3}(3)}{N^{1/3}}\frac{g_1(z,\theta)}{g_2(z,\theta)}\frac{T_c^B}{T}}. \tag{4.88}$$

thus, the Dunkl heat capacity reads

$$\begin{aligned}\frac{C_{>}^{D}}{Nk_B} &= 12\left(\frac{T}{T_c^B}\right)^3 \frac{g_4(z,\theta)}{\zeta(3)} + 6\gamma\left(\frac{T}{T_c^B}\right)^2 \frac{1}{N^{1/3}}\frac{g_3(z,\theta)}{\zeta^{2/3}(3)} \\ &\quad - \frac{3T_c^B}{T}\frac{g_3(z,\theta)}{g_2(z,\theta)}\left[3\left(\frac{T}{T_c^B}\right)^4 \frac{g_3(z,\theta)}{\zeta(3)} + \frac{2\gamma}{N^{1/3}}\left(\frac{T}{T_c^B}\right)^3 \frac{g_2(z,\theta)}{\zeta^{2/3}(3)}\right] \\ &\quad \times \frac{1+\frac{2\gamma}{3}\frac{\zeta^{1/3}(3)}{N^{1/3}}\frac{g_2(z,\theta)}{g_3(z,\theta)}\frac{T_c^B}{T}}{1+\gamma\frac{\zeta^{1/3}(3)}{N^{1/3}}\frac{g_1(z,\theta)}{g_2(z,\theta)}\frac{T_c^B}{T}}.\end{aligned} \tag{4.89}$$

In the large-N limit, the previous expression of this heat capacity simplifies to:

$$\frac{C_{>}^{D}}{Nk_B} = 12\frac{g_4(z,\theta)}{g_3(z,\theta)} - 9\frac{g_3(z,\theta)}{g_2(z,\theta)}. \tag{4.90}$$

Therefore C^D presents a discontinuity at the critical point; the the jump at $T = T_c$ reads:.

$$\frac{C_{>}^{D} - C_{<}^{D}}{Nk_B} = 9\frac{g_3(1,\theta)}{g_2(1,\theta)}, \tag{4.91}$$

which reduces to the known expression $9\zeta(3)/\zeta(2) \simeq 6.577$ for $\theta = 0$; the non-deformed case.

In the high-temperature (classical) limit,: This regime is reached for $z << 1$, where

$$g_s(z,\theta) \simeq \frac{z}{(1+2\theta)^{\,s-1}}, . \tag{4.92}$$

As a consequence, Eq. (4.90) yields

$$\frac{C_{>}^{D}}{Nk_B} \simeq \frac{3}{1+2\theta}. \tag{4.93}$$

This result shows that, although quantum effects vanish at high temperature, the Dunkl deformation parameter θ induces a persistent modification of the classical equipartition value $C/Nk_B = 3$.

The thermodynamic behavior of the Dunkl-deformed Bose gas confined in a harmonic potential exhibits distinct regimes across the condensation transition. Below the critical temperature T_c^D, the heat capacity follows a dominant T^3 scaling, characteristic of harmonically trapped Bose gases, with additional subleading corrections arising from the Dunkl deformation. Above T_c^D, the heat capacity remains finite and is governed by generalized Bose functions, reflecting the modified statistical structure of the system. At the transition temperature, the heat capacity displays a finite discontinuity, signaling the onset of Bose–Einstein condensation; the magnitude of

this jump is controlled by the Wigner parameter and continuously reduces to the standard Bose–Einstein result in the undeformed limit. In the high-temperature regime, the system approaches a classical behavior, with a heat capacity renormalized by the Dunkl deformation, indicating an effective reduction of the available degrees of freedom due to the underlying reflection symmetry.

Chapter 5

Thermodynamics of Ideal Bose Gases in Power-Law Traps within the Dunkl Formalism

In this chapter, we investigate the properties of an ideal Bose gas confined by a power-law trapping potential within the framework of the Dunkl formalism. This study extends our previous analyses of Dunkl-deformed Bose systems by considering a broad class of confining geometries that interpolate between harmonic traps [19,21, 58] and more general external potentials. Power-law confinement provides a unified and flexible setting in which the combined effects of dimensionality, trap geometry, and generalized quantum statistics can be systematically explored.

We begin by analyzing the Dunkl Bose gas subjected to power-law confinement in one and two spatial dimensions. These low-dimensional systems are of particular interest, as they highlight the role of quantum fluctuations and confinement-induced effects on Bose–Einstein condensation under Dunkl deformation. The extension to higher dimensions is then carried out in a unified manner, allowing us to formulate the theory for an arbitrary D-dimensional system within the same framework.

A central objective of this chapter is the investigation of the thermodynamic properties of the Dunkl-deformed Bose gas in power-law traps. Explicit analytical expressions are derived for key thermodynamic quantities, including the internal energy, heat capacity, and condensate fraction.

These quantities are analyzed both below and above the condensation temperature, revealing how the Dunkl deformation alters the thermodynamic behavior relative to the standard ideal Bose gas. An important outcome of this analysis is the emergence of universality classes characterized by a single parameter s, which encapsulates the combined influence of spatial dimensionality and trap geometry. Remarkably, we show that the thermodynamic properties depend only on this parameter, rather than on the specific form of the power-law potential. This result demonstrates that all regular power-law traps fall into a limited number of universality classes, extending earlier findings obtained for harmonically confined systems.

Finally, we address the thermodynamic consistency of the Dunkl formalism in the presence of arbitrary power-law confinement. we demonstrate that the Wigner parameter must lie within the interval $]-1/2, 1/2]$. This constraint generalizes the results obtained for harmonic traps and establishes that the same bounds apply to arbitrary regular potentials in any spatial dimension. Together, these results provide a comprehensive and unified description of Dunkl-deformed Bose gases under power-law confinement and clarify the fundamental role played by symmetry, dimensionality, and generalized statistics in Bose–Einstein condensation.

5.1 1-D power law confinement

Let us begin by considering a one-dimensional system confined by a power-law potential of the form

$$V(x) = V_0 \left|\frac{x}{L}\right|^{\eta}, \tag{5.1}$$

where U_0 sets the energy scale of the confinement, x denotes the spatial coordinate, L is a characteristic length, and η controls the steepness of the trapping potential.

Within the semiclassical approximation, the density of states is given by

$$\rho(\varepsilon) = \frac{\sqrt{2m}}{h} \int_{-l(\varepsilon)}^{l(\varepsilon)} \frac{dx}{\sqrt{\varepsilon - V(x)}}, \tag{5.2}$$

where $l(\varepsilon)$ is determined from $U(l) = \varepsilon$ and reads

$$l(\varepsilon) = L \left(\frac{\varepsilon}{U_0}\right)^{1/\eta}. \tag{5.3}$$

By introducing the dimensionless variable $y = x/l(\varepsilon)$, the integral in Eq. (5.2)

can be evaluated explicitly, yielding

$$\rho(\varepsilon) = \frac{2}{\eta}\frac{\sqrt{2m}}{h} L\, V_0^{-1/\eta}\sqrt{\pi}\,\frac{\Gamma\left(\frac{1}{\eta}\right)}{\Gamma\left(\frac{1}{\eta}+\frac{1}{2}\right)}\varepsilon^{\frac{1}{\eta}-\frac{1}{2}}. \tag{5.4}$$

As performed previously, we compute the sums ((4.30)- (4.28)) by using (5.4) to obtain:

$$N = N_0^D + \frac{2}{\eta}\frac{\sqrt{2m}}{h} LF(\eta)\, V_0^{-1/\eta}(kT)^{\frac{1}{\eta}+\frac{1}{2}}\Gamma\left(\frac{1}{2}+\frac{1}{\eta}\right) g_{\frac{1}{2}+\frac{1}{\eta}}(z,\theta). \tag{5.5}$$

where $F(\eta) = \displaystyle\int_0^1 \frac{y^{\frac{1}{\eta}-1}}{\sqrt{1-y}}\,dy$ When $\theta \to 0$, we recover the standard result [21]:

$$N = N_0 + \frac{2}{\eta}\frac{\sqrt{2m}}{h} LF(\eta)\, V_0^{-1/\eta}(kT)^{\frac{1}{\eta}+\frac{1}{2}}\Gamma\left(\frac{1}{2}+\frac{1}{\eta}\right) g_{\frac{1}{2}+\frac{1}{\eta}}(z). \tag{5.6}$$

By setting $N_0 = 0$ and $z = 1$ the condensation temperature T_c^D, is given by

$$k_B T_c^D = \left[\frac{\eta}{2}\frac{Nh\sqrt{2m}}{V_0^{1/\eta}LF(\eta)}\frac{1}{\Gamma\left(\frac{1}{2}+\frac{1}{\eta}\right) g_{\frac{1}{2}+\frac{1}{\eta}}(1,\theta)}\right]^{\frac{2\eta}{\eta+2}}. \tag{5.7}$$

The condensate fraction is also obtained

$$\frac{N_0^D}{N} = 1 - \left(\frac{T}{T_c^D}\right)^{\frac{1}{2}+\frac{1}{\eta}}. \tag{5.8}$$

In the limit $\theta \to 0$, equation (5.8) reduces to the standard case:

$$\frac{N_0^D}{N} = 1 - \left(\frac{T}{T_c^B}\right)^{\frac{1}{2}+\frac{1}{\eta}}. \tag{5.9}$$

where T_c^B represents the non-deformed critical temperature. Let us examine the thermodynamic behavior of of this system. The first step consists in determining the internal energy of the system, expressed as:

$$U = \int_0^\infty n(\varepsilon)\,\varepsilon\,d\varepsilon \tag{5.10}$$

given by

$$U^D = U_0[2^{-\left(\frac{1}{\eta}+\frac{1}{2}\right)} g_{3/2+1/\eta}(z^2) - \frac{1}{(1+2\theta)^{1/\eta-1/2}} g_{3/2+1/\eta}(-z^{1+2\theta})], \tag{5.11}$$

where

$$U_0 = \frac{2\sqrt{2m}L^2F(\eta)}{\eta h V_0^{1/\eta}}\,\Gamma\left(\frac{1}{\eta}+\frac{3}{2}\right)\,(k_BT)^{1/\eta+3/2}. \tag{5.12}$$

-Heat Capacity for $T < T_c$

Setting $z = 1$, we compute from (5.11)

$$\begin{aligned} C_<^D &= \left(\frac{\partial U^D}{\partial T}\right)_{N,V} \\ &= \frac{2}{\eta}\frac{\sqrt{2m}}{h}L\,k_B\left(\frac{1}{\eta}+\frac{3}{2}\right)F(\eta)\,\Gamma\left(\frac{1}{\eta}+\frac{3}{2}\right)(k_BT)^{1/\eta+1/2}\,g_{3/2+1/\eta}(1,\theta). \end{aligned} \tag{5.13}$$

Heat Capacity for $T > T_c$

Since for $T > T_c$ the fugacity z depends implicitly on T through the number constraint $N = \text{const},$: so

$$C_>^D = \left.\frac{\partial U^D}{\partial T}\right|_z + \left.\frac{\partial U^D}{\partial z}\right|_T \cdot \left.\frac{dz}{dT}\right|_N \tag{5.14}$$

Differentiating U^D with respect to T at fixed z gives:

$$\begin{aligned} \left.\frac{\partial U^D}{\partial T}\right|_{z,N} &= \left(\frac{1}{\eta}+\frac{3}{2}\right)\frac{U^D}{T} \\ &= \frac{2\sqrt{2m}}{\eta\hbar}\,Lk_B\,\frac{\left(\frac{1}{\eta}+\frac{3}{2}\right)}{U_0^{1/\eta}}\,F(\eta)\,\Gamma\left(\frac{1}{\eta}+\frac{3}{2}\right) \\ &\quad\times (k_BT)^{\frac{1}{\eta}+\frac{1}{2}}\,g_{\frac{1}{\eta}+\frac{3}{2}}(z,\theta) \end{aligned} \tag{5.15}$$

then computing the second term of (5.14), we can express it as:

$$C_>^D = C_1 + C_2\left(-\frac{\left(\frac{1}{\eta}+\frac{1}{2}\right)\,g_{1+\frac{1}{2}}(z,\theta)}{T\,g_{\frac{1}{\eta}-\frac{1}{2}}(z,\theta)}\right) \tag{5.16}$$

where

$$C_1 = \frac{2\sqrt{2m}}{\eta\hbar}\,L\,\frac{k_B}{U_0^{1/\eta}}\,F(\eta)\,\Gamma\left(\frac{1}{\eta}+\frac{3}{2}\right)(k_BT)^{\frac{1}{\eta}+\frac{1}{2}}\,g_{\frac{1}{\eta}+\frac{3}{2}}(z,\theta) \tag{5.17}$$

and

$$C_2 = \frac{2\sqrt{2m}}{\eta\hbar}\, L\, \frac{1}{U_0^{1/\eta}}\, F(\eta)\, \Gamma\left(\frac{1}{\eta}+\frac{3}{2}\right) (k_B T)^{\frac{1}{\eta}+\frac{3}{2}}\, g_{\frac{1}{\eta}+\frac{1}{2}}(z,\theta) \tag{5.18}$$

5.2 2-D power law confinement

In this section, we turn our attention to the two-dimensional case. The calculation procedure is similar to that of the one-dimensional case so:

Knowing that the density of states is given by

$$\rho(\varepsilon) = \frac{1}{h^2}\int d^2r\, d^2p\, \delta\left(\varepsilon - \frac{p^2}{2m} - V(r)\right). \tag{5.19}$$

and integrating over momentum space yields

$$\rho(\varepsilon) = \frac{2\pi m}{h^2}\int d^2r\, \Theta\big(\varepsilon - V(r)\big), \tag{5.20}$$

where Θ is the Heaviside step function. For an isotropic power-law potential $U(r) = V_0(r/a)^\eta$, the condition $\varepsilon \geq U(r)$ defines a classical turning radius $r_{\max} = a(\varepsilon/V_0)^{1/\eta}$. one finally obtains the density of states

$$\rho(\varepsilon) = \frac{2\pi^2 m a^2}{h^2}\left(\frac{\varepsilon}{V_0}\right)^{\frac{2}{\eta}}. \tag{5.21}$$

and therefore the number of particles is:

$$N = N_0 + \frac{2\pi^2 m a^2}{h^2}\frac{1}{V_0^{2/\eta}}(kT)^{\frac{2}{\eta}+1}\Gamma\left(\frac{2}{\eta}+1\right) g_{\frac{2}{\eta}+1}(z,\theta). \tag{5.22}$$

Consequently the Dunkl-critical temperature in the 2-d dimension is given by

$$kT_c^D = \left[\frac{Nh^2}{2\pi^2 m a^2} V_0^{2/\eta}\frac{1}{\Gamma\left(\frac{2}{\eta}+1\right) g_{\frac{2}{\eta}+1}(z,\theta)}\right]^{\frac{\eta}{2+\eta}}. \tag{5.23}$$

and the condensate fraction versus the reduced temperature , where T_C^B is the non-deformed critical temperature and is given by :

$$\frac{N_0^D}{N} = 1 - \left\{1 + \frac{g_{\frac{2}{\eta}+1}(-1)}{g_{\frac{2}{\eta}+1}(1)}\left[1-(1+2\theta)^{-\frac{2}{\eta}}\right]\right\}\left(\frac{T}{T_c^B}\right)^{\frac{2}{\eta}+1} \tag{5.24}$$

Finally, we derive the internal energy in the Dunkl-framework and we obtain

$$U^D = \frac{2\pi^2 ma^2}{\eta^2 V_0^{\frac{2}{\eta}}}\,\Gamma\left(\frac{2}{\eta}+2\right)(k_BT)^{\frac{2}{\eta}+2}\left\{2^{-\left(\frac{2}{\eta}+1\right)}g_{\frac{2}{\eta}+2}(z^2)-\frac{1}{(1+2\theta)^{\frac{2}{\eta}-1}}\,g_{\frac{2}{\eta}+2}\left(-z^{1+2\theta}\right)\right\} \tag{5.25}$$

In the same way as before, we obtain the following results for $T < T_c$:

$$C_<^D = \frac{2\pi^2 ma^2}{\eta^2 U_0^{\frac{2}{\eta}}}\,\Gamma\left(\frac{2}{\eta}+2\right)K\left(\frac{2}{\eta}+2\right)(KT)^{\frac{2}{\eta}+1}\,g_{\frac{2}{\eta}+2}(1,\theta) \tag{5.26}$$

and for $T > T_c$we get:

$$C_>^D \;=\; C_3^D + C_4^D\left(-\frac{\frac{2}{\eta}+1}{T}\,\frac{g_{\frac{2}{\eta}+1}(z,\theta)}{g_{\frac{2}{\eta}}(z,\theta)}\right) \tag{5.27}$$

where the calculated expressions for C_3^D and C_4^D are obtained as follows :

$$C_3^D = \frac{2\pi^2 ma^2}{\eta^2 U_0^{\frac{2}{\eta}}}\Gamma\left(\frac{2}{\eta}+2\right)k_B\left(\frac{2}{\eta}+2\right)(k_BT)^{\frac{2}{\eta}+1}g_{\frac{2}{\eta}+2}(z,\theta), \tag{5.28}$$

$$C_4^D = 2\frac{2\pi^2 ma^2}{\eta^2 U_0^{\frac{2}{\eta}}}\Gamma\left(\frac{2}{\eta}+2\right)(k_BT)^{\frac{2}{\eta}+2}g_{\frac{2}{\eta}+1}(z,\theta). \tag{5.29}$$

According to our analysis, the condensation temperature and the condensate fraction are both considerably altered by the Dunkl parameters. The present results confirm those reported in Refs. [21, 58].

In the next section, we will generalize the whole previous result for a power-law potential (including the harmonic oscillator) for any shape and at any spatial dimension . this will allow us to formulate a general theory for confined Dunkl-Bose gases.

5.3 Arbiratry dimensional power law confinement

The choice of trapping potential significantly influences the behavior of confined quantum gases. While much of the existing literature focuses on harmonic confinement—motivated by its experimental prevalence and mathematical simplicity—real experimental potentials often deviate from perfect harmonicity. Anharmonic corrections, geometric constraints, and engineered potential landscapes all lead to more general functional forms.

The spatial dimension in which a Bose gas is confined exerts a profound influence on its statistical properties and phase transition characteristics. This dimensional dependence is not merely a technical detail but reflects fundamental aspects of quantum statistics and fluctuation phenomena. In three dimensions, the ideal homogeneous Bose gas undergoes a sharp phase transition at a well-defined critical temperature. The density of states grows as $\sqrt{\epsilon}$, ensuring that the excited states can accommodate only a finite fraction of particles at any given temperature below T_c, thereby necessitating macroscopic ground-state occupation. The celebrated Mermin–Wagner–Hohenberg theorem [59, 60] establishes that continuous symmetry cannot be spontaneously broken in one and two dimensions at finite temperature, due to the proliferation of long-wavelength thermal fluctuations. For the ideal Bose gas, this translates into the impossibility of achieving true BEC in one or two dimensions without external confinement. The critical question then becomes: under what conditions on the trap geometry and dimensionality does genuine BEC occur? The answer lies in the energy dependence of the density of states $\rho(\epsilon)$ near the ground state. If $\rho(\epsilon)$ vanishes sufficiently rapidly as $\epsilon \to 0$, the ground state acquires macroscopic weight relative to the excited states, enabling condensation. Conversely, if $\rho(\epsilon)$ remains finite or diverges at low energies, quasi-condensation rather than true BEC emerges. This observation naturally leads to the concept of universality classes—categories of systems characterized by the same functional form of $\rho(\epsilon)$ and consequently exhibiting identical thermodynamic behavior. In this chapter, we investigate the thermodynamic properties of an ideal Bose gas confined by a power-law trapping potential within the framework of the Dunkl formalism. We begin by deriving the density of states in arbitrary D-dimensional space, which provides the fundamental basis for the subsequent thermodynamic analysis [61].

Next, Explicit analytical expressions are obtained for the main thermodynamic quantities, including the number of excited particles, the internal energy, the heat capacity, and the condensate fraction. These quantities are analyzed both below and above the critical condensation temperature.

5.3.1 Density of States

We consider a D-dimensional system of bosons of mass m confined in a power-law potential $V(\mathbf{x}) = V_0\Big(\frac{x}{a}\Big)^{\eta}$. The density of states is defined by

$$\rho(\varepsilon) = \frac{1}{(2\pi\hbar)^D}\int d^D p\, d^D x\; \delta\!\left(\varepsilon - \frac{p^2}{2m} - V(\mathbf{x})\right). \tag{5.30}$$

Using spherical symmetry in both momentum and position spaces, and performing the angular integrations, one obtains

$$\rho(\varepsilon) = \frac{(2\pi)^{D/2}}{\Gamma\big(\frac{D}{2}\big)}\frac{1}{(2\pi\hbar)^D}\int_0^{\infty} dp\, p^{D-1}\int_0^{x_{\max}} dx^D\; \delta\!\left(\varepsilon - \frac{p^2}{2m} - V(x)\right). \tag{5.31}$$

Using the delta-function property

$$\delta(f(x)) = \sum_i \frac{\delta(x - x_i)}{|f'(x_i)|} \tag{5.32}$$

that is equal to $\delta(p - p_0)/|f'(p_0)|$ where the term involving $\delta(p + p_0)$ does not contribute, since the integration domain is restricted to $p \geq 0$

With $f(p) = \varepsilon - p^2/(2m) - V(x)$, $p_0 = [2m(\varepsilon - V(x))]^{1/2}$ and $f'(p_0) = p_0/m$, the momentum integral gives:

$$\int_0^{\infty} dp\, p^{D-1}\,\delta\!\left(\varepsilon - \frac{p^2}{2m} - V(x)\right) = p_0^{D-2}\cdot m, \tag{5.33}$$

so that

$$\rho(\varepsilon) = \frac{(2\pi)^{D/2}}{\Gamma\big(\frac{D}{2}\big)\,(2\pi\hbar)^D}\cdot m\int_0^{x_{\max}} x^{D-1}\;[2m(\varepsilon - V(x))]^{\frac{D-2}{2}}\,dx. \tag{5.34}$$

To evaluate this integral, we begin by introducing a change of variables for $V(x) = V_0(x/a)^{\eta}$:

We set $t = \Big(\frac{x}{a}\Big)^{\eta}$, so that $x = a\,t^{1/\eta}$ and $dx = \frac{a}{\eta}\,t^{\frac{1}{\eta}-1}dt$. The upper limit $x_{\max} = a\,(\varepsilon/V_0)^{1/\eta}$ maps to $t_{\max} = \varepsilon/V_0$, hence $t \in [0, \varepsilon/V_0]$. Substituting into (5.34) gives :

$$\rho(\varepsilon) = \frac{(2\pi)^D}{\big[\Gamma\big(\frac{D}{2}\big)\big]^2\,(2\pi\hbar)^D}\cdot m\cdot\frac{a^D}{\eta}\int_0^{\varepsilon/V_0} t^{\frac{D}{\eta}-1}\,[2m(\varepsilon - V_0 t)]^{\frac{D-2}{2}}\,dt. \tag{5.35}$$

A second change of variable $y = t\,V_0/\varepsilon$ (so $t = \varepsilon y/V_0$, $dt = (\varepsilon/V_0)dy$, $y \in [0,1]$)

followed by identification with the Beta-function integral $\int_0^1 y^{b-1}(1-y)^{c-1}dy = B(b,c) = \Gamma(b)\Gamma(c)/\Gamma(b+c)$ with $b = D/\eta$ and $c = D/2$ gives

$$\int_0^{\varepsilon/V_0} t^{\frac{D}{\eta}-1}\left[2m(\varepsilon - V_0 t)\right]^{\frac{D-2}{2}} dt = (2m)^{\frac{D-2}{2}} \left(\frac{\varepsilon}{V_0}\right)^{\frac{D}{\eta}+\frac{D}{2}-1} \frac{\Gamma\left(\frac{D}{\eta}\right)\Gamma\left(\frac{D}{2}\right)}{\Gamma\left(\frac{D}{\eta}+\frac{D}{2}\right)}. \tag{5.36}$$

The final expression for the density of states is therefore

$$\rho(\varepsilon) = \frac{(2\pi)^D}{(2\pi\hbar)^D\left[\Gamma\left(\frac{D}{2}\right)\right]^2} \cdot \frac{(2m)^{D/2}}{\eta} \cdot \frac{a^D}{V_0^{D/\eta}} \cdot \frac{\Gamma\left(\frac{D}{2}\right)\Gamma\left(\frac{D}{\eta}\right)}{\Gamma\left(\frac{D}{2}+\frac{D}{\eta}\right)}\, \varepsilon^{\frac{D}{2}+\frac{D}{\eta}-1}. \tag{5.37}$$

We may write this compactly as $\varrho(\varepsilon) = A\,\varepsilon^{s-1}$ with $s = \dfrac{D}{2} + \dfrac{D}{\eta}$ and prefactor

$$A = \frac{2}{\eta}\frac{\Gamma\left(\frac{D}{\eta}\right)}{\Gamma\left(\frac{D}{2}\right)\Gamma\left(\frac{D}{\eta}+\frac{1}{2}\right)} \left(\frac{ma^2}{2\hbar^2}\right)^{D/2} \left(\frac{1}{V_0}\right)^{D/\eta} \tag{5.38}$$

5.3.2 Number of Particles and Transition Temperature:

- **a)Number of particles:** The number of excited Dunkl bosons, reads:

$$N_\varepsilon = \int_0^\infty d\varepsilon\; \rho(\varepsilon)\left[\frac{2}{z^{-2}e^{2\beta\varepsilon}-1} + \frac{\nu}{z^{-\nu}e^{\beta\nu\varepsilon}+1}\right], \tag{5.39}$$

where $z = e^{\mu/k_BT}$ is the fugacity, $\beta = 1/k_BT$, and we use $\nu = 1 + 2\theta$ as the Dunkl deformation parameter instead of θ. Using $\rho(\varepsilon) = A\,\varepsilon^{s-1}$ and splitting into two integrals $N_\varepsilon = I_1 + I_2$:

$$I_1 = 2A\int_0^\infty d\varepsilon\; \frac{\varepsilon^{s-1}}{z^{-2}e^{2\beta\varepsilon}-1}, \qquad I_2 = \nu A\int_0^\infty d\varepsilon\; \frac{\varepsilon^{s-1}}{z^{-\nu}e^{\beta\nu\varepsilon}+1}. \tag{5.40}$$

Recalling the standard Bose and Fermi integrals

$$\frac{1}{\Gamma(s)}\int_0^\infty dx\,\frac{x^{s-1}}{z^{-1}e^x-1} = g_s(z) \quad \text{(Bose)}, \qquad \frac{1}{\Gamma(s)}\int_0^\infty dx\,\frac{x^{s-1}}{z^{-1}e^x+1} = f_s(z) \quad \text{(Fermi)}, \tag{5.41}$$

and the identity $f_s(z) = -g_s(-z)$, one evaluates I_1 and I_2:

$$I_1 = \frac{\Gamma\left(\frac{D}{2}+\frac{D}{\eta}\right)}{2^{\frac{D}{2}+\frac{D}{\eta}-1}}\left(\frac{1}{\beta}\right)^{\frac{D}{2}+\frac{D}{\eta}} g_{\frac{D}{2}+\frac{D}{\eta}}(z^2), \tag{5.42}$$

$$I_2 = -\frac{\Gamma\left(\frac{D}{2}+\frac{D}{\eta}\right)}{\nu^{\frac{D}{2}+\frac{D}{\eta}-1}}\left(\frac{1}{\beta}\right)^{\frac{D}{2}+\frac{D}{\eta}} g_{\frac{D}{2}+\frac{D}{\eta}}(-z^\nu). \tag{5.43}$$

Setting $s = \dfrac{D}{2}+\dfrac{D}{\eta}$ and combining, we obtain

$$N_\varepsilon = A\,\Gamma(s)\left(\frac{1}{\beta}\right)^s\left[\frac{1}{2^{s-1}}\,g_s(z^2) - \frac{1}{\nu^{s-1}}\,g_s(-z^\nu)\right]. \tag{5.44}$$

Using the polylogarithm identity $g_s(z)+g_s(-z) = 2^{1-s}\,g_s(z^2)$, equation (5.44) can be rewritten as

$$N_\varepsilon = A\,\Gamma(s)\left(\frac{1}{\beta}\right)^s g_s(z,\nu), \tag{5.45}$$

where $g_s(z,\nu)$ is the generalised function defined previously (4.56)

$$g_s(z,\nu) = g_s(z) + g_s(-z) - \frac{1}{\nu^{s-1}}\,g_s(-z^\nu). \tag{5.46}$$

Substituting the explicit form of A from (5.38), the number of exited particles becomes

$$N_\varepsilon = \frac{2}{\eta}\,\frac{\Gamma\left(\frac{D}{\eta}\right)}{\Gamma\left(\frac{D}{2}\right)}\cdot\left(\frac{V_0}{2\hbar^2}\right)^{D/2}\cdot\left(\frac{ma^2}{1}\right)^{D/2}\cdot\left(\frac{k_BT}{V_0}\right)^s g_s(z,\nu). \tag{5.47}$$

- **b)Universality classes:** At this stage, we can extract the condition for the occurrence of Bose–Einstein condensation. In order for condensation to take place, the number of excited particles N_e given by the previous equation (5.47) must remain finite in the limit $z \to 1$. This requires that the function $g_s(1,\nu)$ be convergent. Since $g_s(1) = \zeta(s)$ diverges for $s \leq 1$, the existence of Bose–Einstein condensation requires $s > 1$ which leads to the mixed condition on the trap exponent and space dimension:

$$\frac{1}{\eta} > \frac{1}{D} - \frac{1}{2}. \tag{5.48}$$

This condition has the following implications for specific dimensions:

D=2 : condition (5.48) gives $\eta > 0$, so BEC occurs for any positive trap exponent.

D=1 : $\eta < 2$ is required; BEC is possible only for sufficiently steep traps.

D=3 : for $\eta > 0$, the condition $1/\eta > -1/6$ is always satisfied, so BEC occurs for any $\eta > 0$. For $\eta < 0$: $|\eta| > 6$ is required, meaning a trap of the form $1/r^{|\eta|}$ with $|\eta| > 6$ allows BEC.

Figure 5.1 depicts the various universality classes arising from the distinct domains of the (η, D) plane for which the condition $s > 1$ is satisfied.

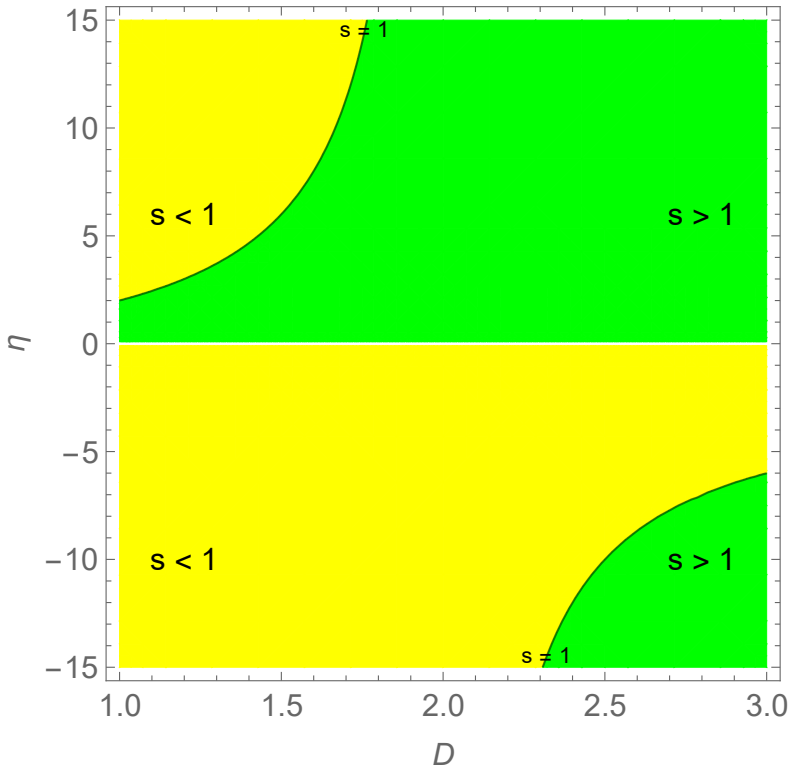

Figure 5.1: Universality classes characterized by the parameter s as a function of spatial dimension D and potential exponentη . Green regions correspond to where true Bose–Einstein condensation occurs ($s > 1$), while yellow regions indicate regimes where quasi-condensation is expected ($s < 1$). The boundary at $s = 1$ separates these distinct phases

In the regions $s < 1$, Physically significant situations are included , such as steep attractive potentials with $\eta > 2$ in one dimension and repulsive power-law potentials $\eta < 0$ in all dimensions. This behavior is particularly evident in three-dimensional systems for inverse power-law potentials in the range

$-6 < \eta < 0$, which can be experimentally accessible by manipulated inter-particle interactions or designed optical potentials.

For $s > 1$ the ground state weight disappears in the continuum limit and must be explicitly separated from the excited-state spectrum. Consequently true Bose-Einstein condensation becomes possible.

c-Transition Temperature: At the critical temperature T_c, the condensate fraction vanishes ($N_0 \approx 0$), $z \to 1$, then $N = N_\varepsilon(T_c)$ and according to the equations (5.47) we finally get :

$$\frac{k_B T_c}{V_0} = \left[\frac{\eta}{2} \cdot \frac{\Gamma\left(\frac{D}{2}\right)}{\Gamma\left(\frac{D}{\eta}\right)} \cdot \frac{N}{g_s(1,\nu)}\right]^{\frac{1}{s}} \left(\frac{2\hbar^2}{ma^2}\right)^{\frac{\eta}{2+\eta}}. \tag{5.49}$$

In order to more effectively observe the impact of the deformation parameter ν on the variation of the critical temperature T_c, we compare it to that of the undeformed case $\nu = 1$.

$$\frac{T_c(\nu)}{T_c(1)} = \left[\frac{g_s(1)}{g_s(1,\nu)}\right]^{1/s}, \qquad s = \frac{D(2+\eta)}{2\eta}, \tag{5.50}$$

In the strong-deformation limit $\nu \to \infty$, one can show that $\nu^{1-s} \to 0$, so that $g_s(1,\nu) \to g_s(1) + g_s(-1)$, where

$$g_s(-1) = \left(2^{1-s} - 1\right)\zeta(s)$$

giving finally:

$$\frac{T_c(\nu)}{T_c(1)} \xrightarrow{\nu\to\infty} \left[\frac{g_s(1)}{g_s(1) + g_s(-1)}\right]^{1/s} = 2^{-1/s}, \tag{5.51}$$

which recovers the known harmonic trap result, $\eta = 2$.

To better visualize the dependance of the Dunkl critical temperature with the deformation parametter , we illustrates in the figure 5.2 the ratio (5.50) for different values of the universality parameter s

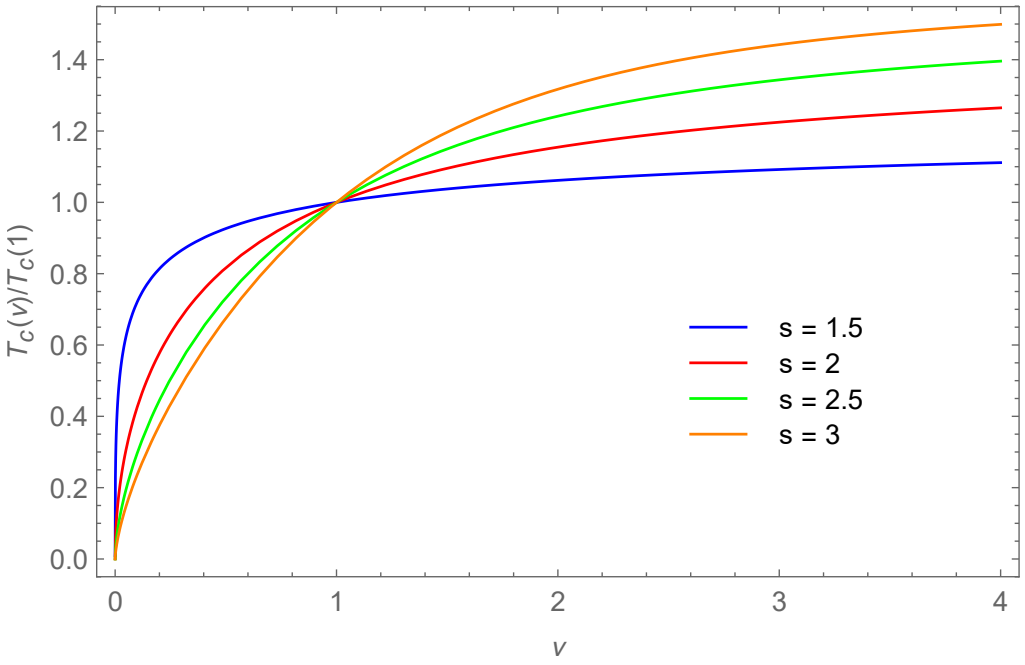

Figure 5.2: ratio $\frac{T_c(\nu)}{T_c(1)}$ versus the deformation parameter ν

We first see that the critical temperature $T_c(\nu)$ presents a dependence on both the universality parameter s and the deformation parameter ν and in second, as s increases, we observe a crossover behavior at $\nu = 1$ in such a way that:

For $\eta < 1$: $T_c(\nu)$ decreases with increasing s.

For $\eta > 1$: $T_c(\nu)$ increases with increasing s This crossover behavior manifests in two complementary ways as follows:

-fixed potential shape: In this situation we observe that higher-dimensional, systems exhibit lower critical temperatures for $\nu < 1$. but higher critical temperatures for $\nu > 1$.

-Fixed dimensionality: We observe that an increase in the trap exponent η raises the critical temperature for $\nu < 1$, while it lowers it for $\nu > 1$. In three dimensions, for example, a quartic confinement ($\eta = 4$) produces a transition temperature T_c higher than that of a harmonic trap ($\eta = 2$) for $\nu < 1$, whereas the ordering reverses for $\nu > 1$.

d) Condensate fraction: Another important parameter used to describe the evolution of a BEC as a function of the critical temperature T_c is the condensate fraction $\frac{N_0}{N}$. Combining equations (5.45) and equation (5.49), we get:

$$\frac{N_0}{N} = 1 - \left(\frac{T}{T_c}\right)^s \tag{5.52}$$

The figure 5.3 illustrates the behavior of this fraction. As predicted, the condensate fraction vanishes at the critical temperature and increases monotonically as the temperature decreases, ultimately reaching unity at absolute zero. For small s, the curve drops steeply, meaning the system is more sensitive to thermal fluctuations. Unlike large s the condensate remains more robust against thermal agitation — the curve remains high over a wider range of $T/T_c(\nu)$, meaning particles stay condensed up to temperatures closer to $T_c(\nu)$. These results confirm the predictions made by the theory regarding Bose-Einstein condensation in systems with varying confining geometries or dimensionality [62–73].

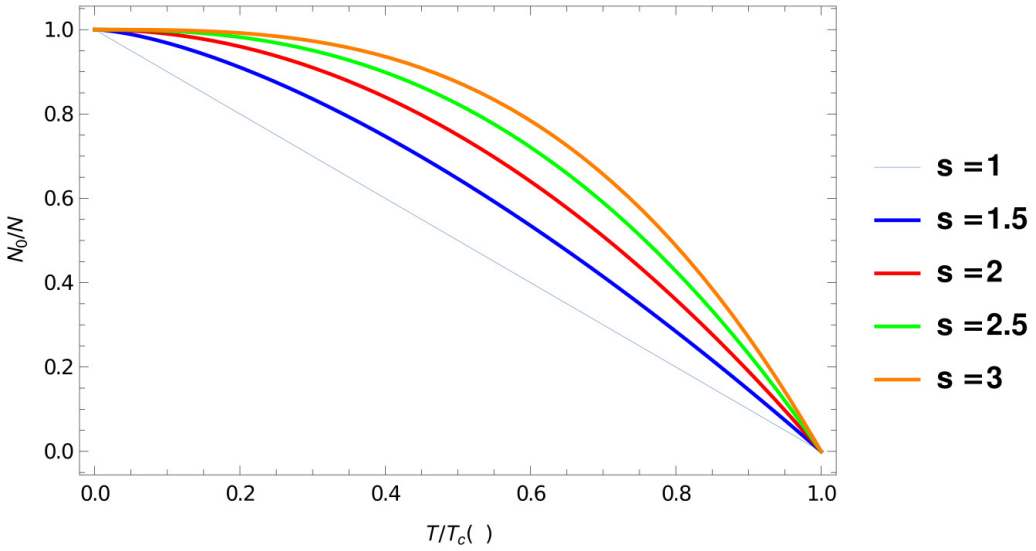

Figure 5.3: ratio $\frac{N_0}{N}$ versus $\frac{T}{T_c(\nu)}$

5.3.3 Thermodynamics

We proceed by calculating the internal energy of the system under consideration. Assuming a continuous energy spectrum, the internal energy of the system is given by:

$$U = \int_0^\infty d\varepsilon\, \varepsilon\, \rho(\varepsilon) \left[\frac{2}{(z^{-1}e^{\beta\varepsilon})^2 - 1} + \frac{\nu}{(z^{-1}e^{\beta\varepsilon})^\nu + 1} \right] \tag{5.53}$$

Using Eq (5.37), we one easily gets

$$\frac{U}{A} = \frac{\Gamma(s+1)}{\beta^{s+1}}\, g_{s+1}(z,\nu) \tag{5.54}$$

Noting that:

$$N_\varepsilon = A\, \frac{\Gamma(s)}{\beta^s}\, g_s(z,\nu) \tag{5.55}$$

the equation (5.54) leads to the more readable expression :

$$U = Nk_BT \left(s\,\Gamma(s) \cdot \frac{g_{s+1}(z,\nu)}{g_s(z,\nu)} \right) \tag{5.56}$$

$$= s\, Nk_BT \left(\frac{T}{T_c(\nu)} \right)^s \frac{g_{s+1}(z,\nu)}{g_s(1,\nu)} \tag{5.57}$$

This expression reveals, on the one hand, significant deviations from the classical equipartition result $U = sNk_BT$, and on other hand,shows that all thermodynamic properties are determined by only two parameters: the universality parameter $''s''$

and the deformation parameter $''\nu''$

Now let's investigate the heat capacity of a the Dunkl-boson system under consideration. This quantity represent one of the most basic thermodynamic concepts in statistical physics since it describes the system's capability to either absorb or release energy in response to a change in temperature. It provides important details on the nature of phase transitions: the beginning of a phase transition is indicated by a divergence or cusp in the heat capacity as a function of temperature. Using the internal energy given in (5.56) we deduce the heat capacity from its following definition:

$$C = \left.\frac{\partial U}{\partial T}\right|_{z,N} = A\, k_B\, \frac{\Gamma(s+1)}{\beta^{s-1}} \left[\frac{s+1}{\beta}\, g_{s+1}(z,\nu) - \frac{1}{z}\, g_s(z,\nu)\, \frac{dz}{d\beta}\right] \tag{5.58}$$

Since the energy given above depends on the temperature explicitly and implicitly trough the fugacity z the heat capacity behaves differently according to $T < T_c$ or $T > T_c$.

Heat capacity for $T < T_c$: For this case, the fugacity is $z = 1$, and therefore the internal energy depends explicitly only on T, then :

$$C_< = A\, k_B\, (s+1)\, \Gamma(s+1)\, \frac{1}{\beta^s}\, g_{s+1}(1,\nu) \tag{5.59}$$

and, finally

$$\frac{C_<}{N k_B} = s(s+1)\, \frac{g_{s+1}(1,\nu)}{g_s(1,\nu)} \left(\frac{T}{T_c(\nu)}\right)^s \tag{5.60}$$

This finding, as indicated in Ref [74], demonstrates the preservation of the T^s dependance of the heat capacity in the degenerate regime, despite the deformation of the underlying Heisenberg algebra. For $\eta \to \infty$ homogeneous case, $\eta = 2$ harmonic, and $\eta = 4$ quartic, we recover the results of the dependence; $T^{D/2}$, T^D and $T^{3D/4}$ dependences respectively reported in Refs [58, 75], respectively.

In order to letter examine the effect of the Dunkl defomation, we compute the ratio of $C_<$ ratio to the undeformed case, giving:

$$\frac{C_<(\nu)}{C_<(1)} = \frac{g_{s+1}(1,\nu)}{g_{s+1}(1)} = \frac{1}{2^s}\left[1 + \frac{2^s - 1}{\nu^s}\right] \tag{5.61}$$

For strong deformation, this ration tends to :

$$\frac{C_<(\nu)}{C_<(1)} \xrightarrow{\nu\to\infty} \frac{1}{2^s} \tag{5.62}$$

which is a kind for BEC saturation.

Applying the obtained equation to the harmonic oscillator case in 3D ($s = 3$) we recover the results reported in [58]:

$$\frac{C_<(\nu)}{C_<(1)} = \frac{g_4(1,\nu)}{g_4(1)} = \frac{1}{8}\left[1 + \frac{7}{\nu^3}\right] \tag{5.63}$$

In the case of 2-dimensional harmonic oscillator:

$$\frac{C_<(\nu)}{C_<(1)} = \frac{1}{8}\left[1 + \frac{7}{\nu^3}\right] \tag{5.64}$$

And for a 1-dimensional harmonic oscillator:

$$\frac{C_<(\nu)}{C_<(1)} = \frac{\nu+1}{2\,\nu} \xrightarrow{\nu\to\infty} \frac{1}{2} \tag{5.65}$$

Heat capacity for $T > T_c(\nu)$: If one recalls that $N_0 << N_e \simeq N$, we can simplify the implicit relation between z and T to get

$$\left(\frac{T_c}{T}\right)^s = \frac{g_s(z,\nu)}{g_s(1,\nu)} \tag{5.66}$$

therefore

$$\frac{dz}{d\beta} = \frac{z\,g_s(1,\nu)\,s\,\beta^{s-1}}{g_{s-1}(z,\nu)\,\beta_c^s}, \tag{5.67}$$

which yealds

$$\frac{C_>(\nu)}{Nk_B} = s\left[(s+1)\,\frac{g_{s+1}(z,\nu)}{g_s(z,\nu)} - s\,\frac{g_s(z,\nu)}{g_{s-1}(z,\nu)}\right] \tag{5.68}$$

As an illustration n the case $s = 3$, we recover the result of the $3D$ harmonic oscillator [58]:

$$\frac{C_>(\nu)}{Nk_B} = 12\,\frac{g_4(z,\nu)}{g_3(z,\nu)} - 9\,\frac{g_3(z,\nu)}{g_2(z,\nu)} \tag{5.69}$$

and for the $1D$ harmonic oscillator with $s = 1$, we find:

$$\frac{C_>(\nu)}{Nk_B} = 2\,\frac{g_2(z,\nu)}{g_1(z,\nu)} - \frac{g_1(z,\nu)}{g_2(z,\nu)} \tag{5.70}$$

It is important to underline that the expressions (5.60) and (5.68) for $C_<$ and $C_>$ represent natural generalizations of the results reported in [21, 56, 58, 74–76].

Another important point, though less apparent, is the overall dependence of $C_>$, which remains unchanged by the deformation parameter. This can be seen by examining its behavior in the vicinity of the critical temperature $T \to T_c^+$ $(z \to 1^-)$.

From equation (5.66) we obtain :

$$1-z \simeq \frac{(1-\nu^{1-s})(1-2^{1-s})\,\zeta(s)}{(1-\nu^{2-s})(1-2^{2-s})\,\zeta(s-1)} - \frac{1}{(1-\nu^{2-s})(1-2^{2-s})\,\zeta(s-1)} \left(\frac{T_c}{T}\right)^s \quad (5.71)$$

Expanding the generalized Bose functions in Eq.(5.68) around $z = 1$, and employing Eq.(5.71), we readily obtain the following expression.

$$\frac{C_>(\nu)}{Nk_B} = a(\nu, s) + b(\nu, s) \left(\frac{T_c}{T}\right)^s \quad (5.72)$$

where a and b are functions of ν and s alone. This result clearly demonstrates that the deformation does not modify the characteristic T^{-s} critical behavior of the heat capacity. This very deep and related the preserved symetry of the Hamiltonian

In figure 5.4 we display the heat capacity as a function of the reduced temperature T/T_c for four values of the parameter s: $s = 3/2$ (upper left), $s = 2$ (upper right), $s = 5/2$ (lower left) and $s = 3$ (lower right). In each panel, three values of the deformation parameter are considered: $\nu = 0.5$ (blue), $\nu = 1$ (red, corresponding to the undeformed case), and $\nu = 1.5$ (green).

The characteristic λ-point behavior is observed throughout the entire range of investigated values of s and ν. In general, the heat capacity exhibits a finite discontinuity at the critical temperature T_c, which is the hallmark of a second-order phase transition. A remarkable exception arises at $s = 2$, where the heat capacity displays a sharp but continuous peak at the transition point, rather than a discontinuous jump. This qualitative distinction stems directly from Eq. (5.68), in which the second term involves the function $g_1(z, \nu)$, which diverges logarithmically as $z \to 1^-$, thereby inducing a fundamentally different critical behavior at this particular value of s. The continuity at $s = 2$ was reported in [74] for the case of two-dimensional harmonic oscillator.

This behavior, characteristic of the universality class defined by $s = 2$, includes a $x^2/3$ potential in one dimension and a r^6 potential in three dimensions. For $0 < \nu < 1$, the heat capacity is found to exceed that of the undeformed case ($\nu = 1$), which indicates an enhancement of energy fluctuations. Conversely, for $\nu > 1$, the heat capacity is systematically suppressed below its standard counterpart, reflecting a reduction fluctuations under the influence of stronger deformations.

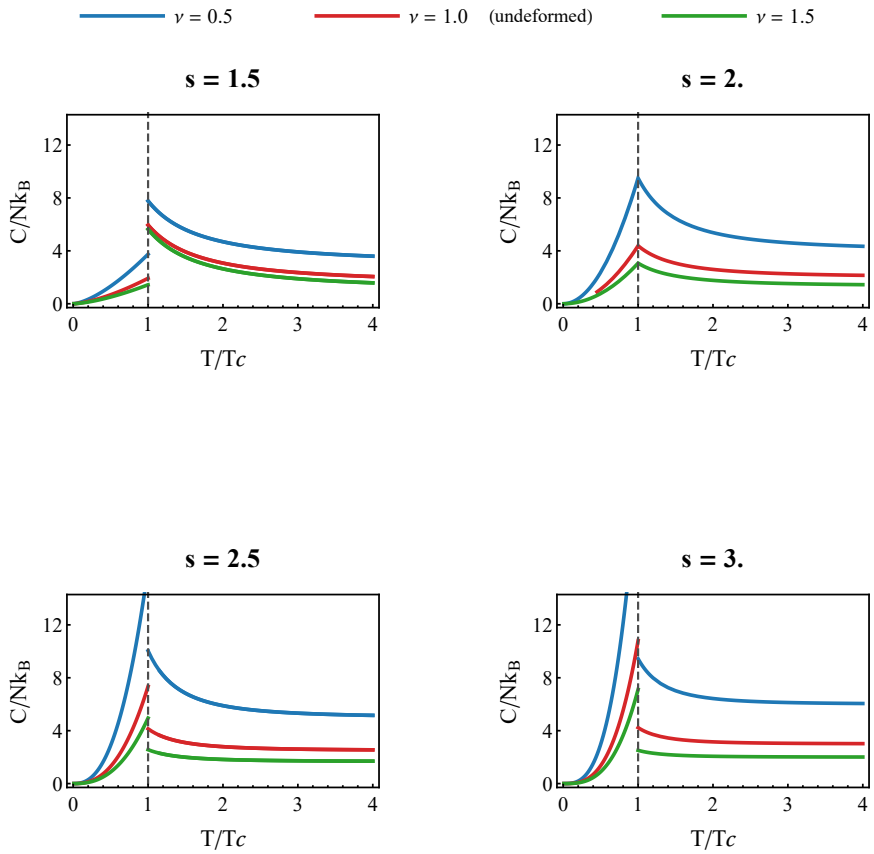

Figure 5.4: Heat capacity (normalized to Nk_B) as a function of reduced temperature T/T_c for various uni versality parameter values s. The four panels show $s = 1.5$ (upper left), $s = 2.0$ (upper right), $s = 2.5$ (lower left), and $s = 3.0$ (lower right). Three deformation parameters are displayed: $\nu = 0.5$ (blue curves),$\nu = 1.0$ (red curves, undeformed case), and $\nu = 1.5$ (green curves). The vertical dashed line marks the critical temperature T_c . Note that $s = 2.0$ exhibits a continuous transition without discontinuity, while all other s values show characteristic jumps at the phase transition

To develop a more thorough understanding of how the heat capacity behaves at the critical point, we investigate the discontinuity at $T_c(\nu)$.

After evaluating the polylogarithmic functions entering the expression, the discontinuity is obtained:

$$\left.\frac{C_< - C_>}{Nk_B}\right|_{T_c} = \Delta C = s^2 \, \frac{g_s(1,\nu)}{g_{s-1}(1,\nu)} \tag{5.73}$$

$$= \frac{s^2}{2} \, \frac{\zeta(s)}{\zeta(s-1)} \cdot \frac{1}{\nu} \cdot \frac{\nu^{s-1} + 2^{s-1} - 1}{\nu^{s-2} + 2^{s-2} - 1} \tag{5.74}$$

This equation show that for $\nu = 1$ this discontinuity reduces to the following expression $s^2\,\zeta(s)/\zeta(s-1)$ and reproduces the results reported in ref [58, 74] for the three harmonic oscillator, which is $54\,\zeta(3)/\pi^2$ and confirms the case $s = 2$ by giving $\Delta C = 0$.

In the figure 5.5, we represent this discontinuity as a function of both deformation ν and universality parameter s. The phase transition has standard behavior with positive heat capacity changes ($\Delta C > 0$) for $s > 2$, but becomes atypical with negative changes $\Delta C < 0$ in the interval $1 < s < 2$.

This anomalous regime encompasses $\frac{2}{3} < \eta < 2$ (one dimension), $\eta > 2$ (two dimensions), and $\eta > 6$ or $\eta < -6$ (three dimensions). The negative discontinuity indicates unexpected thermodynamics: Heat capacity drops upon condensation, reflecting increased thermal stability below T_c.This behavior is notably independent of the deformation parameter, hence characterizing entire universality classes rather than specific trap geometries.

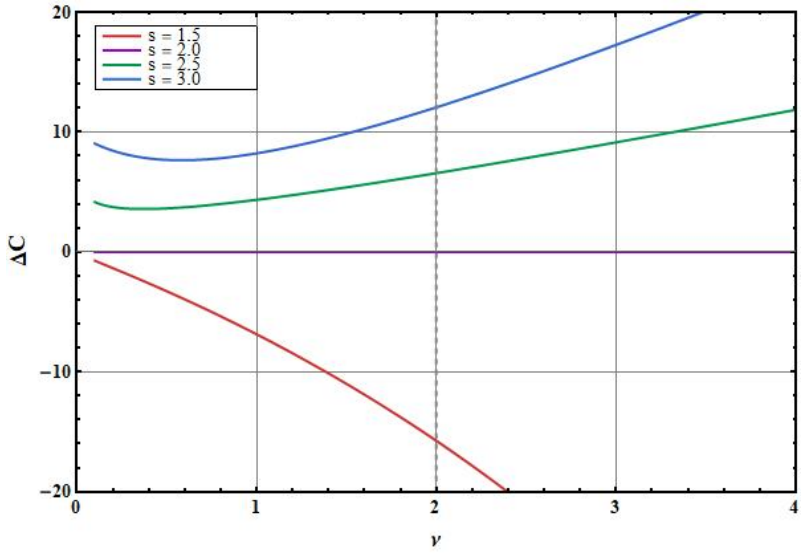

Figure 5.5: Discontinuity ΔC versus the deformation parameter ν for four universality parameters. $s = 1.5$ (red): $\Delta C < 0$, $s = 2$ (purple): continuous BKT-like transition, $s = 2.5$ (green) and $s = 3$ (blue): $\Delta C > 0$. The vertical dashed line at $\nu = 2$ depicts the critical boundary for the physical validity of the Dunkl formalism

5.3.4 Classical Limit and Physical Consistency

In this subsection, we investigate the classical limit and verify the consistency of the theory by recovering the equipartition theorem in the high-temperature limit.

As follows from Eq.(5.66), in the high-temperature regime $T >> T_c$, the $g_s(z,\nu) << 1$. Since $g_s(z) = \sum_{k=1}^{\infty} \frac{z^k}{k^s}$, it is easily seen that is:

$$g_s(z,\nu) = \frac{z^2}{2^{s-1}} + 2\cdot\frac{z^4}{4^s} + \cdots + \frac{1}{\nu^{s-1}}\left[\frac{z^\nu}{1^s} + \frac{z^{2\nu}}{2^s} - \frac{z^{3\nu}}{3^s} + \cdots\right] \tag{5.75}$$

Case $0 < \nu < 2$**:** Since $z^2 \ll z^\nu$ as $z \to 0$ the dominant term is z^ν, hence

$$g_s(z,\nu) \simeq \frac{z^\nu}{\nu^{s-1}} \tag{5.76}$$

Therefore the heatcapacity behave as

$$\frac{C_>}{Nk_B} \simeq \frac{s}{\nu} \tag{5.77}$$

Setting $\nu = 1$, we retrieve the undeformed classical case $\frac{c_>}{Nk_B}$ while we observe enhancement of $c_>$ for $0 < \nu < 1$ and suppression for $\nu > 1$ as compared to the undeformed case.

-Case : $\nu = 2$ The leading terms are z^2 and z^ν. This leads to which exactly the classical undeformed case.

$$\frac{C_>}{Nk_B} = s \tag{5.78}$$

Case : $\nu > 2$ Since $z^\nu \ll z^2$ as $z \to 0$, the leading term z^2 : thus, giving a heat capacity:

$$\frac{C_>}{Nk_B} \simeq \frac{s}{2} \tag{5.79}$$

which different to the undeformed situation, this ν-independent finding shows thermodynamically incompatible behavior. Physical consistency therefore indicates that the range where classical thermodynamics is correctly recovered is defined by $0 < \nu \leq 2$. For $\nu > 2$, while mathematically allowed, the heat capacity saturates at $C = \frac{s}{2}Nk_B$, reflecting a reduction in the effective degrees of freedom This constraint generalizes previous results [74] to arbitrary power-law traps in any spatial dimension. Our analysis provides universal upper and lower bounds, in contrast to previous studies that treated it as a free parameter with only a lower constraint. As a result, the validity of the Dunkl deformation is essentially limited: regard-

less of trap shape or spatial dimension, classical consistency imposes the universal limitation $0 < \nu \leq 2$.

The central result of this chapter is the emergence of a universal parameter $s = D(1/\eta + 1/2)$, which completely governs the thermodynamic behavior of the system. This universality implies that physically distinct systems, differing in spatial dimension D and confinement exponent η, exhibit identical thermodynamic properties whenever they share the same value of s. Bose-Einstein condensation is found to occur exclusively for $s > 1$, in accordance with the Mermin-Wagner-Hohenberg theorem. The heat capacity displays characteristic power-law scaling, following a T^s dependence below T_c and a T^{-s} behavior in the vicinity of the critical point. The BEC transition remains second order for all $s \neq 2$, whereas the case $s = 2$ gives rise to a continuous transition reminiscent of Berezinskii-Kosterlitz-Thouless transition.

Conclusion

The present thesis is devoted to a systematic investigation of Bose gases systems, within the Dunkl formalism and the ensuing physical implications.

The first chapter provides a self-contained introduction to the concept of deformed algebras, establishing their mathematical foundations and elucidating their relevance in the context of quantum mechanics and statistical physics. Since the objective of this thesis is to investigate ideal-Bose gases systems within the framework of the deformed Heisenberg algebra, it is natural to begin by recalling in chapter-2 the origins and fundamental principles of this algebra. In this context, we revisit the seminal contributions of Wigner and Yang, and trace the subsequent mathematical developments that, through the foundational work of Dunkl, culminated in the rigorous formulation of the Dunkl differential-difference operator and its associated algebraic structure. Simultaneously, by employing the Wigner-Dunkl deformation formalism, the present investigation extends beyond the standard quantum mechanical framework, revealing novel spectral structures and modified quantum states in paradigmatic systems such as the particle in a box and the harmonic oscillator.

Chapter 3 is devoted to Bose-Einstein condensation of an ideal Bose gas, providing a rigorous treatment of the phenomenon from the perspective of quantum statistical mechanics. Particular attention is devoted to the derivation and analysis of the key thermodynamic quantities governing the condensation, including the partition function, density of states and occupation number in the standard framework.

Chapter 4 develops a systematic investigation of the statistical mechanics of an ideal Bose gas within the Dunkl formalism, built upon a novel approach based on the reflection operator. Starting from the homogeneous untrapped case and extending to harmonically confined systems, the analysis covers arbitrary spatial dimensions with particular attention to $D = 1$, $D = 2$, and $D = 3$. The central focus is the role of the Wigner deformation parameter ν, whose influence on the thermodynamic behavior of the gas is examined through three key quantities: the density of states, the critical transition temperature, and the heat capacity. The results consistently show that the Dunkl deformation induces significant and systematic departures from the

standard Bose–Einstein statistics, with modifications that grow with ν and persist across all dimensions and confinement geometries considered.

In the last chapter, we examine the thermodynamic of ideal Bose gas in power law within the Dunkl formalism, covering both the general case of arbitrary dimension and the specific cases $D = 1$, $D = 2$, and $D = 3$.

Beyond the results obtained in this thesis, several questions remain open and provide promising directions for future research. In particular, the extension of the present analysis to interacting systems, the study of fermionic gases within the Dunkl framework, and the investigation of dynamical properties constitute natural perspectives that could further clarify the physical implications of the deformation parameter.

Appendix A

Confluent Hypergeometric Function and the Frobenius Series Solution

In this appendix, we detail the identification of the Frobenius series solution of the radial eigenvalue equation with the confluent hypergeometric function ${}_0F_1$, and establish the explicit form of the energy eigenfunctions in terms of this special function [77–79].

The Confluent Hypergeometric Function ${}_0F_1$

The confluent hypergeometric function ${}_0F_1$ is defined by the power series:

$$ {}_0F_1(b;\, z) = \sum_{n=0}^{\infty} \frac{z^n}{(b)_n\, n!}, \tag{A.1} $$

where $(b)_n$ denotes the Pochhammer symbol (rising factorial), defined by:

$$ (b)_n = b(b+1)(b+2)\cdots(b+n-1), \qquad (b)_0 = 1, \tag{A.2} $$

or equivalently in terms of the Gamma function:

$$ (b)_n = \frac{\Gamma(b+n)}{\Gamma(b)}. \tag{A.3} $$

The series converges absolutely for all $z \in \mathbb{C}$, provided $b \notin \{0, -1, -2, \ldots\}$.

The Frobenius Series and Recurrence Relation

The Frobenius method applied to the eigenvalue equation yields a series solution of the form:

$$\psi(x) = \sum_{n=0}^{\infty} a_n \, x^{2n+\lambda}, \tag{A.4}$$

where λ is the indicial exponent determined by the indicial equation, and the coefficients $\{a_n\}$ satisfy the two-term recurrence relation:

$$a_n = \frac{2mE_+}{(2n+\lambda)(2n-1+\lambda+2\nu)} \, a_{n-1}, \qquad n \geq 1, \tag{A.5}$$

with a_0 an arbitrary normalization constant. The entire series is therefore determined by a_0 through successive iteration of (A.5).

Iteration and Identification with Pochhammer Symbols

We now iterate the recurrence relation (A.5) explicitly. At the first few orders:

$$a_1 = \frac{2mE_+}{(2+\lambda)(1+\lambda+2\nu)} \, a_0, \tag{A.6}$$

$$a_2 = \frac{(2mE_+)^2}{(2+\lambda)(4+\lambda)(1+\lambda+2\nu)(3+\lambda+2\nu)} \, a_0, \tag{A.7}$$

$$a_3 = \frac{(2mE_+)^3}{(2+\lambda)(4+\lambda)(6+\lambda)(1+\lambda+2\nu)(3+\lambda+2\nu)(5+\lambda+2\nu)} \, a_0. \tag{A.8}$$

The pattern is now manifest: the numerator accumulates powers of $2mE_+$, while the denominator organizes into two independent chains of consecutive factors. These chains are precisely rising factorials. Indeed, introducing the parameters:

$$\alpha = \frac{\lambda}{2} + 1, \qquad \beta = \frac{\lambda}{2} + \nu + \frac{1}{2}, \tag{A.9}$$

one verifies that:

$$(2+\lambda)(4+\lambda)\cdots(2n+\lambda) = 2^n \, (\alpha)_n, \tag{A.10}$$

$$(1+\lambda+2\nu)(3+\lambda+2\nu)\cdots(2n-1+\lambda+2\nu) = 2^n \, (\beta)_n. \tag{A.11}$$

Substituting into the iterated recurrence, the general coefficient takes the closed form:

$$\boxed{a_n = \frac{(mE_+)^n}{n!\,(b)_n}\,a_0,} \tag{A.12}$$

where the parameter b encodes the dependence on λ and ν through the Pochhammer structure of the denominator, and is given by:

$$b = \frac{\lambda + 2\nu + 1}{2}. \tag{A.13}$$

Identification with ${}_0F_1$

Substituting the closed-form expression for a_n into the Frobenius series:

$$\psi(x) = \sum_{n=0}^{\infty} a_n\, x^{2n+\lambda} = a_0\, x^{\lambda} \sum_{n=0}^{\infty} \frac{(mE_+)^n}{n!\,(b)_n}\, x^{2n}, \tag{A.14}$$

and comparing with the standard definition of ${}_0F_1$, one recognizes immediately that:

$$\psi(x) = a_0\, x^{\lambda} \sum_{n=0}^{\infty} \frac{(mE_+x^2)^n}{(b)_n\, n!} = a_0\, x^{\lambda}\, {}_0F_1\big(b;\, mE_+\, x^2\big)\,. \tag{A.15}$$

Hence the Frobenius series solution is expressed compactly as:

$$\boxed{\psi(x) = a_0\, x^{\lambda}\, {}_0F_1\left(\frac{\lambda + 2\nu + 1}{2};\; mE_+\, x^2\right),} \tag{A.16}$$

which constitutes the exact closed-form eigenfunction in terms of the confluent hypergeometric function ${}_0F_1$.

Termination Condition and Energy Quantization

For the solution $\psi(x)$ to be physically admissible, it must be square-integrable. Since the asymptotic growth of ${}_0F_1(b; z)$ for large $|z|$ is exponential, the series must terminate at a finite order. This occurs if and only if the numerator of a_n vanishes at some $n = N$, which requires:

$$mE_+ = 0 \quad \text{or} \quad N \in \mathbb{N}, \tag{A.17}$$

imposing a quantization condition on the energy E_+ and yielding a discrete spectrum. In this case, ${}_0F_1$ reduces to a polynomial of degree N, and the eigenfunctions

become square-integrable.

Appendix B

The Generalized Bose–Einstein Function

This appendix provides a rigorous and self-contained treatment of the generalized Bose–Einstein function $g_s(z, \theta)$

The Standard Bose–Einstein Function

The standard Bose–Einstein function of order $s \in \mathbb{C}$ and fugacity $z \in \mathbb{C}$ is defined by the power series:

$$g_s(z) \;=\; \sum_{k=1}^{\infty} \frac{z^k}{k^s}, \qquad |z| \leq 1, \quad \mathrm{Re}(s) > 0. \tag{B.1}$$

This coincides with the polylogarithm $\mathrm{Li}_s(z)$. At $z = 1$ the series reduces to the Riemann zeta function,

$$g_s(1) = \zeta(s), \qquad \mathrm{Re}(s) > 1, \tag{B.2}$$

while at $z = -1$ one obtains the Dirichlet eta function,

$$g_s(-1) = -\eta(s) = -(1 - 2^{1-s})\,\zeta(s), \qquad \mathrm{Re}(s) > 0. \tag{B.3}$$

The integral representation, derived in full in Section B.0.2, reads:

$$g_s(z) = \frac{1}{\Gamma(s)} \int_0^{\infty} \frac{x^{s-1}}{e^x z^{-1} - 1}\, dx, \qquad 0 < z \leq 1, \quad \mathrm{Re}(s) > 0. \tag{B.4}$$

A key identity that relates the Bose–Einstein function at z and $-z$ to the function

at z^2 is the following.

For all z with $|z| < 1$ and $s \in \mathbb{C}$:

$$g_s(z) + g_s(-z) = 2^{1-s}\, g_s(z^2). \tag{B.5}$$

Starting from the series definitions:

$$g_s(z) + g_s(-z) = \sum_{k=1}^{\infty} \frac{z^k}{k^s} + \sum_{k=1}^{\infty} \frac{(-z)^k}{k^s} = \sum_{k=1}^{\infty} \frac{z^k + (-z)^k}{k^s}. \tag{B.6}$$

Since $z^k + (-z)^k = 0$ for odd k and $2z^k$ for even k, only the even terms survive. Setting $k = 2j$:

$$g_s(z) + g_s(-z) = \sum_{j=1}^{\infty} \frac{2\, z^{2j}}{(2j)^s} = 2 \sum_{j=1}^{\infty} \frac{(z^2)^j}{2^s\, j^s} = \frac{2}{2^s} \sum_{j=1}^{\infty} \frac{(z^2)^j}{j^s} = 2^{1-s}\, g_s(z^2). \tag{B.7}$$

The Generalized Bose–Einstein Function $g_s(z, \theta)$

In the Dunkl formalism, the statistical mechanics of a confined Bose gas leads naturally to a combination of Bose–Einstein functions of z, $-z$, and $-z^{1+2\theta}$

Let $s \in \mathbb{C}$ with $\mathrm{Re}(s) > 0$, let $z \in (0, 1]$ be the fugacity. The generalized Bose–Einstein function is defined as:

$$g_s(z, \theta) \;=\; g_s(z) + g_s(-z) - \frac{1}{(1+2\theta)^{s-1}}\, g_s\big(-z^{1+2\theta}\big)\,. \tag{B.8}$$

Using the symmetry identity (B.5), the definition can be rewritten in the equivalent compact form:

$$g_s(z, \theta) \;=\; 2^{1-s}\, g_s(z^2) - \frac{1}{(1+2\theta)^{s-1}}\, g_s\big(-z^{1+2\theta}\big)\,, \tag{B.9}$$

Setting $\theta = 0$ and using (B.5):

$$g_s(z, 0) = g_s(z) + g_s(-z) - g_s(-z) = g_s(z), \tag{B.10}$$

we recover the standard case.

B.0.1 Series Expansion

Applying the series (B.1) to each term in (B.8):

$$\begin{aligned} g_s(z,\theta) &= \sum_{k=1}^{\infty} \frac{z^k}{k^s} + \sum_{k=1}^{\infty} \frac{(-z)^k}{k^s} - \frac{1}{(1+2\theta)^{s-1}} \sum_{k=1}^{\infty} \frac{(-z^{1+2\theta})^k}{k^s} \\ &= \sum_{k=1}^{\infty} \frac{z^k \left[1+(-1)^k\right]}{k^s} - \frac{1}{(1+2\theta)^{s-1}} \sum_{k=1}^{\infty} \frac{(-1)^k\, z^{k(1+2\theta)}}{k^s}. \end{aligned} \tag{B.11}$$

Since $1+(-1)^k$ vanishes for all odd k and equals 2 for all even k, setting $k = 2j$ in the first sum:

$$g_s(z,\theta) = \frac{2}{2^s} \sum_{j=1}^{\infty} \frac{z^{2j}}{j^s} - \frac{1}{(1+2\theta)^{s-1}} \sum_{k=1}^{\infty} \frac{(-1)^k\, z^{k(1+2\theta)}}{k^s}, \tag{B.12}$$

which agrees with (B.9) expressed in series form. The conditions of validity are $|z| < 1$ and $|z|^{1+2\theta} < 1$, both of which are satisfied simultaneously for $|z| < 1$ and $\theta \geq 0$.

B.0.2 Integral Representation

[Integral Representation For $\mathrm{Re}(s) > 0$ and $0 < z \leq 1$:

$$g_s(z) = \frac{1}{\Gamma(s)} \int_0^{\infty} \frac{x^{s-1}}{e^x z^{-1} - 1}\, dx. \tag{B.13}$$

Proof. Starting from the series $g_s(z) = \sum_{k=1}^{\infty} z^k/k^s$, apply the integral representation of the Gamma function to each term:

$$\frac{1}{k^s} = \frac{1}{\Gamma(s)} \int_0^{\infty} t^{s-1}\, e^{-kt}\, dt, \qquad \mathrm{Re}(s) > 0, \quad k \geq 1. \tag{B.14}$$

Substituting:

$$g_s(z) = \frac{1}{\Gamma(s)} \sum_{k=1}^{\infty} z^k \int_0^{\infty} t^{s-1}\, e^{-kt}\, dt. \tag{B.15}$$

To interchange sum and integral, we bound the sum of absolute values:

$$\sum_{k=1}^{\infty} \int_0^{\infty} t^{s-1}\, |z|^k\, e^{-kt}\, dt = \Gamma(s)\, g_s(|z|) < \infty, \tag{B.16}$$

which is finite for $|z| < 1$ and $\mathrm{Re}(s) > 0$. By Fubini's theorem the interchange is

justified, giving:

$$g_s(z) = \frac{1}{\Gamma(s)} \int_0^\infty t^{s-1} \underbrace{\sum_{k=1}^{\infty} \left(z\, e^{-t}\right)^k}_{= ze^{-t}/(1-ze^{-t})}\, dt = \frac{1}{\Gamma(s)} \int_0^\infty \frac{t^{s-1}}{z^{-1}e^t - 1}\, dt. \tag{B.17}$$

□

Applying Proposition B.0.2 to each of the three terms in Definition B:

$$g_s(z,\theta) = \frac{1}{\Gamma(s)} \int_0^\infty x^{s-1} \left[\frac{1}{z^{-1}e^x - 1} + \frac{1}{z^{-1}e^x + 1} - \frac{1}{(1+2\theta)^{s-1}} \cdot \frac{1}{z^{-(1+2\theta)}e^x + 1} \right] dx. \tag{B.18}$$

The first two integrands combine as:

$$\frac{1}{z^{-1}e^x - 1} + \frac{1}{z^{-1}e^x + 1} = \frac{2\, z^{-1}e^x}{(z^{-1}e^x)^2 - 1} = \frac{2}{z^{-2}e^{2x} - 1}, \tag{B.19}$$

leading to the more compact form:

$$g_s(z,\theta) = \frac{1}{\Gamma(s)} \int_0^\infty x^{s-1} \left[\frac{2}{z^{-2}e^{2x} - 1} - \frac{1}{(1+2\theta)^{s-1}} \cdot \frac{1}{z^{-(1+2\theta)}e^x + 1} \right] dx. \tag{B.20}$$

.

B.0.3 Convergence Properties

Convergence of the Standard Function

From the series (B.1), the ratio test gives absolute convergence for $|z| < 1$ for all $s \in \mathbb{C}$. At $|z| = 1$ convergence depends on $\mathrm{Re}(s)$:

- $\mathrm{Re}(s) > 1$: $g_s(\pm 1)$ is absolutely convergent and finite; $g_s(1) = \zeta(s)$.
- $0 < \mathrm{Re}(s) \leq 1$: $g_s(1)$ diverges; $g_s(-1)$ converges conditionally for $\mathrm{Re}(s) > 0$.
- $\mathrm{Re}(s) \leq 0$: both series diverge at $|z| = 1$.

B.0.4 Convergence of the Generalized Function

For $g_s(z,\theta)$ as defined in (B.8), the conditions of convergence are determined by the most restrictive of the three constituent series:

$$|z| < 1 \quad \text{and} \quad |z|^{1+2\theta} < 1, \tag{B.21}$$

both of which reduce to $|z| < 1$ for $\theta \geq 0$. At $z = 1$, convergence of $g_s(1, \theta)$ requires:

$$g_s(1) = \zeta(s) < \infty \quad \Longleftrightarrow \quad \mathrm{Re}(s) > 1, \tag{B.22}$$

$$g_s(-1) = -\eta(s) < \infty \quad \Longleftrightarrow \quad \mathrm{Re}(s) > 0, \tag{B.23}$$

$$g_s(-1) = -\eta(s) < \infty \quad \Longleftrightarrow \quad \mathrm{Re}(s) > 0. \tag{B.24}$$

Therefore $g_s(1, \theta) < \infty$ if and only if $\mathrm{Re}(s) > 1$, which is precisely the condition for Bose–Einstein condensation to occur.

B.0.5 Asymptotic Expansions and Critical Behavior

B.0.5.1 Behavior as $z \to 1^-$: Standard Function

The Laurent expansion of $g_s(z)$ around $z = 1$ (equivalently, around $\mu = 0$ with $z = e^{\mu/k_B T}$ and $\mu \to 0^-$) for non-integer $s > 1$ is given by the Sommerfeldtype expansion:

$$g_s(z) = \Gamma(1 - s)\,(-\ln z)^{s-1} + \sum_{n=0}^{\infty} \frac{\zeta(s - n)}{n!}\,(\ln z)^n, \qquad z \to 1^-. \tag{B.25}$$

The dominant singular behavior is:

$$g_s(z) \simeq \zeta(s) + \Gamma(1 - s)\left(\frac{|\mu|}{k_B T}\right)^{s-1} + \mathcal{O}(|\mu|/k_B T), \qquad \mu \to 0^-. \tag{B.26}$$

For $s > 1$, the power $(s - 1) > 0$, so the singular term vanishes as $\mu \to 0^-$ and $g_s(1) = \zeta(s)$ is approached continuously. For $0 < s \leq 1$, the singular term diverges, indicating that $g_s(z)$ cannot be bounded as $z \to 1^-$, and BEC is suppressed.

B.0.5.2 Critical Behavior of $g_s(z, \theta)$

At the critical point $z = 1$ and for $s > 1$, the generalized function evaluates to:

$$\begin{aligned} g_s(1, \theta) &= g_s(1) + g_s(-1) - \frac{1}{(1 + 2\theta)^{s-1}}\, g_s(-1) \\ &= \zeta(s) - \eta(s)\left[1 - \frac{1}{(1 + 2\theta)^{s-1}}\right] \\ &= \zeta(s) - (1 - 2^{1-s})\,\zeta(s)\left[1 - \frac{1}{(1 + 2\theta)^{s-1}}\right], \end{aligned} \tag{B.27}$$

where we used $\eta(s) = (1 - 2^{1-s})\zeta(s)$. This can be simplified to:

$$g_s(1, \theta) = \zeta(s) \left[2^{1-s} + (1 - 2^{1-s}) \frac{1}{(1 + 2\theta)^{s-1}} \right]. \tag{B.28}$$

For $\theta = 0$: $g_s(1, 0) = \zeta(s)\left[2^{1-s} + (1 - 2^{1-s})\right] = \zeta(s)$, confirming the recovery of the standard result.

B.0.6 High-Temperature (Classical) Limit

For $z \ll 1$, the series (B.12) is dominated by its first term. Using (B.9):

$$g_s(z, \theta) \simeq 2^{1-s}\, z^2 + \frac{1}{(1 + 2\theta)^{s-1}}\, z^{1+2\theta} + \mathcal{O}(z^4,\, z^{2(1+2\theta)}), \qquad z \to 0, \tag{B.29}$$

recovering the Maxwell–Boltzmann limit with modifications in the effective fugacity powers due to the deformation.

Recurrence Relations and Special Values

B.0.7 Differentiation Identity

From the series definition (B.1), differentiation with respect to $\ln z$ yields the fundamental recurrence:

$$z \frac{d}{dz}\, g_s(z) = g_{s-1}(z), \qquad s \in \mathbb{C}. \tag{B.30}$$

For the generalized function, applying the same operation to (B.8):

$$z \frac{d}{dz}\, g_s(z, \theta) = g_{s-1}(z, \theta), \tag{B.31}$$

which shows that $g_s(z, \theta)$ and $g_{s-1}(z, \theta)$ are linked by the same recurrence as the standard functions.

B.0.8 Special Values

The most frequently encountered values in the thermodynamic calculations of this thesis are collected here for reference:

$$g_{3/2}(1) = \zeta(3/2) \approx 2.612, \tag{B.32}$$

$$g_{5/2}(1) = \zeta(5/2) \approx 1.342, \tag{B.33}$$

$$g_{3/2}(-1) = -(1 - 2^{-1/2})\,\zeta(3/2) \approx -0.765, \tag{B.34}$$

$$g_{5/2}(-1) = -(1 - 2^{-3/2})\,\zeta(5/2) \approx -0.451. \tag{B.35}$$

From (B.28), the critical values of the generalized function are:

$$g_s(1, \theta) = \zeta(s)\left[2^{1-s} + (1 - 2^{1-s})\,(1 + 2\theta)^{1-s}\right], \qquad \mathrm{Re}(s) > 1. \tag{B.36}$$

Appendix C

Coxeter Groups and Reflection Symmetries

Definition of Coxeter Groups

A *Coxeter group* G is a group generated by a finite set of elements $\{s_1, s_2, \ldots, s_m\}$, called *simple reflections*, subject to the relations

$$(s_i)^2 = 1, \qquad (s_i s_j)^{m_{ij}} = 1 \quad \text{for } i \neq j,$$

where $m_{ij} = m_{ji} \in \mathbb{N} \cup \{\infty\}$, with $m_{ii} = 1$. The integer m_{ij} determines the order of the product $s_i s_j$.

These relations completely determine the algebraic structure of the group.

Geometric Realization as a Reflection Group

A Coxeter group admits a natural realization as a subgroup of the orthogonal group $O(\mathbb{R}^N)$, generated by reflections. Each generator s_i is represented as a reflection with respect to a hyperplane orthogonal to a vector $v_i \in \mathbb{R}^N$:

$$s_i(x) = x - 2\frac{\langle x, v_i \rangle}{\langle v_i, v_i \rangle} v_i.$$

The associated hyperplane is

$$H_i = \{x \in \mathbb{R}^N \mid \langle x, v_i \rangle = 0\}.$$

Thus, the group G is generated by reflections across a finite collection of hyper-

planes.

Interpretation of the Coxeter Relations

The relation

$$(s_i s_j)^{m_{ij}} = 1$$

has a direct geometric interpretation. The composition of two reflections s_i and s_j is a rotation in the plane spanned by v_i and v_j, with rotation angle equal to $2\theta_{ij}$, where θ_{ij} is the angle between the two reflecting hyperplanes.

The above condition implies

$$2\theta_{ij} = \frac{2\pi}{m_{ij}} \quad \Longrightarrow \quad \theta_{ij} = \frac{\pi}{m_{ij}}.$$

Thus, the integers m_{ij} encode the angles between the reflecting hyperplanes and determine the geometry of the group.

Root Systems and Reflection Representation

Associated with a Coxeter group is a set of vectors $R \subset \mathbb{R}^N$, called a *root system*, such that:

- For each $\alpha \in R$, the reflection σ_α leaves R invariant.
- If $\alpha \in R$, then $-\alpha \in R$.
- The group G is generated by reflections σ_α for $\alpha \in R$.

Each reflection can be written as

$$\sigma_\alpha(x) = x - 2\frac{\langle x, \alpha \rangle}{\langle \alpha, \alpha \rangle}\alpha.$$

In this framework, the vectors v_j introduced in the main text correspond to elements of the root system.

Conjugacy Classes of Reflections

Two reflections θ_i and θ_j are said to be conjugate if there exists $g \in G$ such that

$$\theta_j = g\theta_i g^{-1}.$$

Reflections in the same conjugacy class share identical geometric properties. In particular, it is natural to assume that the corresponding vectors satisfy

$$|v_i| = |v_j| \quad \text{whenever } \theta_i \sim \theta_j,$$

which implies that

$$v_i = \pm v_j$$

up to the action of the group.

Bibliography

[1] Albert Einstein. Quantentheorie des einatomigen idealen gases. *Sitzungsberichte der Preussischen Akademie der Wissenschaften, Physikalisch-mathematische Klasse*, XXII:261–267, 1924. Published 10 July 1924.

[2] Albert Einstein. Quantentheorie des einatomigen idealen gases. zweite abhandlung. *Sitzungsberichte der Preussischen Akademie der Wissenschaften. Physikalisch-mathematische Klasse*, 3:3–14, 1925. Berlin: Verlag der Akademie der Wissenschaften, in Kommission bei Walter de Gruyter u. Co.

[3] Wolfgang Ketterle and N. J. van Druten. Bose–einstein condensation of a finite number of particles trapped in one or three dimensions. *Physical Review A*, 54(1):656–660, 1996.

[4] M. H. Anderson, J. R. Ensher, M. R. Matthews, C. E. Wieman, and E. A. Cornell. Observation of bose–einstein condensation in a dilute atomic vapor. *Science*, 269(5221):198–201, 1995.

[5] V. Genest, L. Vinet, and A. Zhedanov. *Journal of Physics: Conference Series*, 512:012010, 2014.

[6] V. Genest, M. Ismail, L. Vinet, and A. Zhedanov. *Communications in Mathematical Physics*, 329:999–1029, 2014.

[7] V. Genest, M. Ismail, L. Vinet, and A. Zhedanov. *Journal of Physics A: Mathematical and Theoretical*, 46:145201, 2013.

[8] V. Genest, M. Ismail, L. Vinet, and A. Zhedanov. *Journal of Physics A: Mathematical and Theoretical*, 46:325201, 2013.

[9] M. R. Ubriaco. *Physica A*, 414:128–135, 2014.

[10] W. S. Chung and H. Hassanabadi. *Modern Physics Letters A*, 34:1950190, 2019.

[11] D. Ojeda-Guillén, R. D. Mota, M. Salazar-Ramírez, and V. D. Granados. *Modern Physics Letters A*, page 2050255, 2020.

[12] Y. Kim, W. S. Chung, and H. Hassanabadi. *Revista Mexicana de Física*, 66(4):411–417, 2020.

[13] S. H. Dong, W. H. Huang, W. S. Chung, P. Sedaghatnia, and H. Hassanabadi. *Europhysics Letters*, 135:30006, 2021.

[14] H. Hassanabadi, M. de Montigny, W. S. Chung, and P. Sedaghatnia. *Physica A*, 580:126154, 2021.

[15] A. Merad and M. Merad. *Few-Body Systems*, 62:98, 2021.

[16] R. D. Mota, D. Ojeda-Guillén, M. Salazar-Ramírez, and V. D. Granados. *Annals of Physics*, 411:167964, 2019.

[17] R. D. Mota, D. Ojeda-Guillén, M. Salazar-Ramírez, and V. D. Granados. *Modern Physics Letters A*, 36(10):2150066, 2021.

[18] R. D. Mota, D. Ojeda-Guillén, M. Salazar-Ramírez, and V. D. Granados. *Modern Physics Letters A*, 36(23):2150171, 2021.

[19] B. Hamil and B. C. Lütfüoğlu. *Physica A*, 623:128841, 2023.

[20] B. Hamil and B. C. Lütfüoğlu. *Few-Body Systems*, 63:74, 2022.

[21] F. Merabtine, B. Hamil, B. C. Lütfüoğlu, A. Hocine, and M. Benarous. *Journal of Statistical Mechanics: Theory and Experiment*, 2023(5):053102, 2023.

[22] B. Hamil and B. C. Lütfüoğlu. *European Physical Journal Plus*, 137:812, 2022.

[23] A. Hocine, F. Merabtine, B. Hamil, B. C. Lütfüoğlu, and M. Benarous. *Indian Journal of Physics*, 2024.

[24] B. Hamil and B. C. Lütfüoğlu. *European Physical Journal Plus*, 137:1241, 2022.

[25] S. Kakei. *Journal of Physics A: Mathematical and General*, 29:L619–L624, 1996.

[26] L. Lapointe and L. Vinet. *Communications in Mathematical Physics*, 178(2):425–452, 1996.

[27] M. S. Plyushchay. *Annals of Physics*, 245:339–360, 1996.

[28] M. Plyushchay. *Nuclear Physics B*, 491:619–634, 1997.

[29] M. Plyushchay. *International Journal of Modern Physics A*, 15:3679–3698, 2000.

[30] C. F. Dunkl and Y. Xu. *Orthogonal Polynomials of Several Variables*, volume 81 of *Encyclopedia of Mathematics and its Applications*. Cambridge University Press, Cambridge, 2001.

[31] H. de Bie, B. Ørsted, P. Somberg, and V. Souček. *Transactions of the American Mathematical Society*, 364:3875–3902, 2012.

[32] M. Durdevich and S. B. Sontz. *SIGMA: Symmetry, Integrability and Geometry: Methods and Applications*, 9:040, 2013.

[33] S. Ghazouani, I. Sboui, M. A. Amdouni, and M. B. El Hadj Rhouma. *Journal of Physics A: Mathematical and Theoretical*, 52:225202, 2019.

[34] A. Aliano, G. Kaniadakis, and E. Miraldi. Bose-einstein condensation in the framework of κ-statistics. *Physica B*, 325:35–40, 2003.

[35] G. Kaniadakis. Nonlinear kinetics underlying generalized statistics. *Physica A*, 296:405–425, 2001.

[36] L. Accardi and F. Fidaleo. Bose-einstein condensation and condensation of q-particles in equilibrium and nonequilibrium thermodynamics. *Reports on Mathematical Physics*, 77(2):153–182, 2016.

[37] Q. A. Wang, M. Pezeril, and A. Le Méhauté. *Physica A*, 278:337–348, 2000.

[38] C. Tsallis. Possible generalization of boltzmann-gibbs statistics. *Journal of Statistical Physics*, 52(1-2):479–487, 1988.

[39] C. Tsallis. *Introduction to Nonextensive Statistical Mechanics: Approaching a Complex World*. Springer, Berlin, 2009.

[40] W. S. Chung and H. Hassanabadi. *European Physical Journal Plus*, 136:239, 2021.

[41] C. F. Dunkl. Differential-difference operators associated to reflection groups. *Transactions of the American Mathematical Society*, 311(1):167–183, 1989.

[42] Murray Gerstenhaber. On the deformation of rings and algebras. *Annals of Mathematics*, 79(1):59–103, 1964.

[43] F. Bayen, M. Flato, C. Frønsdal, A. Lichnerowicz, and D. Sternheimer. Deformation theory and quantization. *Annals of Physics*, 111(1):61–110, 1978.

[44] E. Noether. Invariante Variationsprobleme. *Nachrichten von der Gesellschaft der Wissenschaften zu Göttingen, Mathematisch-Physikalische Klasse*, 1918:235–257, 1918.

[45] P. A. M. Dirac. The fundamental equations of quantum mechanics. *Proceedings of the Royal Society A*, 109:642–653, 1925.

[46] W. Heisenberg. Über quantentheoretische Umdeutung kinematischer und mechanischer Beziehungen. *Zeitschrift für Physik*, 33:879–893, 1925.

[47] Paul Adrien Maurice Dirac. *The Principles of Quantum Mechanics*. International Series of Monographs on Physics. Oxford University Press, Oxford, 4th edition, 1958.

[48] E. Schrödinger. Quantisierung als Eigenwertproblem. *Annalen der Physik*, 384(4):361–376, 1926.

[49] E. P. Wigner. Do the equations of motion determine the quantum mechanical commutation relations? *Physical Review*, 77(5):711–712, 1950.

[50] L. M. Yang. Some exact results for the many-body problem in quantum mechanics. *Physical Review*, 84(4):788–792, 1951.

[51] George B. Arfken, Hans J. Weber, and Frank E. Harris. *Mathematical Methods for Physicists*. Academic Press, 7 edition, 2013.

[52] George F. Simmons. *Differential Equations with Applications and Historical Notes*. McGraw-Hill, 2 edition, 1991.

[53] R. K. Pathria and P. D. Beale. *Statistical Mechanics*. Elsevier, 3rd edition, 2011.

[54] W. Greiner, L. Neise, and H. Stöcker. *Thermodynamics and Statistical Mechanics*. Springer, New York, 1995.

[55] Franco Dalfovo, Stefano Giorgini, Lev P. Pitaevskii, and Sandro Stringari. Theory of Bose-Einstein condensation in trapped gases. *Rev. Mod. Phys.*, 71(3):463–512, 1999.

[56] Siegfried Grossmann and Martin Holthaus. On bose–einstein condensation in confined systems. *Zeitschrift für Naturforschung A*, 50:921–930, 1995.

[57] Siegfried Grossmann and Martin Holthaus. On bose–einstein condensation in confined systems. *Zeitschrift für Naturforschung A*, 51:921–930, 1996.

[58] A. Hocine, B. Hamil, F. Merabtine, B. C. Lütfüoğlu, and M. Benarous. *Revista Mexicana de Física*, 70:051701, 2024.

[59] N. D. Mermin and H. Wagner. Absence of ferromagnetism or antiferromagnetism in one- or two-dimensional isotropic heisenberg models. *Physical Review Letters*, 17(22):1133–1136, 1966.

[60] P. C. Hohenberg. Existence of long-range order in one and two dimensions. *Physical Review*, 158(2):383–386, 1967.

[61] M. Medani, M. Benarous, A. Hocine, and F. Merabtine. Thermodynamics of a general power-law trapped ideal dunkl-deformed bose gas. *Journal of Low Temperature Physics*, 222:24, 2026.

[62] A. Görlitz, J. M. Vogels, A. E. Leanhardt, C. Raman, T. L. Gustavson, J. R. Abo-Shaeer, A. P. Chikkatur, S. Gupta, S. Inouye, T. Rosenband, and W. Ketterle. Realization of bose-einstein condensates in lower dimensions. *Physical Review Letters*, 87(13):130402, 2001.

[63] Z. Hadzibabic, P. Krüger, M. Cheneau, S.P. Rath, and J. Dalibard. *New J. Phys.*, 10:045006, 2008.

[64] L. Chomaz, L. Corman, T. Bienaimé, R. Desbuquois, C. Weitenberg, S. Nascimbène, J. Beugnon, and J. Dalibard. Emergence of coherence via transverse condensation in a uniform quasi-two-dimensional Bose gas. *Nat. Commun.*, 6:6162, 2015.

[65] F. Delfino and E. Vicari. Dimensional crossover of Bose-Einstein-condensation phenomena in quantum gases confined within slab geometries. *Phys. Rev. A*, 96:043623, 2017.

[66] D.S. Petrov, G.V. Shlyapnikov, and J.T.M. Walraven. Regimes of quantum degeneracy in trapped 1D gases. *Phys. Rev. Lett.*, 85:3745, 2000.

[67] D.S. Petrov, M. Holzmann, and G.V. Shlyapnikov. Bose-einstein condensation in quasi-2D trapped gases. *Phys. Rev. Lett.*, 84:2551, 2000.

[68] W. Ketterle. Realization of Bose-Einstein condensates in lower dimensions. *Phys. Rev. Lett.*, 87:130402, 2001.

[69] B.P. van Zyl, R.K. Bhaduri, and J. Sigetich. Dilute Bose gas in a quasi-two-dimensional trap. *J. Phys. B: At. Mol. Opt. Phys.*, 35:1251, 2002.

[70] N.P. Proukakis. Coherence of trapped one-dimensional (quasi-) condensates and continuous atom lasers in waveguides. *Las. Phys.*, 13:527, 2003.

[71] U. Al Khawaja, N.P. Proukakis, J.O. Andersen, M.W.J. Romans, and H.T.C. Stoof. Dimensional and temperature crossover in trapped Bose gases. *Phys. Rev. A*, 68:043603, 2003.

[72] D.S. Petrov, D.M. Gangardt, and G.V. Shlyapnikov. Low-dimensional trapped gases. *J. Phys. IV France*, 116:5, 2004.

[73] A. Richaud, P. Massignan, V. Penna, and A.L. Fetter. Dynamics of a massive superfluid vortex in r^k confining potentials. *Phys. Rev. A*, 106(6):063307, 2022.

[74] M. Benarous, A. Hocine, B. C. Lütfüoğlu, and B. Hamil. Bounding the wigner deformation parameter in harmonically trapped bose gases. *Journal of Statistical Mechanics: Theory and Experiment*, 2025(5):053102, 2025.

[75] S. Gautam and D. Angom. *The European Physical Journal D*, 46:151–155, 2008.

[76] A. Hocine, B. Hamil, F. Merabtine, B. C. Lutfuoglu, and M. Benarous. *Revista Mexicana de Física*, 70:051701, 2024.

[77] M. Abramowitz and I. A. Stegun. *Handbook of Mathematical Functions*. Dover Publications, New York, 1965.

[78] F. W. J. Olver et al. *NIST Handbook of Mathematical Functions*. Cambridge University Press, Cambridge, 2010.

[79] G. Arfken, H. Weber, and F. Harris. *Mathematical Methods for Physicists*. Academic Press, New York, 7th edition, 2013.